Summer 2022

Long Non-coding RNA PVT1 – An Exploratory Study in Ovarian and Endometrial Cancer

Kevin Tabury

LONG NON-CODING RNA PVT1 – AN EXPLORATORY STUDY IN OVARIAN AND ENDOMETRIAL CANCER

By

Kevin Tabury

Bachelor of Science
HEL, 2009

Master of Engineering
KU Leuven, 2016

Submitted in Partial Fulfillment of the Requirements

For the Degree of Doctor of Philosophy in

Biomedical Engineering

College of Engineering and Computing

University of South Carolina

2022

Accepted by:

Mythreye Karthikeyan, Major Professor

Tarek Shazly, Major Professor

R. Michael Gower, Committee Member

Michael Shtutman, Committee Member

Roel Quintens, Committee Member

Tracey L. Weldon, Vice Provost and Dean of the Graduate School

DEDICATION

This PhD thesis is dedicated to my family and in particular to my grandfather who lost the fight against cancer during this PhD.

ACKNOWLEDGEMENTS

The end of a long journey has arrived which would have not been possible without the help and support from many people. Limited to one page, my appreciation goes beyond. I would like to acknowledge my advisor, Prof. Mythreye Karthikeyan, for her continual guidance and abundant support throughout this journey. I would like to acknowledge my second advisor, Prof. Tarek Shazly, for his continuous support and who made this journey possible. I would like to thank Dr. Roel Quintens, my mentor, for his continuous critical assessment and discussion of this work. I would also like to acknowledge my committee members Prof. R. Michael Gower and Prof. Michael Shtutman for their devoted time, help and effort to this work. A special thank you to Prof. Sarah Baatout who inspired and supported me in my transformation process from being a lab technician to a researcher. Thank you Mehri for your crucial help and collaboration in finalizing my first manuscript. To Ben and Choi, my lab partners in crimes, thank you for making the time with you so memorable. My appreciation to Nazli and Liya for always backing me up with my crazy adventures. To Tine, thank you for starting this journey with me. My deepest appreciation to all my colleagues at the Belgian Nuclear Research Center for your patience and continuous support. I am looking forward to tackle the next challenges together. To my family and friends for always believing in me, Thank you!

ABSTRACT

Gynecological cancers, ovarian and endometrial cancer, are still leading causes of cancer-related death in women worldwide. Early detection methods as well as treatment resistance remain a challenge. Long non-coding RNAs (lncRNAs) are emerging as therapeutic targets with diagnostic and prognostic potential with lncRNA PVT1 being one of them.

Here I test and demonstrate the role of PVT1 in ovarian cancer growth and metastasis. PVT1 is amplified and overexpressed in ovarian cancer and has predictive value for survival and response to targeted therapeutics. We find that expression of PVT1 is regulated by tumor cells in response to cellular stress, particularly loss of cell-cell contacts and changes in matrix rigidity occurring in a YAP1-dependent manner. Induction of PVT1 promotes tumor cell survival, growth, and migration. Conversely, reducing PVT1 levels robustly abrogates metastatic behavior and tumor cell dissemination in cell lines and syngeneic transplantation models in vivo. We find that reducing PVT1 causes widespread changes in the transcriptome leading to alterations in cellular stress response and metabolic pathways including doxorubicin metabolism, which impacts chemo sensitivity in ovarian cancer. We further investigated the role of PVT1 DNA alterations and RNA expression in endometrial cancer. We find that PVT1 has predictive value for survival and potentially treatment response. High PVT1 RNA expression combined with PVT1 amplification

results in poor patient survival, is characterized by an enrichment of cell cycle progression through E2F and MYC target genes and corresponds to type 2 endometrial cancer. On the other hand, PVT1 diploid patients have the best survival without consideration of PVT1 RNA expression and correspond to type 1 endometrial cancer. PVT1 low RNA expression combined with PVT1 diploid is characterized by an enrichment of the estrogen signaling pathway, suggesting PVT1 as a good candidate to explore for response to hormonal therapy.

Together, these findings implicate PVT1 as a promising therapeutic target as well as a potential biomarker of survival and treatment response in ovarian and endometrial cancer.

TABLE OF CONTENTS

LIST OF TABLES

LIST OF FIGURES

CHAPTER 1

INTRODUCTION

1.1 NON-CODING RNA

The central dogma of molecular biology states that ‘Once information has got into a protein it can’t get out again. Information here means the sequence of the amino acid residues, or other sequences related to it.’, a statement elaborated by Crick in 1956 [1] and published in 1970 [2]. The scientific community responded by a simplification of it as describing the flow of genetic information, from DNA to RNA to proteins. Although it is true that DNA is transcribed into messenger RNA (mRNA) which in turns is translated into proteins, describing it as “the flow” is incorrect and was also not what Crick intended to imply [2]. The complexity hidden within the central dogma is only slowly being revealed. Until recently, mRNAs were thought to be the most prevalent and important entities of the human transcriptome as proteins are responsible for orchestrating nearly every structural and functional component of the cell. Yet, the sequencing of the human genome, in 2001, exposed that only ~2 % of our transcriptome is encoding for proteins [3]. The remaining ~98 % was believed to be simply nonfunctional “DNA junk”, although divergent opinions were existing [4, 5]. The ENCODE project, in 2012, showed that the non-protein coding portion of the genome is transcribed into thousands of RNA molecules [6]. These RNA molecules, commonly termed as non-coding RNAs (ncRNAs), are composing the majority

of the transcriptome and are functional. NcRNAs are very heterogeneous in terms of their length, conformation and cellular function.

1.2 NON-CODING RNA CLASSIFICATION

NcRNAs can be separated into two main classes, broadly based upon an arbitrary size threshold. The most widely studied class of ncRNAs are small ncRNAs called microRNAs (miRNAs - ~22 nucleotides) that function as translational repressors [7] in many biological processes such as embryogenesis [8] and human disease [9] as examples. Yet, many other types of small ncRNAs also have major roles in cellular homeostasis and disease. Amongst others, PIWI-interacting RNAs (piRNAs - ~28 nucleotides) that function as a transposon silencer [10], small nucleola RNAs (snoRNAs - ~70 nucleotides) that guide RNAs in the post-transcriptional synthesis of 2′-O-methylated nucleotides and pseudo uridines in ribosomal RNAs [11] and long non-coding RNAs (lncRNAs – longer than 200 nucleotides). The ENCODE project annotated ~9,600 lncRNAs [6]. Initially these lncRNAs were seen as “transcriptional noise” as these have low evolutionary primary sequence conservation [12], low levels of expression [13] and lack of long open reading frames (longer than 300 nucleotides) to code for proteins [14], hence thought to be nonfunctional. Recent research, however, showed that some lncRNAs contain short open reading frames coding for small peptide [15], some are conserved by sequence [16] or structure [17], and have regulatory functions [18]. Besides the use of size, lncRNAs have also been proposed to be classified based on their genomic location with respect to protein coding genes as intronic, intergenic, sense, antisense and bidirectional/divergent [19]. Intronic lncRNAs are located within the intronic region of a coding gene. Intergenic lncRNAs (also called lincRNAs) are located between two coding genes. Sense lncRNAs

are transcribed from the sense strand of protein-coding genes while antisense are transcribed from the antisense strand of protein-coding genes. Bidirectional/divergent lncRNAs have their sequences located on the opposite strand from a protein coding gene. Subcellular localization was also proposed as a classification method where lncRNAs can be classified as nuclear or cytoplasmic [20]. Even though, lncRNAs can also be found only in specific organelles [20]. Another class of lncRNAs are circular RNAs. circular RNAs are a class of RNA transcripts that originate or from back-spliced exons (circRNAs) or from spliced intron (ciRNAs) [21]. The mode of action to regulate gene expression has also been proposed as a classification method, which broadly includes cis- and trans- acting. Cis-acting lncRNAs regulate gene expression of nearby genes while trans-acting leave the site of transcription to regulate gene expression of distant genes [22]. To note that not all lncRNAs fall within these classes and that overlaps between the different classification method are seen.

Although, the balance of scientific opinion has moved away from classifying lncRNAs as “transcriptional noise”, the aforementioned classification methods are non-exhaustive and incomplete as exceptions are regularly found. It might take a decade of analyses to fully define and classify lncRNAs.

1.3 LONG NON-CODING RNA BIOGENESIS

Compared to messenger RNAs (mRNAs) (which code for proteins), lncRNAs share common but also unique features in their biogenesis. Most lncRNAs (lincRNAs) are processed through RNA polymerase II and have similarly to mRNAs a 7-Methyl guanosine (m^7G) capping at the 5′ end a 3′ poly(A) tail RNA transcripts to which splice events might have occurred but fewer than with mRNAs [23]. Yet, alternative processing to mitigate

their degradation such as RNase P cleavage to generate a mature 3′ end, capping by snoRNAs at both ends or the 5′ end [23] as well as the forming of circular structures [21] are also seen. Furthermore, lincRNAs are usually shorter and contain fewer exons than mRNAs [24]. Also, Melé et al. showed that lincRNAs appear to have fewer histone marks and transcription factors bound to their promoters compared to mRNAs suggesting that their expression are more specific [24].

1.4 LONG NON-CODING RNA FUNCTION

To date, only a hand full of lncRNAs have been characterized. These lncRNAs have been involved in multiple physiological [25] and pathological processes including cancer [26]. LncRNAs have functions at the level of transcriptional regulation, post-transcriptional regulation, cell organelle formation and structural organization. These functions are completed through the interaction between lncRNAs and other molecules such as DNA, RNA as well as protein and was recently reviewed by Statello et al. [18].

At the transcriptional level, lncRNAs can induce chromatin remodulation through indirect interaction (recruitment or inhibition of chromatic modifiers) or direct interaction (cis-acting and trans-acting) [18]. The most well know example is lncRNA XIST which inactivate the X-chromosome in mammals through DNA methylation and histone modifications [27]. In addition, lncRNAs can act as guide where lncRNAs bind to proteins and direct the formed complex to a specific genomic location. Example of guide is the well-studied lncRNA HOTAIR direct the chromatin modifier Polycomb Repressive Complex 2 to the developmental HOXD locus resulting in chromatin silencing [28]. LncRNAs can also function as scaffolds, which act as platforms to host the formation of molecule complexes [18]. LncRNA NEAT1 is a well-known scaffold, essential for the

formation of paraspeckles [29]. Decoy lncRNAs, also known as competing endogenous RNAs (ceRNAs), regulate transcription by binding to miRNAs, transcription factors or RNA binding protein to annihilate their transcriptional activities [18]. An example of decoy lncRNA is lncRNA MALAT1 which interacts with serine/arginine splicing factors to regulate alternative splicing [30].

At the post-transcriptional level, lncRNAs are found in the nucleus and the cytosol where they mainly act as ceRNAs or scaffold to alter mRNA splicing or degradation as well as the regulation of signaling pathways [18]. LncRNA H19 is an example of lncRNA scaffold that binds to K homology-type splicing regulatory protein to promote mRNA encoding the cell cycle regulator Nucleophosmin in C2C12 cells [31]. Modulation of miRNA availability by lncRNA as ceRNAs is also a central regulatory process [32]. Finally, the formation of exosomes encompassing lncRNAs has emerged, increasing their complexity in regulatory functions [33].

1.5 LONG NON-CODING RNA PVT1

Plasmacytoma variant translocation 1 (Pvt1) has been first described in the mouse as being involved in a variant translocation in plasmacytomas [34]. Subsequent study revealed Pvt1 participation in recurrent translocations between chromosome 8 and chromosome 2 and 22 in Burkitt's lymphomas indicating a first correlation with Myc [35]. Pvt1 is also a common retroviral integration site in murine leukemia virus induced T lymphomas [36]. With the avenues of transcriptome analysis technologies and the identification of locus 8q24 has oncogenic, increase interest has been shown in recent years in PVT1. LncRNA PVT1 has recently been extensively reviewed [37-39] and will therefore only shortly be introduced here.

PVT1 is a lincRNA located ~53 kb downstream of MYC on chromosome 8q24.21. Multiple linear and circular transcript have been reported with PVT1-224 / ENST00000651587.1 isoform (identified here as PVT1) and hsa_circ_0001821 (identified here as circPVT1) transcripts being the most studied [39]. Specific transcript appears to have also specific function. While PVT1b, including exon 1b in place of 1a, is described as a tumor suppressor [40], PVT1 is mostly observed as amplified and upregulated in different pathologies including cancer. Both linear and circular form are able to act independently from each other [41] and PVT1 transcript also encompasses multiple miRNAs [42]. PVT1 is enriched in the nucleus but can also be found in the cytosol while circPVT1 is mor prevalent in the cytosol [39]. Functionally, PVT1 (linear and circular) promote cell proliferation, invasion, migration, apoptosis resistance, drug resistance and increase cellular metabolism [39]. These functions result from PVT1 acting (cis- and trans-acting) as a chromatin modifier, ceRNAs and scaffold [39]. Also, due to PVT1 proximity to MYC, accumulating evidences shows that PVT1 and MYC have separate and distinct oncogenic potential. However, their interaction remain unclear.

Although increasing knowledge is being acquired, the complexity of lncRNA PVT1 activity is only emerging and more insights into the underlying mechanisms involving PVT1 is needed. Yet, it is clear that PVT1 is an excellent candidate as potential therapeutic target or as biomarker of diagnosis and prognosis.

1.6 LONG NON-CODING RNA PVT1 IN GYNECOLOGICAL CANCERS

Gynecological cancers, mainly including ovarian, cervical and endometrial cancers, are still the leading cause of cancer related death worldwide [43]. Ovarian cancer accounts for ~2% of all new cancer diagnoses and ~4% of all cancer-related deaths in

women worldwide [43]. Yet, ~39% of all cancer related death from cancer of the female genital tract are ovarian cancer [43] because of asymptomatic and hidden growth of the tumor, delayed onset of symptoms, and lack of proper screening that result in its detection mostly at an advanced stage [44]. The incidence rate increases proportionately with age with the largest proportion of patients being in the 60–64 years age group [45]. The fist-line of treatment are surgery and chemotherapy. Although the response rate of treatment is high, most patients relapse within the subsequent 5 years mainly due to treatment resistant cancer cells [46]. Most cervical cancer arise from long-term persistent infection by one of the high-risk human papilloma virus (HPV) [47]. Through HPV vaccination as preventive measure and screening for precancerous lesions as early detection method, cervical cancer is almost eliminated in developed countries [48]. Yet, approximately 90% of cervical cancers occur in low-income and middle-income countries that lack organized screening and HPV vaccination programs [48]. Cervical cancer accounts for ~1.5% of all new cancer diagnoses and ~1.5% of all cancer-related deaths in women, while ~13% of all cancer related deaths from cancer of the female genital tract are cervical cancers worldwide [43]. The fist-line of treatment are surgery and radiation therapy, with chemotherapy as valuable adjunct [48]. According to Siegel et al., endometrial cancer accounts for ~7% of all new cancer diagnoses and ~4% of all cancer-related deaths in women worldwide [43]. Yet, ~38% of all cancer related death from cancer of the female genital tract are endometrial cancer [43]. The fist-line of treatment consists of hysterectomy and bilateral salpingo-oophorectomy [43].

To further explore gynecological cancers, we first clarify their histopathological subtypes (Figure 1. 1). At first, ovarian cancers are classified as Type 1 (low grade) or Type

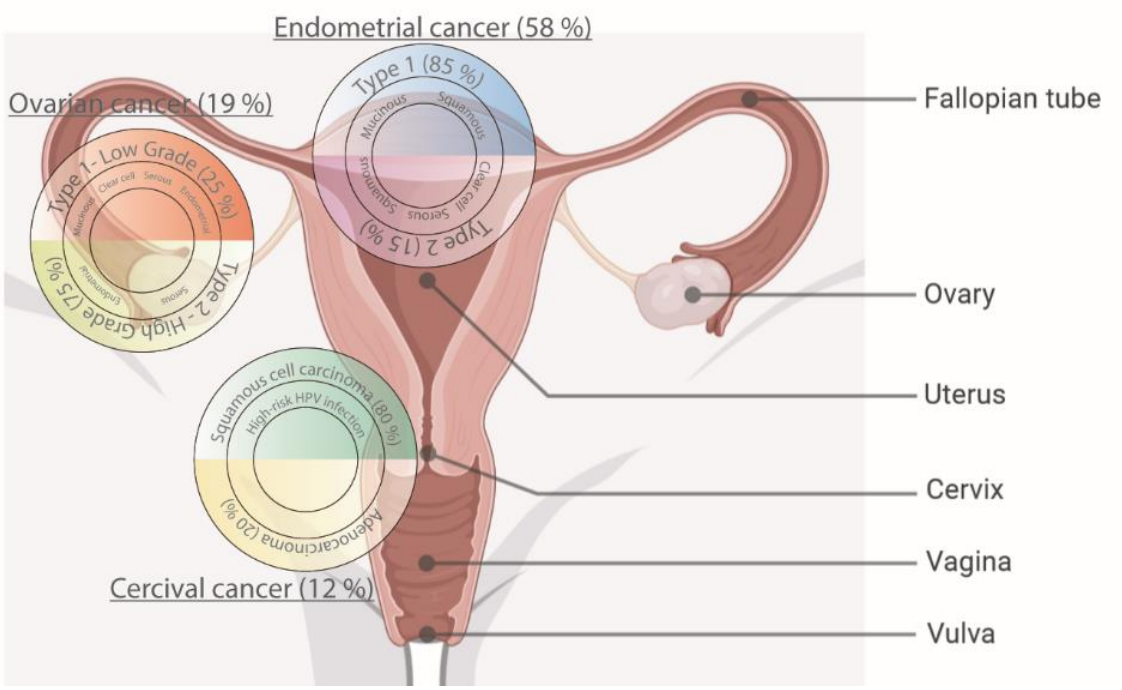

Figure 1. 1: Overview of the female reproductive system together with a representation of the three most occurring histopathological subtypes of gynecological cancers, created with BioRender.

2 (high-grade) carcinoma. Type 1 is less common (~25%), detected at early stage and has thus a better prognosis. Type 1 can be further classified into low-grade serous, low-grade endometrial, clear cell and mucinous. On the contrary, Type 2 is more common (~75%), detected at an advanced stage and accounts for most ovarian cancer-related deaths. In addition, Type 2 is mostly composed of high grade serous (HGSC) and to a lesser extent high grade endometrioid cancer (Table A.1) [49-51]. Furthermore, there is currently a paradigm shift regarding the origin of HGSC that postulate serous tubal intraepithelial carcinoma precursor lesions in the fallopian tube as onset of HGSC [52]. Lastly, although combination of cytoreductive surgery and chemotherapy is effective, ~70% of patients experience relapse [53]. Next, cervical cancers are classified as squamous-cell carcinoma (~80%) or adenocarcinoma (~20%) (Table A.1) [54]. At last, endometrial cancers are classified as Type 1 (endometrioid) or Type 2 (nonendometrioid). Type 1 is more common

(~85%) and consist of adenocarcinoma mucinous, and squamous. Type 2 is less common (~15%) and consist of clear cell carcinoma, serous carcinoma and carcinosarcoma subtypes (Table A.1). Yet, Type 2 is more aggressive and has a relatively unfavorable prognosis [55-57].

Despite an indication that PVT1 is dysregulated in the most aggressive subtypes, its dysregulation has been observed in all major types of gynecological cancers (Table A.1).

1.6.1 PVT1 IN OVARIAN CANCER

PVT1 expression (linear and circular form) is upregulated in both subtypes of ovarian cancer. In these, PVT1 is involved in promoting cell proliferation, migration, invasion, cell cycle progression, apoptosis resistance, sphere forming and paclitaxel resistance.

Predominantly, PVT1 acts as a competitive endogenous RNA for miR-133a [58], miR-140 [59], miR-17-5p [60], miR-543 [61], miR-370-5p and miR-526-5p [62]. Similarly, circPVT1 acts as a competitive endogenous RNA for miR-149 [63]. Yet, PVT1 can also epigenetically suppress miR-214 by binding to EZH2 [64]. Downstream effectors of these miRNAs are multiple. Expression of miR-133a restore cell proliferation, cell cycle progression, migration and invasion after PVT1 knockdown [58] by targeting IGF1R [65]. Cell proliferation is repress by PDGFRA [66] or MAPK1 [67] through miR-140. Expression of miR-17-5p inhibits cell proliferation, cell cycle progression and apoptosis resistance by targeting PTEN [60, 68] or YES1 [69]. Cell proliferation, migration, invasion, sphere formation and apoptosis resistance targeted by SERPINI1 [61] or TWIST1 [70] can be repressed by miR-543. Expression of miR-370-5p suppress cell proliferation and cell cycle progression by targeting FOXM1 [62]. Yet, PVT1 can also post-transcriptionally

stabilize FOXM1 protein by directly binding to it [62]. Expression of miR-149 impede cell proliferation and apoptosis resistance [63] by targeting XIAP [71]. Also, expression of miR-214 reduces cell proliferation, migration, invasion and EMT [64] by targeting PTEN [72, 73].

Furthermore, PVT1 expression can be modulated by the stress responsive transcription factor FOXO4 [74] through direct binding to its promoter [59]. PVT1 expression has also been associated to chemo resistance by activating apoptosis resistance pathways [75, 76]. However, contradictory association has also be observed [77]. Interestingly, compared to other gynecological cancers, ovarian cancer is the first to point out differences between PVT1 copy number amplification and RNA expression [78]. Indeed, the concept of copy number amplification corresponding to high RNA expression is challenged. PVT1 copy number and RNA expression is often studied in parallel with the oncogene MYC due to their proximity. However, the understanding of their interaction and correlation remains unclear. Looking at those, MYC and PVT1 correlation as well as their individual copy number versus mRNA expression seem to be histopathological subtype and tissue reference dependent [79, 80]. Consequently, conclusions on the prognostic potential of PVT1 can be contradictory [79, 81, 82] and emphasize the need of novel studies tackling the differences between copy number amplification and RNA expression.

1.6.2 PVT1 IN CERVICAL CANCER

PVT1 expression (linear and circular form) is upregulated in both subtypes of cervical cancer. In these, PVT1 is involved in promoting cell proliferation, migration, invasion, cell cycle progression, apoptosis resistance, EMT and paclitaxel resistance. Multiple mechanisms of action have been reported. Predominantly, PVT1 acts as a

competitive endogenous RNA for miR-424 [83], miR-140-5p [84] and miR-486-3p [85]. Yet, PVT1 can also repress microRNA expression using the epigenetic machinery by binding to EZH2 and as such induce H3K27 methylation on the promoter of miR-200b [86] and miR-195 [87]. Expression of miR-424 induces cell cycle arrest, apoptosis and radiation sensitivity by targeting KDM5B or aprataxin [88, 89]. Targets of SMAD3 [84] or ADAM10 [90] involved in migration, invasion, cell cycle progression and EMT can be inhibited by miR-140-5p. Cell proliferation and invasion is repressed by EMP1 through miR-486-3p [91]. Expression of miR-200b inhibits cell cycle progression, apoptosis resistance and EMT by targeting RhoA [92]. Expression of miR-195 inhibits cell proliferation, cell cycle progression, migration, invasion and paclitaxel induced EMT by direct binding to cyclin D1 [93], DCUN1D1 [94] or YAP1 [95]. Furthermore, PVT1 seem to be responsive to cellular stressors such as hypoxia and immune activation by INF-α [96]. Also PVT1 has been found to colocalize with Nucleolin in the cytoplasmic and plasma membrane compartments [96]. PVT1 is mainly located in the cytoplasm but can also be found in the nucleus [85]. Similarly, circular PVT1 acts as a competitive endogenous RNA for miR-1286 promoting thus migration and invasion through EMT regulation [97].

The linear form of PVT1 has also been proposed as a biomarker to monitor cervical cancer progression. Indeed, significant correlation was found between PVT1 level in patient-derived serum with PVT1 expression in the corresponding cervical cancer tissue as well as correlation with tumor size, clinical stage, and lymph node metastasis [98, 99]. Similarly, circular PVT1 has been proposed as a biomarker of prediction. Indeed, levels of circular PVT1 in patient-derived plasma correlated with tumor size, clinical stage and

lymph node metastasis [100]. Finally, circular PVT1 can also be measured in plasma and urine exosomes [97].

1.6.3 PVT1 IN ENDOMETRIAL CANCER

PVT1 expression is so far upregulated in patients with endometrial carcinomas (type 2). In these, PVT1 is involved in promoting cell proliferation, migration, invasion, cell cycle progression, apoptosis resistance, sphere-forming and paclitaxel resistance [101-103]. Mechanistically, PVT1 seems to act as a competitive endogenous RNA for miR-195-5p [101] and can be modulated by the protein UPF1 through direct protein-RNA binding [103]. Expression of miR-195-5p inhibits epithelial-mesenchymal transition (EMT) by targeting G protein-coupled estrogen receptor 1 [104]. AN overview of PVT1 mechanism of action is described in Figure 1. 2.

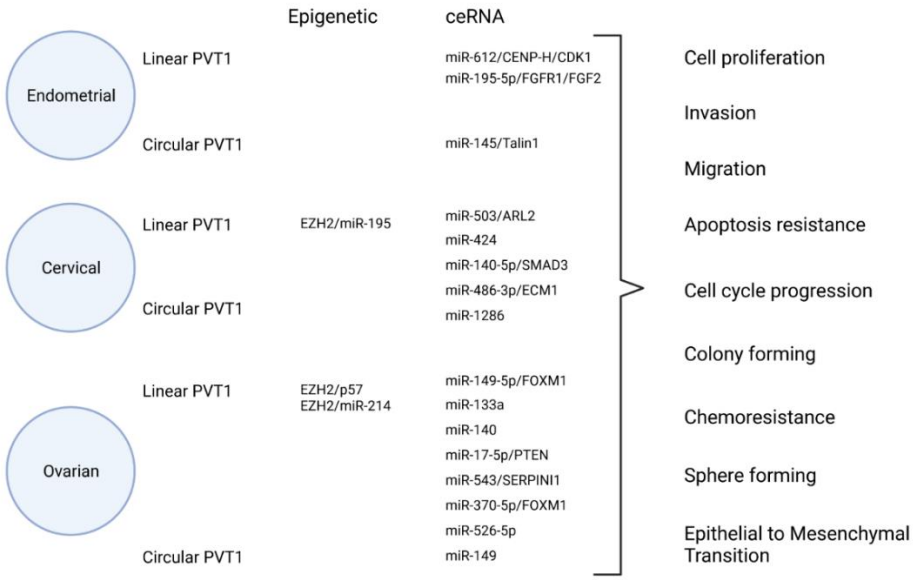

Figure 1. 2: Overview of PVT1 (linear and circular form) mechanisms of action and functional impact based on the literature (Table A.1).

1.7 PHD AIMS

Constant transcriptomic advances are resulting in the recognition of lncRNAs as important regulator of the expression of the genome and in particular in cancer. Yet, knowledge gaps in our understanding of lncRNAs, including their functional, range of action and mechanistic, hamper their potential as therapeutic targets.

This PhD sought to bring insights in the regulatory mechanisms of lncRNA PVT1 in ovarian cancer and to investigate the potential implications of lncRNA PVT1 copy number alteration and RNA expression in endometrial cancer, envisioning PVT1 as a potential therapeutic target. Chapter 2 aimed at 1) uncovering mechanisms that regulate lncRNA PVT1 in ovarian cancer and 2) investigating functions of lncRNA PVT1 in ovarian cancer. Chapter 3 aimed at exploring the clinical relevance of lncRNA PVT1 copy number alteration and RNA expression in endometrial cancer.

CHAPTER 2

PVT1 IS A STRESS-RESPONSIVE LNCRNA THAT DRIVES OVARIAN CANCER METASTASIS AND CHEMORESISTANCE [1]

Metastatic growth of ovarian cancer cells into the peritoneal cavity requires adaptation to various cellular stress factors to facilitate cell survival and growth. Here, we demonstrate the role of PVT1, one such stress induced long non-coding RNA, in ovarian cancer growth and metastasis. PVT1 is an amplified and overexpressed lncRNA in ovarian cancer with strong predictive value for survival and response to targeted therapeutics. We find that expression of PVT1 is regulated by tumor cells in response to cellular stress, particularly loss of cell–cell contacts and changes in matrix rigidity occurring in a YAP1-dependent manner. Induction of PVT1 promotes tumor cell survival, growth, and migration. Conversely, reducing PVT1 levels robustly abrogates metastatic behavior and tumor cell dissemination in cell lines and syngeneic transplantation models in vivo. We find that reducing PVT1 causes widespread changes in the transcriptome leading to alterations in cellular stress response and metabolic pathways including doxorubicin metabolism, which impacts chemosensitivity. Together, these findings implicate PVT1 as

[1] Kevin Tabury, Mehri Monavarian, Eduardo Listik, Abigail K. Shelton, Alex Seok Choi, Roel Quintens, Rebecca Arend, Nadine Hempel, C. Ryan Miller, Balázs Győrffy, Karthikeyan Mythreye. Deposited to bioRxiv and published at Life Science Alliance

a promising therapeutic target to suppress metastasis and chemoresistance in ovarian cancer.

2.1 INTRODUCTION

A feature of successful metastasis is the ability of cancer cells to adapt and survive under cellular stress. Mechanisms to do so include increased genomic instability, transcriptional and epigenetic changes, and acquisition of mutations [105]. Such changes are coupled with signaling pathways and gene expression alterations that facilitate cancer cell survival and thereby tumor progression. Cellular stressors impacting most cancers include changes in oxygen tension (hypoxia), changes in ECM composition and matrix rigidity, alterations in cell-cell contacts and changes in anchorage-independent survival capabilities, oxidative, and metabolic stress as well as therapeutic treatments. Thus, defining stress dependent alterations is critical to our understanding of metastatic mechanisms.

Ovarian cancer is the fifth leading cause of cancer deaths with the highest mortality among all gynecological cancers [106]. Yet, the full etiology and pathophysiology continues to be delineated [107]. Epithelial ovarian cancer (EOC) is the most common type of ovarian cancer and is classified into different subtypes (high-grade serous carcinoma [HGS, low-grade serous carcinoma, mucinous carcinoma, endometroid carcinoma, and clear cell carcinoma) [108] that are marked by different genome amplification and genetic instability [109]. All subtypes are exposed to cellular stressors during metastasis that involve the ovaries, the omentum, and the peritoneum. The metastatic peritoneal spread involves cell-ECM detachment, loss of cell-cell contacts, epithelial-mesenchymal transition (EMT) and shedding of cells from the tumor, followed

by anchorage independent survival, re-attachment to new locations and re-establishment of cell-cell contacts [110]. Primary tumors in the fallopian tube and ovaries and secondary peritoneal growths in the abdominal cavity can also be hypoxic [111], potentially further driving metastasis and chemo resistance in a feed forward manner [111, 112]. In addition, several prior studies have reported changes to cellular stiffness during metastasis in ovarian cancer [113, 114]. Similarly, changes to the ECM and thereby matrix rigidity can also directly impact EMT responses and metastasis [115].

The Human Genome Project launched the era of non-coding RNAs (ncRNAs) [116]. In these ncRNA's, small ncRNAs (<200 nucleotides) such as microRNAs, small interference RNAs and PIWI- interacting RNAs have been intensively investigated for many years [10, 117]. However, long ncRNAs (lncRNAs) (>200 nucleotides) and the contexts of their significance are still poorly understood. In ovarian cancer, several lncRNAs including *MALAT1*, *HOTAIR* and *H19* are pivotal players in response to cellular stressors particularly genotoxic stress, metabolic stress and hypoxia and are also associated with tumorigenesis, metastasis and chemo resistance [118]. *PVT1* is one such lncRNA located on chr8q24.21 that is expressed at low levels in normal tissues but is also designated as an oncogene due to its amplification/upregulation status in multiple cancers [78, 119] acting as a potential competing endogenous RNA for miRNAs [120, 121]. PVT1 has complex roles in cancers including ovarian. On one hand it has been reported to suppress cell growth [77], while in others it has been reported to promote growth [62]. Given the significant genetic instability of ovarian cancers and the ability of lncRNAs to impact metastasis through multiple mechanisms [122], a first step to precisely defining lncRNA

expression outcomes is to delineate and establish contexts that regulate lncRNA expression and activity.

Here we investigate in detail the contexts and mechanisms of lncRNA PVT1 expression and metastatic activities particularly in response to various stress factors in ovarian cancer. Our findings uncover PVT1 as a YAP1 dependent stress-responsive lncRNA, that can be altered transiently to drive metastasis and chemo resistance. We also discover a novel contribution of PVT1 in the regulation of doxorubicin resistance in this process.

2.2 RESULTS

2.2.1 CLINICAL SIGNIFICANCE OF PVT1 IN OVARIAN CANCER

To evaluate in detail PVT1 expression and amplification in broad cancer types, we evaluated The Cancer Genome Atlas (TCGA) datasets using cBioportal [123, 124]. Analysis of somatic focal copy number gain events identified by GISTIC (v2.0) for serous ovarian cancers identified chromosome loci 8q24.21 as exhibiting the highest copy number gains (Figure 2. 1A). Notably, MYC is located on 8q24.21 (Figure 2. 1B). PVT1 was most significantly co-expressed with MYC, (*Figure* 2. 1C and 1D - Pearson factor of 0.70 ($P = 3.11 \times 10^{-46}$)). Among all cancers within the TCGA Firehose Legacy studies, serous ovarian cancer exhibited the highest frequency of alterations in PVT1 (43 %) (Figure 2. 1E and Table 2.1).

Because serous ovarian cancers are marked by genome amplification [125], we evaluated the effect of PVT1 amplification on PVT1 expression, by comparing PVT1 amplification versus expression and found that amplification and expression were highly correlated in ovarian cancer patients (Pearson factor of 0.46 P = 4.27 x 10-17, Figure 2.

1F). Hence to evaluate the clinical significance of PVT1 expression changes alone, we conducted Kaplan-Meier survival analysis using KM plotter [126] in TCGA datasets that included all ovarian cancer patients with a best cutoff analysis [127]. Log-rank statistics were used to calculate the P-value and Hazard Ratio (HR). We found that patients with higher PVT1 expression had shorter overall survival (OS) (Figure 2. 1G) and significantly shorter progression-free survival (PFS) (Figure 2. 1H). Effects of PVT1 expression on PFS were also grade (Figure B. 1A) and stage dependent (Figure 2. 1I) with an increased hazard ratio for Grade 2 (HR: 2.753, P = 0.0256) (Figure B. 1A) and cancer Stage 4 (HR= 2.374, P = 0.007) (Figure 2. 1I). Kaplan-Meier analysis also suggests that patients with high PVT1 expression may benefit from targeted therapy (HR: 0.3344, P = 0.033) compared to other treatment strategies such as chemotherapy (Figure 2. 1J). This suggests that PVT1 has predictive value for survival and may play an important role in ovarian cancer and treatment outcomes.

Table 2.1: Copy number alteration distribution from Figure 2.1E.

Cancer Type	Alteration Frequency	Alteration Type	Alteration Count
Ovarian Cancer	0.345423143	Homozygous deletion	2
Ovarian Cancer	43.00518135	Amplification	249
Breast Cancer	0.186046512	Homozygous deletion	2
Breast Cancer	21.30232558	Amplification	229
Esophagogastric Cancer	0.32	Homozygous deletion	2
Esophagogastric Cancer	16.8	Amplification	105
Hepatobiliary Cancer	0.24691358	Homozygous deletion	1
Hepatobiliary Cancer	16.79012346	Amplification	68
Head and Neck Cancer	0.383141762	Homozygous deletion	2
Head and Neck Cancer	11.30268199	Amplification	59
Endometrial Cancer	0.168067227	Homozygous deletion	1
Endometrial Cancer	11.42857143	Amplification	68
Pancreatic Cancer	11.41304348	Amplification	21

Non-Small Cell Lung Cancer	10.12782694	Amplification	103

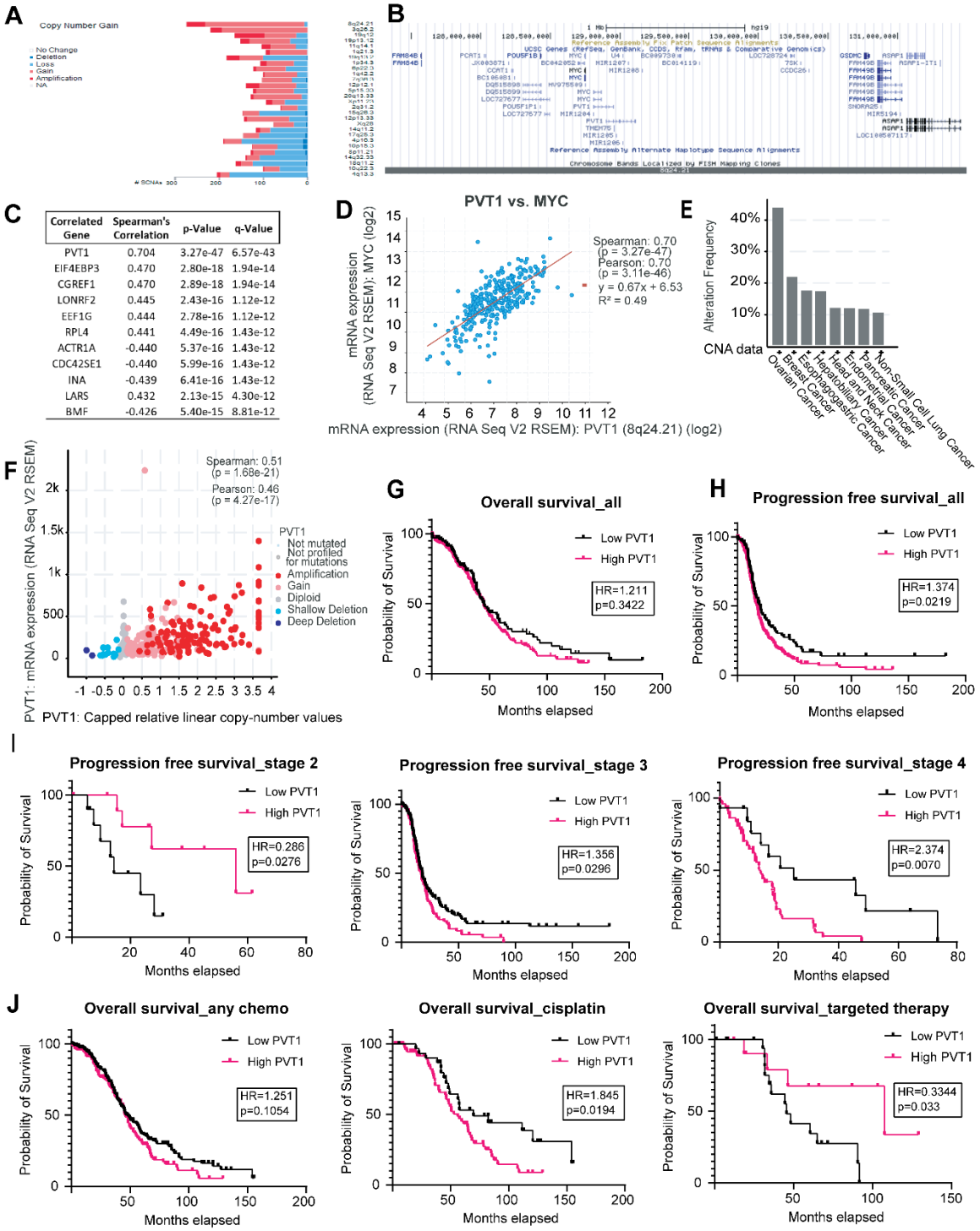

Figure 2. 1: PVT1 is amplified in ovarian cancer and impacts patient outcomes.
(A) PVT1 Chromosomal loci copy number gain in ovarian cancer patients from TCGA. (B) Genomic view of chromosome loci 8q24.21. (C) Top 10 correlated genes with MYC (Spearman's correlation). (D) MYC versus PVT1 RNA co-expression in the TCGA ovarian cancer patient datasets (Pearson factor of 0.70 - $P = 3.11 \times 10^{-46}$). (E) PVT1 copy number alterations in cancers (top 8) (F) PVT1 RNA expression versus copy number alterations (Pearson factor of 0.46 - $P = 4.27 \times 10^{-17}$). (G) Kaplan–Meier analysis for overall survival (log-rank statistics) for ovarian cancer from TCGA. (H) Kaplan–Meier analysis for progression-free survival (log-rank statistics) for ovarian cancer from TCGA. (I) Kaplan–Meier analysis for progression-free survival by stage (log-rank statistics) for ovarian cancer from TCGA (J) Kaplan–Meier analysis for overall survival by treatment (log-rank statistics) for ovarian cancer from TCGA (most patients with targeted therapy received bevacizumab).

2.2.2 PVT1 EXPRESSION LEVELS ARE ALTERED IN RESPONSE TO CELL DENSITY CHANGES

Given the significant amplification of PVT1 in ovarian cancer and the apparent clinical impact of increased expression of PVT1 (Figure 2. 1), we examined the effect of stressors, that may pertain to the metastatic trajectory of ovarian cancers and by altering PVT1 expression in different cell lines. We first evaluated PVT1 expression at baseline using primers spanning PVT1 transcript isoforms containing – exon 1-2, exon 2-3 and exon 6-7 (Figure B. 1B) in a panel of human ovarian cancer (OVCA) cells lines, normal immortalized fallopian tube epithelial cells (p211) and surface epithelial cells (IOSE80) (Figure 2. 2A). Whereas the detectable RNA levels varied between the cell lines, SK-OV3 cells exhibited the most robust levels of detectable PVT1 across all three exons of PVT1 (Figure 2. 2A) consistent with prior reports of high PVT1 levels in this cell line [58, 62, 71]. Using SK-OV3s, we next subjected the cells to a panel of pertinent ovarian cancer stressors including hypoxia, growth under anchorage independence and changes in cell density. We find that exposure to acute hypoxia (0.2%) for 24 h led to increased PVT1 RNA levels with reproducible and significant changes across exon 6-7 (Figure 2. 2B P =

0.0069) in SK-OV3 cells. Similarly, growing cells under anchorage independence led to fluctuations in levels of PVT1 as compared to growth under attached conditions, but this comparison did not reach statistical significance (Figure 2. 2C) in SK-OV3 cells. In contrast to the modest changes observed in response to the above-described stressors, we found reproducible and significant changes in PVT1 RNA levels upon changes in cell density (Figure 2. 2D). Specifically, switching cells between high- and low-density growth revealed marked and significant differences in PVT1 RNA levels, with increases across all exons seen in low density conditions (Figure 2. 2D ($P < 0.0001$)). Cell-cell contact, or absence thereof (low density) was confirmed by phase contrast microscopy and actin staining by immunofluorescence (Figure 2. 2D and Figure B. 2A). The effect of changing cell density on PVT1 levels was recapitulated in other cell lines as well, including human high grade serous OV90 cells across one exon (Figure B. 2B) and across exons 2-3 in the mouse ID8 cell line both in the presence and absence of Trp53 (ID8 Trp53-/-), the most commonly altered gene in OVCA (Figure 2. 2E and F) ($P = 0.0112$ and 0.0044 respectively).

However, in a subset of ovarian cancer cell lines including OVCAR3 and OVCA420, cell density alterations failed to induce changes in PVT1 expression (data not shown). We speculated that several serious ovarian cancer cell lines grow in clusters in the presence of cell-cell contacts, unlike SK-OV3 cells, which exhibit mesenchymal morphology and growth patterns [128]. To test if PVT1 changes in response to cell density were a feature of mesenchymal cells, we induced EMT in epithelial ovarian cancer OVCAR3 and OVCA420 cells with TGFβ-1. EMT was confirmed by increases in ZEB1 and SNAIL1 expression (Figure B. 2C). Post EMT mesenchymal cells indicated as

OVCAR3-M and OVCA420-M, were then subjected to either high density or low-density growth conditions followed by evaluation of PVT1 levels. We find that PVT1 levels across all exons were increased under low density in both OVCAR3-M and OVCA420-M cells (

Figure 2. *2*G and H) (OVCAR3: exon 1-2 P = 0.002; exon 2-3 P = 0.0013; exon 6-7 P = 0.0134; OVCA420: exon 2-3 P = 0.0229; exon 6-7 P = 0.0086), mimicking the cell density response in SK-OV3 and ID8 cells (Figure 2. 2D-F). We further expanded the cell density assay to DAOY (human medulloblastoma) and PC3 (human prostate cancer) cell lines and found similarly to SK-OV3 an increase of PVT1 expression under low density (Figure B. 2 and Figure 2. 2E). These data indicate that isogenic mesenchymal cells are particularly sensitive to cell density associated PVT1 changes as compared to their epithelial counterparts. To next evaluate if PVT1 levels correlate with a mesenchymal gene signature in ovarian cancer patients we examined a panel of EMT genes and PVT1 in the ovarian cancer TCGA data. We find a positive correlation between PVT1 and EMT associated genes (Figure 2. 2I) suggesting a strong correlation between post EMT regulation of PVT1 in ovarian cancer.

2.2.3 PVT1 IS DEPENDENT ON YAP1 IN OVARIAN CANCER

Cell density changes can lead to alterations in the cell cycle and concomitant changes to the Hippo pathway, a key modulator of cell survival in response to cellular stressors and a key negative regulator of YAP1 in various models [129-131]. Based on the cell density associated with changes in PVT1 levels, we first evaluated if SK-OV3 cells under high density retain active Hippo signaling, as measured by nuclear YAP1 localization [129, 130]. We found nuclear accumulation of YAP1 in cells plated under low density, with significant exclusion under high density (Figure 2. 3A and B P <0.0001). In

addition, YAP1 target genes including CTGF and CYR61 were significantly upregulated (CYR61 P <0.0001; CTGF P = 0.0084) under low density compared to high density

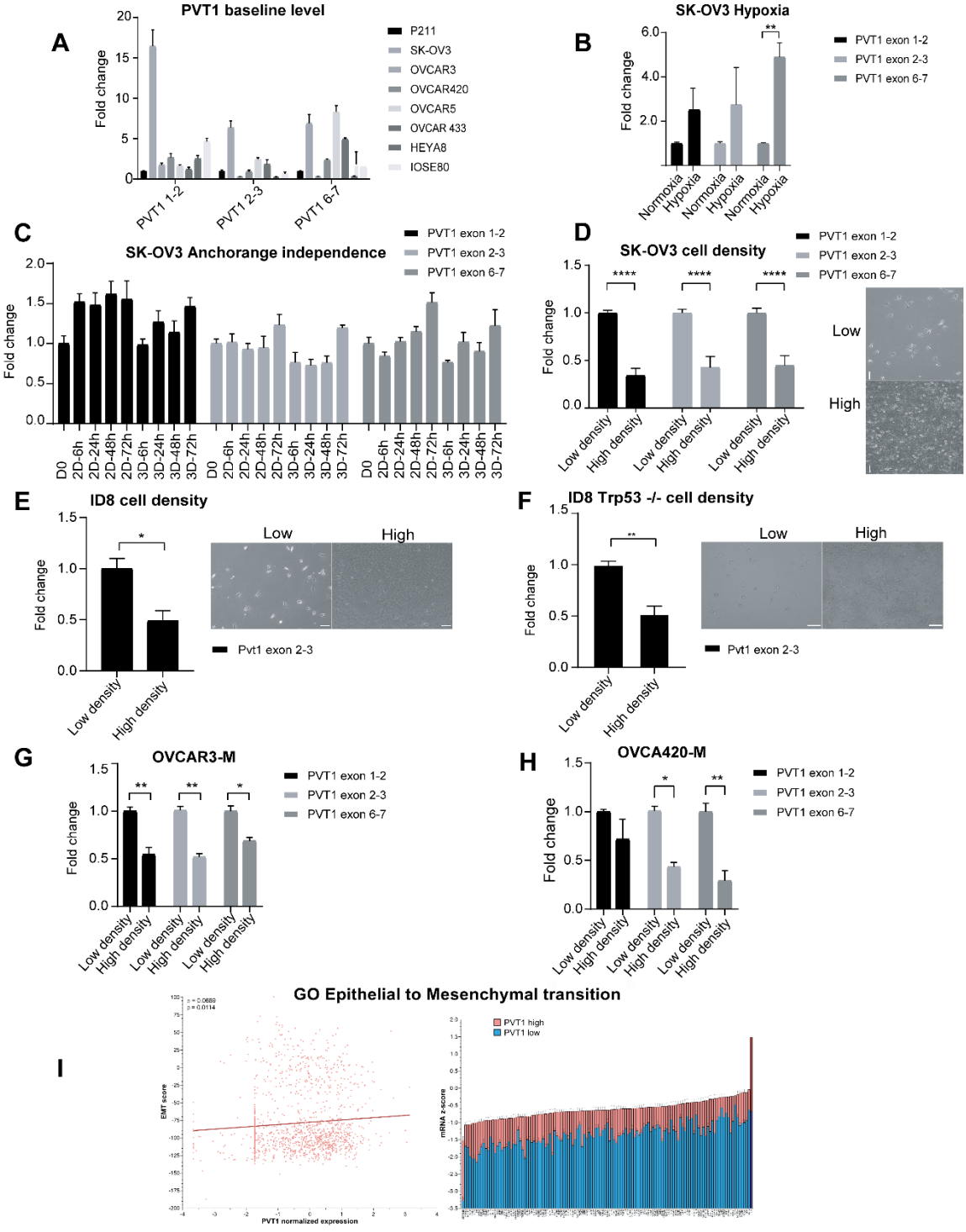

Figure 2. 2: PVT1 levels are altered in response to changes in cell density.
(A) RT-qPCR analysis of PVT1 levels at baseline in a panel of human ovarian cancer and ovarian surface epithelial cell lines normalized to non-oncogenic fallopian tube epithelial cell line p211 (N = 2). (B) RT-qPCR analysis of PVT1 levels in indicated cells grown under hypoxia (0.2% Oxygen) normalized to the respective levels in normoxia conditions (two-way ANOVA-Sidak multiple comparisons test: n = 3; exon 1–2, P = 0.3760; exon 2–3, P = 0.4203; exon 6–7, P = 0.0069; N = 3). (C) RT-qPCR analysis of PVT1 RNA expression under anchorage independence (N = 2) normalized to D0 (day 0 levels). (D) RT-qPCR analysis of PVT1 RNA at different cell densities (inset figures) in SK-OV3 cells normalized to the low density levels (two-way ANOVA-Sidak multiple comparisons test: exon 1–2, P < 0.0001; exon 2–3, P < 0.0001; exon 6–7, P < 0.0001; N = 6).

growth indicative of YAP1 function and activity under low density (Figure 2. 3C). To mechanistically extend the correlative observations of PVT1 RNA changes with YAP1 localization under low density, we tested if changing matrix rigidity would impact PVT1 RNA levels independent of the cell density associated changes.

We first utilized fibronectin conjugated polyacrylamide hydrogels with an elastic modulus of 0.5 kPa (soft), 8 kPa (stiff) and normal plastic plates (in the order of GPa). We find that increasing matrix rigidity leads to increased PVT1 RNA levels (Figure 2. 3D, 0.5 kPa vs 8 kPa: exon 1-2 P = 0.2523; exon 2-3 P = 0.6295; exon 6-7 P = 0.4684; 0.5 kPa vs 8 GPa: exon 1-2 P <0.0001; exon 2-3 P <0.0001; exon 6-7 P <0.0001; 8 kPa vs GPa: exon 1-2 P = 0,0002; exon 2-3 P <0.0001; exon 6-7 P = 0.0002). To confirm the direct correlation between YAP1 activity and substrate rigidity, CYR61 and CTGF mRNA expression was monitored and was found to be upregulated with increasing matrix rigidity (Figure 2. 3E). Serum is a known inhibitor of the Hippo pathway [132] and leads to increased YAP1 activity. To next test if depleting serum from low density cells when Hippo signaling is low and PVT1 is elevated, would lower PVT1 expression, we serum starved low density population of cells and evaluated PVT1 levels. We find that serum starved low density cells, further reduced their levels of PVT1 (Figure 2. 3F) and at the same time also reduced

YAP1 activity as indicated by the decrease of CYR61 and CTGF mRNA expression (Figure 2. 3G). These data point to regulation of PVT1 co-incidentally with, or dependent on YAP1 activity.

To directly test if PVT1 expression depended on YAP1 levels, we used shRNAs' to lower YAP1 levels (Figure 2. 3H) or inhibited the YAP1-TEAD association using the small molecule inhibitor verteporfin (Figure 2. 3I) [133]. We find that specific reduction of YAP1 or the use of verteporfin significantly reduced PVT1 levels compared to control cells (Figure 2. 3H and I). Based on this apparent dependency of PVT1 expression on YAP1 function, we next evaluated the clinical relevance of the PVT1-YAP1 relationship. We found a strong correlation between an inactive Hippo gene signature (where YAP1 target gene signatures are expressed), and PVT1 expression in TCGA ovarian cancer datasets (Figure 2. 3J). Together, these observations indicate a YAP1 dependency of PVT1 expression with functional correlations in ovarian cancer patients.

2.2.4 PVT1 CONFERS SURVIVAL AND PRO-METASTATIC ADVANTAGES TO OVCA CELLS IN VITRO AND IN VIVO

To test the effects of altering PVT1 levels on tumor cell behavior in vitro, we first used shRNAs (Figure 2. 4A and B) to reduce PVT1 levels in both human SK-OV3 cells and mouse ID8 Trp53 -/- cells. We found that lowering PVT1 resulted in reduced proliferation (MTT assay - $P < 0.0001$), migration potential of the tumor cells (transwell migration assay – $P = 0.003$) and clonogenic survival ($P = 0.0088$) in SK-OV3 (Figure 2. 4C-E). Similar results were obtained upon reducing PVT1 levels in mouse ID8 Trp53 -/- cells with shRNA, leading to significant reduction of proliferation (MTT assay – P

<0.0001), as well as migration potential (transwell migration assay – P = 0.0163)

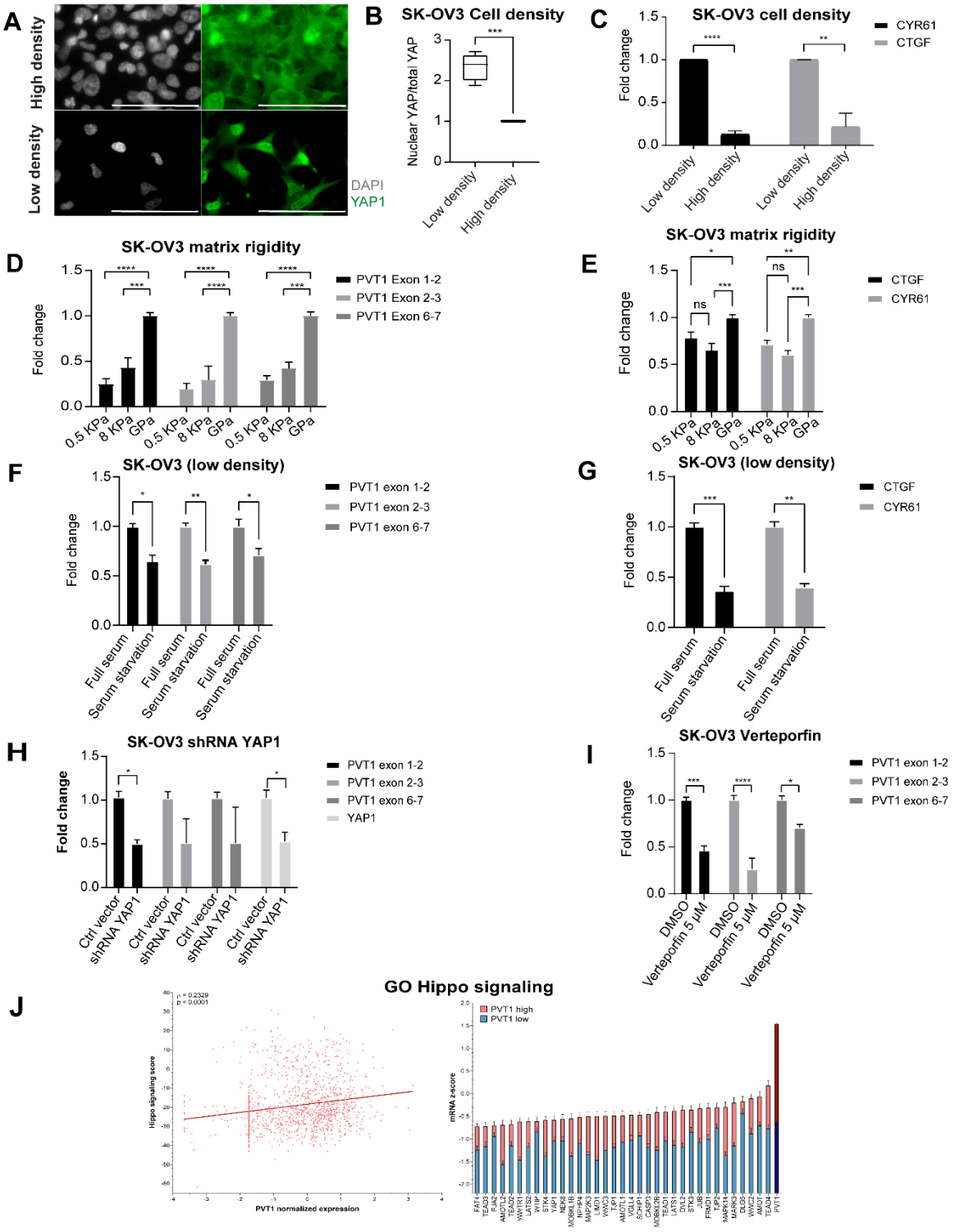

Figure 2. 3: PVT1 is dependent of YAP1.
A) Immunofluorescence of YAP1 under low and high density seeding in SK-OV3 cells (scale bar = 100 μm). (B) Quantification of the ratio of nuclear YAP to total YAP measured as an average intensity of total YAP in the nucleus/total YAP in the cell (unpaired two-tailed t test: number of cells = minimum 70 cells per biological trial, P = 0.0005; N = 3). (C) RT-qPCR of CTGF and CYR61 mRNA expression of cells grown in indicated cell densities normalized to levels in low density (unpaired two-tailed t test: CYR61, P < 0.0001; CTGF, P = 0.0084; N = 3). (D, E) RT-qPCR of (D) PVT1 or (E) indicated genes in cells grown under different matrix rigidity conditions normalized to levels of normal plastic plates (GPa) (two-way ANOVA-Tukey multiple testing; N = 3). (F) RT-qPCR of PVT1 RNA from cells grown at low density and under either full serum or serum starvation as indicated, normalized to levels under full serum (two-way ANOVA-Sidak's multiple testing; –N = 2; exon 1–2, P = 0.0102; exon 2–3, P = 0.0068; exon 6–7, P = 0.0251). (G) RT-qPCR of indicated YAP1 target genes (CTGF and CYR61) of cells grown at low density and under either full serum or serum starvation as indicated, normalized to levels under full serum (two-way ANOVA-Sidak multiple testing: CTGF, P = 0.0009; CYR61, P = 0.0011; N = 2). (H) RT-qPCR of PVT1 RNA in shRNA YAP1 or Ctrl vector cells normalized to levels in Ctrl vector cells (two-way ANOVA-Sidak multiple testing: exon 1–2, P = 0.0199; YAP1, P = 0.0258; N = 2). (I) RT-qPCR of PVT1 RNA expression in cells treated with 5 μM of Verteporfin or DMSO control normalized to levels in DMSO-treated cells (two-way ANOVA-Sidak multiple testing: exon 1–2, P < 0.0001; exon 2–3, P = 0.0002; exon 6–7, P = 0.0153; N = 3). (J) Correlation analysis of PVT1 expression with gene ontology of Hippo signaling pathway (z-score: value indicates the number of standard deviations away from the mean of mRNA expression in all profiled samples). Error bars are indicated as SEM. P-values are reported as ≥ 0.05 (ns), 0.01–0.05 (*), 0.001–0.01 (**), 0.0001–0.001 (***), and < 0.000

(Figure 2. 4F and G). These observations were complemented with siRNAs targeting exon 4-5, exon 6 and 2 different sequences of exon 9 in mouse ID8 Trp53 -/- cells (Figure B. 2F-G). Conversely, to evaluate the effect of increasing PVT1 expression, human PVT1 was cloned into a pcDNA3.1(+) vector and expressed in SK-OV3 cells. Exogenous PVT1 expression was evaluated by RT-qPCR and FISH (Figure 2. 4H and I). We found that overexpressing PVT1 resulted in increased proliferation (Figure 2. 4J.i – P <0.0001), increased migration (Figure 2. 4J.ii - P = 0.0007) and colony formation in a long term clonogenicity assay (Figure 2. 4J.iii - P <0.0001). These data suggest that while mouse and human PVT1 sequences vary between species [134], both have likely conserved functions [135] and promote tumorigenic behavior of cell lines.

Peritoneal growth and metastasis involves changes in cell-cell and cell-ECM contacts and survival of single cells that can attach to peritoneal organs [110, 136]. We therefore tested if reducing PVT1 levels altered intraperitoneal tumor growth. We reduced Pvt1 expression in ID8 Trp53-/- cells with shRNAs targeting Pvt1 (shPvt1 targeting two sequences of exon 9) or non-targeting control (shctrl) (Figure 2. 5A.i) and injected 5×10^6 viable cells within 96 h of Pvt1 knockdown into the peritoneal cavity of C57BL/6J mice (n= 12). Half the mice (n= 6) were sacrificed after 4 weeks to capture earlier effects of Pvt1 expression differences (mid-point of tumor growth as determined from pilot studies) and the remaining 6 mice were sacrificed at 8 weeks when they were moribund (Figure 2. 5B). At the 4-week time point, we found that mice receiving control cells had already developed small omental and intraperitoneal lesions with observable tumor growth (Figure 2. 5A. ii and iii) compared to mice receiving shPvt1 cells (Figure 2. 5A, black arrows). Omental weights were also measurably higher in mice receiving shctrl cells (Figure 2. 5A.iv). The reduction in peritoneal lesions persisted over time, as shPvt1 cells had visibly (Figure 2. 5B.i and ii) and measurably reduced overall tumor burden at 8 weeks (Figure 2. 5B.iii, n=6 for each group with one shctrl receiving mouse moribund prior to 8 weeks). Assessment of the omentum, ovary, and peritoneal wall, all primary target tissues of metastatic ovarian cancer, revealed that cells expressing Pvt1 (shctrl) had seeded the peritoneum efficiently and invaded into omental tissue (Figure 2. 5B.i,ii). In contrast, lowering Pvt1 in shPvt1 cells led to significantly lower amounts of ascites fluid (Figure 2. 5B.iv $P < 0.0001$) and abdominal girth (Figure 2. 5B.v $P < 0.0001$). These striking differences indicate that reducing Pvt1 leads to significantly less intraperitoneal tumor burden and demonstrates the critical role of PVT1 in ovarian cancer growth in vivo.

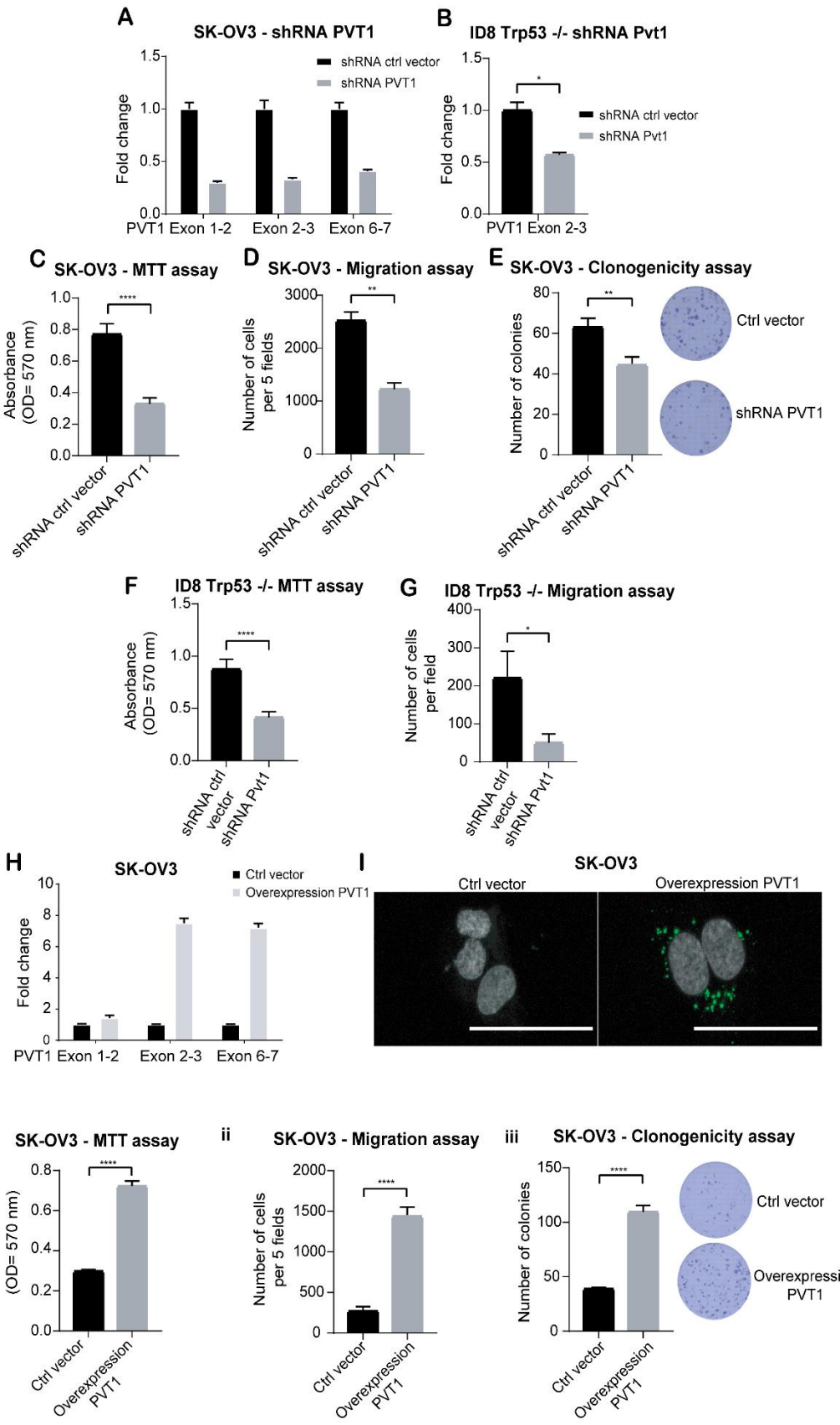
A
SK-OV3 - shRNA PVT1
shRNA ctrl vector
shRNA PVT1
Fold change
PVT1 Exon 1-2
Exon 2-3
Exon 6-7
B
ID8 Trp53 -/- shRNA Pvt1
shRNA ctrl vector
shRNA Pvt1
Fold change
PVT1 Exon 2-3
C
SK-OV3 - MTT assay
Absorbance (OD= 570 nm)
shRNA ctrl vector
shRNA PVT1
D
SK-OV3 - Migration assay
Number of cells per 5 fields
shRNA ctrl vector
shRNA PVT1
E
SK-OV3 - Clonogenicity assay
Number of colonies
Ctrl vector
shRNA PVT1
shRNA ctrl vector
shRNA PVT1
F
ID8 Trp53 -/- MTT assay
Absorbance (OD= 570 nm)
shRNA ctrl vector
shRNA Pvt1
G
ID8 Trp53 -/- Migration assay
Number of cells per field
shRNA ctrl vector
shRNA Pvt1
H
SK-OV3
Ctrl vector
Overexpression PVT1
Fold change
PVT1 Exon 1-2
Exon 2-3
Exon 6-7
I
SK-OV3
Ctrl vector
Overexpression PVT1
J
i
SK-OV3 - MTT assay
Absorbance (OD= 570 nm)
Ctrl vector
Overexpression PVT1
ii
SK-OV3 - Migration assay
Number of cells per 5 fields
Ctrl vector
Overexpression PVT1
iii
SK-OV3 - Clonogenicity assay
Number of colonies
Ctrl vector
Overexpression PVT1
Ctrl vector
Overexpression PVT1

Figure 2. 4: PVT1 confers increased migration invasion and survival advantages to OVCA cells.
(A, B) RT-qPCR of PVT1 in shPVT1 or shCtrl human SK-OV3 and mouse cells (ID8 Trp53−/−) (unpaired two-tailed t test: P = 0.0328) normalized to levels in shCtrl cells. (C) Absorbance values after completion of an MTT assay after 72 h of growth of shRNA PVT1 or shCtrl SK-OV3 cells (unpaired two-tailed t test: P < 0.0001; N = 12). (D) Transwell migration analysis of shRNA PVT1 or shCtrl SK-OV3 cells after 6 h of migration (unpaired two-tailed t test: P = 0.003; N = 3). (E) Numbers of colonies counted from a clonogenicity assay using shRNA PVT1 or shCtrl cells after 10 d (unpaired two-tailed t test: P = 0.0088; N = 6). (F) Absorbance values after completion of a MTT assay after 72 h using shRNA Pvt1 or shCtrl in mouse ID8 Trp53−/− cells (unpaired two-tailed t test: P < 0.0001; N = 12). (G) Transwell migration analysis of shRNA PVT1 or shCtrl mouse ID8 Trp53−/− cells after 6 h of migration (unpaired two- tailed t test: P = 0.0163; N = 3). (H) RT- qPCR of PVT1 in SK-OV3 cells expressing exogenous pcDNA3.1-PVT1 (overexpression PVT1) or ctl vector normalized to levels in control cells. (I) RNA-FISH images of cells expressing pcDNA 3.1 - PVT1 exogenously (overexpression PVT1) or ctl vector in SK-OV3 cells - scale bar 100 μm. (J) (i) Absorbance values after completion of a MTT assay after 72 h in indicated cells using PVT1 exogenously (overexpression PVT1) or ctl vector in SK-OV3 cells (Unpaired two-tailed t test: P < 0.0001; N = 12). (ii) Transwell migration analysis after 6 h of migration (unpaired two-tailed t test: P = 0.0007; N = 3) or (iii) Numbers of colonies counted from a clonogenicity assay in indicated cells (unpaired two-tailed t test: P < 0.0001; N = 6). P-values are reported as ≥0.05 (ns), 0.01–0.05 (*), 0.001–0.01 (**), 0.0001–0.001 (***), and < 0.0001 (****).

2.2.5 PVT1 IMPACTS GLOBAL GENE EXPRESSION AND REGULATES SENSITIVITY TO DOXORUBICIN

Because PVT1 is a lncRNA with likely broad range effects, we evaluated the impact of PVT1 on global gene expression by performing RNA sequencing in human SK-OV3 cells upon silencing PVT1 using siRNAs (siPVT1). We found that 450 protein coding genes were differentially expressed between control (Ctrl vector) and siPVT1 cells with 50 additional genes found to be non-protein coding. The top 50 differentially expressed genes include both downregulated and upregulated genes in response to reducing PVT1 by siRNAs (Figure 2. 6A). Lowered PVT1 levels were confirmed in the RNA-seq dataset (Figure B. 3A) as well as by RT-qPCR in biological replicates (Figure B. 3B). Furthermore, principal component analysis confirmed PVT1 siRNA status as a factor influencing the

gene expression profiles (Figure B. 3C). The gProfiler web analysis tool was used to investigate all significant genes (n=450). We find that PVT1 siRNA leads to substantial changes in the biological pathways associated with several stress responses and metabolism, specifically genes associated with doxorubicin metabolism (Figure 2. 6B and C). Gene set enrichment analysis confirmed the "doxorubicin metabolism process" (Figure 2. 6D) with genes such as AKR1C1, AKR1C2 and AKR1B10 being significantly downregulated in the siPVT1 samples (Figure 2. 6C).

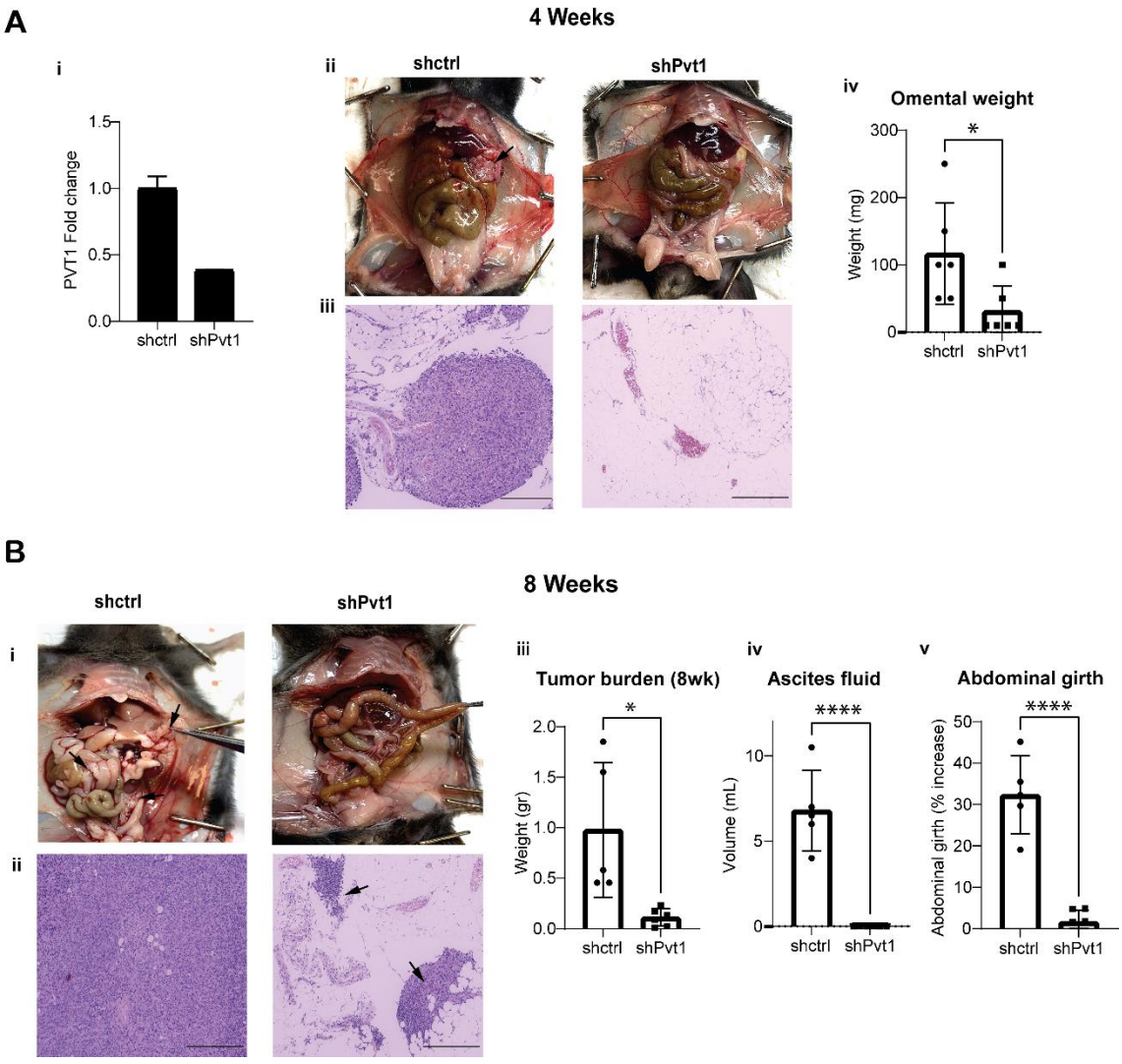

Figure 2. 5: Pvt1 promotes intraperitoneal tumor growth and metastasis in ovarian cancer. (A) (i) RT-qPCR of Pvt1 in shPvt1 or shCtrl mouse ID8 Trp53−/− cells normalized to levels in shctrl cells (N = 1). (ii) Representative mouse peritoneal images (above) and (iii) H&E-stained omental tissue sections after 4 wk following intraperitoneal injection of 5 × 10^6 shPvt1 or shCtrl mouse ID8 Trp53−/− cells. Black arrow in ii points to omental tumor/s. Scale bar = 275 μm. (N = 6 per group). (iv) Weight in grams of the omental tissue at 4 wk (unpaired two-tailed t test: P = 0.0325; N = 6). (B) (i) Representative mouse peritoneal images (above) and (ii) H&E-stained omental tissue sections after 8 wk after intraperitoneal injection of 5 × 106 shPvt1 or shCtrl mouse ID8 Trp53−/− cells. (iii) Weight in grams of the total tumor burden after 8 wk (Unpaired two-tailed t test: P = 0.0113; N = 6). (iv) Volume in mL of ascites fluid collected from mice after 8 wk (unpaired two-tailed t test: P < 0.0001; N = 6). (v) Percent increase in abdominal girth of mice measured from day 40 to day 60. (unpaired two-tailed t test: P < 0.0001; N = 5 for shCtrl and n = 6 for shPvt1).

Expression changes in these genes were also validated and confirmed by RT-qPCR for PVT1 knockdown (Figure 3. 4E). In a reciprocal fashion, overexpression of PVT1 led to increased expression of AKR1C1, AKR1C2 and AKR1B10 (Figure 3. 5F). We next tested if siRNA to PVT1 sensitized SK-OV3 cells to doxorubicin. We found a 1.5-fold reduction in the IC50 to doxorubicin in siPVT1 as compared to siControl SK-OV3 cells (Figure 3. 6G). Because human SK-OV3 cells do not express p53 [137], we evaluated if siPVT1 sensitized cells to doxorubicin even in the presence of p53 as the cell density dependent regulation of Pvt1 was largely p53 independent (Figure 3. 2E and F). To test this, we used mouse ID8-IP2 cells that express wild type Trp53 [138] and evaluated doxorubicin sensitivity. We found that siRNA to Pvt1 significantly lowered doxorubicin IC50 in these cells as well (Figure 2. 7H) indicating conserved functions across species and likely independent of the p53 status. These observations indicate a novel correlation between PVT1 and doxorubicin resistance in ovarian cancer.

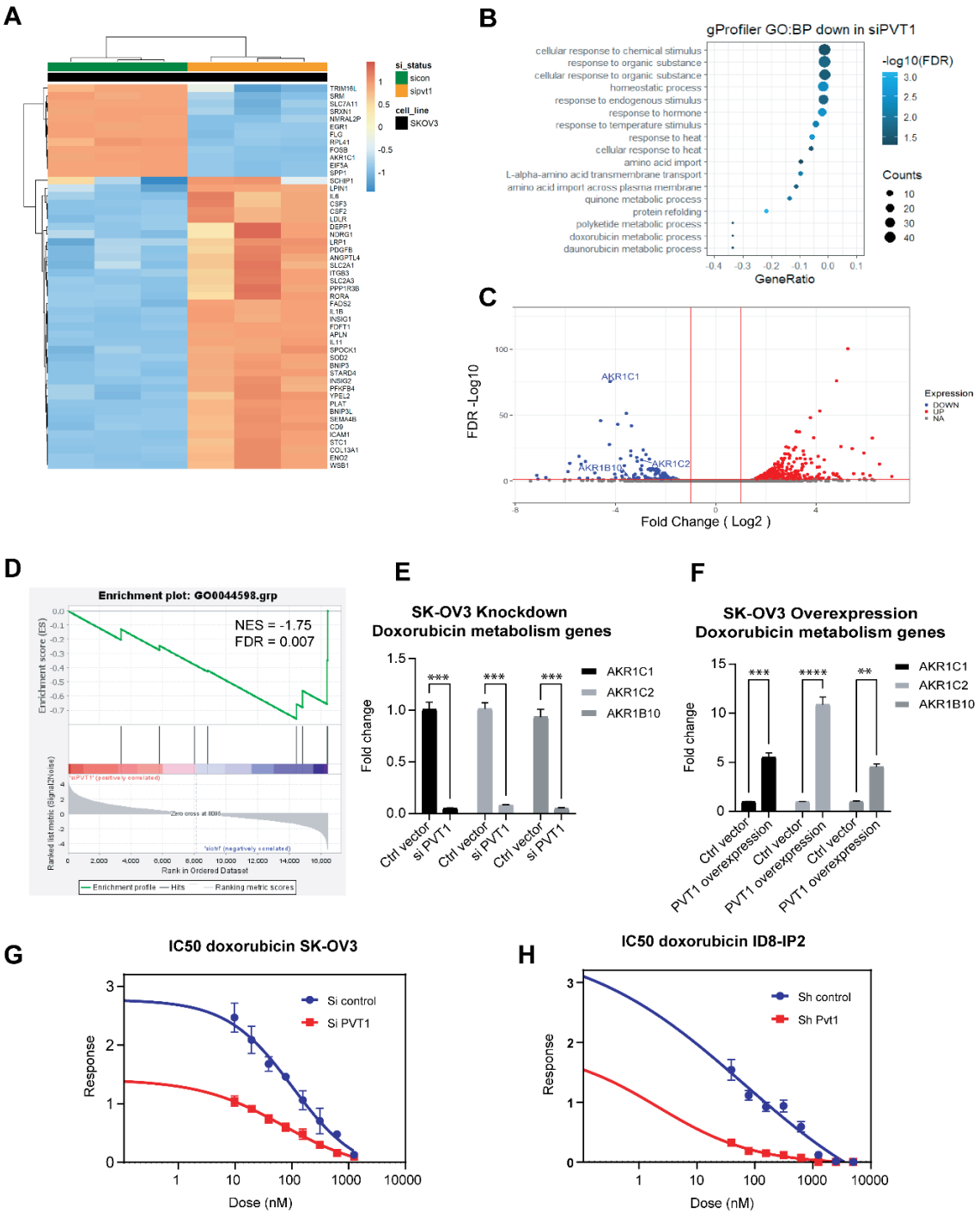

Figure 2. 6: RNA sequencing analysis reveals global transcriptional changes with specific changes to genes associated with doxorubicin resistance.

A) Heat map of the 50 top differentially expressed genes in siPVT1 versus Ctrl vector (sicon) in SK-OV3 cells. (B) gProfiler biological process enrichment analysis in siPVT1 SK-OV3 cells. (C) Volcano plot of doxorubicin resistance target genes (AKR1C1, AKR1C2, and AKR1B10) in siPVT1 SK-OV3 cells. (D) GSEA analysis of doxorubicin metabolic process enriched in siPVT1 SK-OV3 cells. (E) RT-qPCR of AKR1C1,

AKR1C2, and AKR1B10 in siPVT1 and siCtrl cells (two-way ANOVA-Sidak multiple testing: $P < 0.0001$; $N = 3$). (F) RT-qPCR of AKR1C1, AKR1C2, and AKR1B10 in PVT1 overexpression and Ctrl vector SK-OV3 cells (two-way ANOVA-Sidak multiple testing: exon 1–2, $P = 0.0005$; exon 2–3, $P < 0.0001$; exon 6–7, $P = 0.0018$; $N = 2$). (G) IC50 values to doxorubicin (nM) in control and PVT1 knockdown in human SK-OV3. (H) IC50 values to doxorubicin (nM) in control and PVT1 knockdown in mouse ID8-IP2 cells.

2.3 DISCUSSION

Here we demonstrate that PVT1 is a contextual oncogenic lncRNA, amplified along with MYC, and a prognostic indicator in ovarian cancers that is dynamically altered in expression primarily in response to cellular stressors. Notably cell density and matrix stiffness changes, both of which converge on pathways associated with YAP1, lead to changes in PVT1. Our study is the first to report such a mechanism and suggest a potential feedforward relationship between YAP1 and PVT1.

We find a strong correlation between PVT1 and MYC in ovarian cancer, as has been previously documented [119, 139, 140]. Genome-wide association studies have identified chromosome 8q24.21 as a cancer risk locus in multiple cancers [141], but also specifically in ovarian cancer [142, 143]. Besides harboring MYC, dysregulation and amplification of which is found in many human cancers [144], the 8q24.21 locus also harbors lncRNA PVT1 53 kb downstream of MYC. Bioinformatic analysis of TCGA datasets confirmed that chromosome 8q24.21 exhibits the highest copy number amplifications and that copy number alteration (CNA) frequency of PVT1 is among the highest in ovarian cancer (Figure 2. 1), highlighting the significance and relevance of PVT1 to this cancer. Furthermore, PVT1 expression is also correlated with patient survival outcomes. Ovarian cancers are mostly detected at an advanced stage which is one of the causes of poor survival. Our findings are consistent with other reports of higher PVT1 mRNA expression in stage 3 compared to other stages [59, 64]. Interestingly, the impact

of PVT1 expression differs for early-stage patients (stage II) where low PVT1 expression is correlated with poor progression-free survival (Figure 2. 2I). As ovarian cancers are marked by genome amplification, we investigated the correlation between PVT1 amplification and expression. Our data indicated a strong positive correlation between PVT1 amplification on chr 8q24.21 and expression in the TCGA cohort of primary patient tumors (Figure 2. 1F).

We demonstrate here for the first time that PVT1 RNA expression is modulated by cell density, hypoxia, and matrix rigidity in both human and mouse ovarian cancer cell lines. Increases in PVT1 RNA expression under hypoxia have been previously described in non-ovarian cancers [96, 145, 146], but were somewhat modest in the ovarian cancer cell line SK-OV3 we tested here (Figure 2. 2B). The most consistent and reproducible stressors that alter PVT1 expression are changes to cell density and mesenchymal status across cell lines, regardless of their baseline PVT1 levels (Figure 2. 2A). The Hippo signaling pathway is altered in ovarian cancer and causes increased nuclear YAP1 and tumorigenesis [147, 148]. Interestingly, modulation of PVT1 RNA expression after exposure to the stressors followed the RNA expression of YAP1 canonical target genes CTGF and CYR61 [131, 147], indicating a correlation between YAP1 nuclear localization and PVT1 RNA expression, that we also observed in patient data (Figure 2. 3J). PVT1 expression levels were directly dependent on YAP1 levels as investigated through YAP1 knockdown as well as through disrupting YAP/TEAD interaction [131, 149]. In the context of EMT, tumors often exhibit a spectrum of EMT states. Indeed, cell lines such as OVCAR3 and OVCA420 exhibit a more epithelial phenotype, whereas SK-OV3s exhibit a more intermediate to mesenchymal phenotype [150] and were found to be responsive to

cell density dependent changes in PVT1. YAP1 plays a dual role as both inducer and effector of EMT [151] and has been shown to translocate from the cytoplasm to the nucleus after EMT induction through TGFβ treatment [152]. Consistently, we observed a significant sensitivity of EMT induced cells to cell density dependent induction of PVT1 as seen in post EMT OVCAR3 and OVCA420 cells that were rendered sensitive to cell density dependent PVT1 changes (Figure 2. 2). Whereas it is likely that the PVT1 promoter possesses a TEAD binding site [153] the complex of YAP-TEAD on PVT1's promoter has not yet been reported and may involve indirect regulatory mechanisms as well. Little is known about modulators of PVT1 expression itself. Prior studies have demonstrated MYC [119], FOXM1 [154], STAT3 [155] and TP53 [40] as regulators that can bind to PVT1's promoter. For instance, it has been shown that FOXM1, which binds to PVT1's promoter to induce PVT1 RNA expression [154], is a downstream effector of YAP1 [156]. Thus, whether regulation is occurring here, directly or indirectly at the promoter remains to be determined. A surprising observation is the lack of a role of p53 in cell density dependent changes in Pvt1. Several prior studies have demonstrated PVT1 as a direct p53 target [40, 157]. Our findings suggest that the YAP1 dependent mechanism of PVT1 may be p53 independent.

Functional assays with gain or loss of PVT1 RNA expression demonstrated PVT1's role in promoting survival and chemo resistance in ovarian cancer cell lines and during intra peritoneal tumor growth, highlighting a pro-metastatic role for Pvt1 in ovarian cancer. Strikingly short-term knockdown of Pvt1 (within 96 hours of shRNA administration) was sufficient to cause a significant reduction in tumor burden, suggesting that transient dynamic changes occurring during disease progression may be adequate at impacting

disease outcomes. Our studies using the ID8Trp53-/- cells in immunocompetent models are also highly pertinent, as PVT1 was recently reported be significantly correlated with CD8 T- cell infiltration in several cancer types [158].

In the context of the models used here, transcriptomic analysis revealed a novel contribution of PVT1 in the regulation of aldo-keto reductases including AKR1C, AKR1C2, and AKR1B10. Aldo-keto reductases (AKR) have been demonstrated to regulate the metabolic processing of chemotherapeutic drugs such as doxorubicin, cisplatin, and paclitaxel, among others, and to cause chemo resistance in multiple cancers [159, 160]. AKR1B10 has been linked to cellular resistance to doxorubicin by inducing the conversion of doxorubicin to doxorubicinol, which is significantly less toxic [161]. AKR1B10 has also been reported to have an oncogenic role across different cancer types [162]. Indeed, lowering PVT1 increased the sensitivity to doxorubicin. Here again, the effect of Pvt1 on the sensitivity to doxorubicin was Trp53 independent. Therefore, targeting PVT1 to suppress the level of these AKR enzymes and consequently reducing inhibitory concentration of doxorubicin could pave the way toward minimizing the dose dependent cardiotoxicity of doxorubicin [163]. The exact mechanism by which PVT1 regulates AKRs expression remains to be elucidated.

In summary the broad impact of PVT1 on multiple pathways suggest that blocking PVT1 may be an attractive target to simultaneously suppress multiple pathways. Tools to silence lncRNAs are currently available (RNA interference, antisense oligonucleotides and genome editing (CRISPR/Cas9 system), but none have been clinically employed for PVT1 [164] and warrant further investigation for ovarian cancers.

2.4 MATERIAL AND METHODS

2.4.1 CELL LINES AND REAGENTS

Human ovarian cancer cell lines SK-OV3, PC3, DAOY and OV-90-CRL-11732™ were purchased from ATCC. OVCAR3 and OVCAR5 were obtained from NIH (NCI-60). OVCA420 and HeyA8 cells were a gift from Susan K Murphy. P211 were derived as described previously [165, 166], IOSE80 cells were received from the Canadian tissue bank. Mouse ovarian surface epithelial cell line ID8 and ID8-IP2's were a kind gift from Jill K. Slack-Davis and ID8 Trp53-/- were a kind gift from Iain McNeish. SK-OV3, OVCAR3, OVCAR5, OVCAR433, OVCA420, and HeyA8 were cultured in RPMI-1640 (10-040-CV; Corning) supplemented with 10% FBS (35-010-CV; Corning) and 100 U/ml penicillin, 100 μg/ml streptomycin at 37°C in a humidified incubator containing 5% CO_2. PC3 were cultured in Ham's F-12K (21127022; Gibco), whereas DAOY were cultured in EMEM (670086; Gibco), both supplemented with 10% FBS at 37°C in a humidified incubator containing 5% CO_2 . ID8 and ID8 Trp53−/− were cultured in DMEM (10-017-CV; Corning) supplemented with 4% FBS, 5 μg/ml insulin, 5 μg/ml transferrin, 5 ng/ml sodium selenite, and 100 U/ml penicillin, 100 μg/ml streptomycin at 37°C in a humidified incubator containing 5% CO 2. P211 and IOSE80 were cultured in DMEM supplemented with 10% FBS plus 100 U/ml penicillin, 100 μg/ml streptomycin. OV90 cells were cultured in a 1:1 mixture of MCDB 105 medium (M6395-1L; Sigma-Aldrich) and Medium 199 (M5017-10X1L; Sigma-Aldrich) containing 15% fetal bovine serum plus 100 U/ml penicillin and 100 μg/ml streptomycin. All cell lines were grown at 37°C in a humidified incubator containing 5% CO_2.

2.4.2 ANTIBODIES

Monoclonal mouse anti-YAP1 (sc-101199; Santa Cruz Biotechnology), Alexa Fluor 488 goat anti-mouse IgG, H+L (A11001; Invitrogen), and Alexa Fluor 488 Phalloidin (A12379; Invitrogen).

2.4.3 REAGENTS

PolyHema (P3932; Sigma-Aldrich) was used to generate low attachment plates for the anchorage-independent assay; fibronecti Recombinant Human Fibronectin, 8258-FN-050; R&D Systems); BSA (0903-5G; BioExpress); crystal violet (AA22866-14; VWR); PolyBrene (sc-134220; Santacruz Biotechnology); DMSO (BP231-100; Thermo Fisher Scientific); Paraformaldehyde (S898-07; Avantor); Triton-X100 (0694-1L; AMRESCO); absolute ethanol (Decon Laboratories); EMT was induced with 200 pM of Human recombinant TGF-β 1 (240-B; R&D Systems); verteporfin (SML0534-5MG; Sigma-Aldrich); Paclitaxel (328420010; Thermo Fisher Scientific); Doxorubicin (BP25176-10; Fisher Bioreagent); and Cisplatin (HY-17394; Medchem Express).

2.4.4 BIOINFORMATIC ANALYSIS

Somatic focal copy number gain events identified by Genomic Identification of Significant Targets in Cancer (GISTIC) for TCGA ovarian serous cystadenocarcinoma were recovered from firebrowse (http://firebrowse.org/). Genome data viewer was used to investigate genes located in chromosome 8q24.21 (https://www.ncbi.nlm.nih.gov/genome/gdv/). TCGA data for ovarian serous cystadenocarcinoma (TCGA, Firehose Legacy, RNA Seq V2, 307 samples) was recovered from cBioportal (https://www.cbioportal.org/) and used to investigate mRNA expression, mRNA co-expression and CNAs. Survival data was generated from KM Plotter using the

TCGA datasets, all patients and the best cutoff setting [126, 127]. Log-rank statistics were used to calculate the p-value (P) and Hazard ratio (HR).

Z-score normalized RNA-seq data from ovarian cancer patients were retrieved from TCGA datasets. Elements from the "GO Hippo signaling" and "GO Epithelial to Mesenchymal transition" gene sets [167] were filtered, and Hippo signaling score or EMT score was obtained from the direct sum of the gene's z-scores. Spearman rank correlation test was performed to assess whether PVT1 expression correlates to each obtained score. PVT1-high and -low groups of patients were also checked for mRNA expression of each gene within each gene set. Each group contained patients with the highest or lowest 10^{th} percentile of PVT1 expression.

2.4.5 GENERATION OF STABLE OVEREXPRESSION/KNOCKDOWN CELLS

For PVT1 and YAP1 knockdown, SK-OV3 and ID8 Trp53−/− cells were infected with 10 MOI of shRNAs or controls. All virus production was performed by the Functional Genomics Core of the Center for Targeted Therapeutics, University of South Carolina. In short, HEK293-FT cells, cultured in DMEM (high glucose) media with 10% FBS, 2 mM L-glutamine, penicillin (100 IU/ml), and streptomycin (100 mg/ml) were transiently transfected with specific lentiviral constructs and the packaging/envelope plasmids pMD2.G and psPAX2. The Virus-containing medium was collected at 48 and 72 h after transfection and centrifuged at 200g for 5 min at 4°C. The medium was filtered with 0.45-μm PES Syringe Filter and centrifuged at 21,000g for 16 h at 4°C. Pellets of lentivirus were re-dissolved in PBS at one-hundredth of the original volume. Lentiviruses were then diluted with fresh culture media to transduce target cells in the presence of 10 μg/ml PolyBrene (hexadimethrine bromide). Sequences for the multiple shRNAs are in Table 2.2.

Table 2.2: shRNA sequences

	shRNA - knockdown
Human PVT1	Exon 2: GAGCTTCGTTCAAGTATTT Exon 8: GAAATGTCCTCTCGCCTGC
Human control	SMARTvector Non-targeting hCMV-TurboRFP plasmid
Mouse pvt1	Exon 9: CGAGTGTGAAGGAGCGAGT Exon 9: TGACCTTATTGTAGACTAA
Mouse control	pHIV-Zsgreen plasmid
Human YAP1	CCGGCCCAGTTAAATGTTCACCAATCTCGAGATTGGTGAACATTTAAC TGGGTTTTTG CCGGGACCAATAGCTCAGATCCTTTCTCGAGAAAGGATCTGAGCTATT GGTCTTTTTG
Human control	TRCN scr PLKO.1 plasmid

For the overexpression construct, the complete linear RNA PVT1 sequence (1969 bp) was inserted in a pcDNA3.1(+) vector (SC1691 – GenScript). Control samples were achieved using an empty pcDNA3.1(+) plasmid. For YAP1, two shRNAs that include multiple transcript variants were inserted in a pLKO.1 vector (TRCN0000107265 and TRCN0000107268). Control samples were achieved using a TRCN scr PLKO.1 plasmid. The efficiency of knockdown or overexpression was performed by RT-qPCR (list of primers are in Table 2.3).

Table 2.3: Primer sequences

Gene ID	**Primer sequence (5'->3')**	**Specie**
RPL13a	Forw: AGATGGCGGAGGTGCAG Rev: GGCCCAGCAGTACCTGTTTA	Human
PVT1 exon 1-2	Forw: CACCTTCCAGTGGATTTCCTT Rev: GACAGGCACAGCCATCTT	
PVT1 exon 2-3	Forw: CTTCCTGGTGAAGCATCTGAT Rev: TTCAGCCTCCACTTAAAGTACC	
PVT1 exon 6-7	Forw: CTGTTTGCTTCTCCTGTTGC Rev: GAACTCCTCAGCCTCCAAG	

CTGF	Forw: GCGTGTGCACCGCCAAAGAT Rev: CAGGGCTGGGCAGACGAACG	
CYR61	Forw: CGCCTTGTGAAAGAAACCCG Rev: GGTTCGGGGGATTTCTTGGT	
YAP1	Forw: TGACCCTCGTTTTGCCATGA Rev: GTTGCTGCTGGTTGGAGTTG	
SNAIL 1	Forw: AAGATGCACATCCGAAGCCA Rev: CAGTGGGAGCAGGAGAATGG	
ZEB1	Forw: CTGCTCCCTGTGCAGTTACA Rev: GTGCACTTGAACTTGCGGTT	
AKR1C1	Forw: GTCCTGGCCAAGAGCTACAA	
	Rev: CGCACATTTCTGTTTAGGCCAT	
AKR1C2	Forw: ACGGAGTCATTGCCATTCAGA	
	Rev: CATGCAATGCCCTCCATGTTA	
AKR1B10	Forw: AGAAACTGGAGGGCCTGTAA	
	Rev: CATGCAATGCCCTCCATGTTA	
Rpl13a	Forw: CAAGGTTGTTCGGCTGAAGC Rev: GCTGTCACTGCCTGGTACTT	Mouse
Pvt1 exon 2-3	Forw: CACTGAAAACAAGGACCGAAAC Rev: ACAGACATTGGCAGTGGC	

For transient PVT1 knockdown using siRNA, SK-OV3 cells were cultured to 50% confluency in six well plates. Human siRNA for PVT1 was achieved using a mixture of four siRNA (ACCUAUGAGCUUUGAAUAA; GAGAACUGUCCUUACGUGA; CUUCAACCCAUUACGAUU and GUACGAACUUCAUCGCCCA) (smartpool R-029357-00-0005; Dharmacon). Control samples were achieved using Lincode Non-targeting Pool (D-001320-10-05; Dharmacon). 50 nM Pooled siRNA to human PVT1 or non-targeting siRNA from Dharmacon were used to transfect SK-OV3 cells for 48 h in full serum media carefully maintaining cell confluency to not exceed ~80%. Lipofectamine RNAiMAX Transfection Reagent (13778075; Thermo Fisher Scientific) was used to facilitate the transfection. This was followed by RNA extraction and verification of

knockdown using primers to PVT1. Similarly, mouse siRNA for PVT1 was achieved using a mixture of four siRNA (AAGUAUACCCUUUAAGCGU; CGAGUGUGAAGGAGCGAGU; GAUGUCACACAGACGAUAA; and UGACCUUAUUGUAGACUAA) (smartpool R-065730-00-0005; Dharmacon).

2.4.6 FUNCTIONAL ASSAYS

For Transwell migration assay, 8-μm-pore membranes (662638; Greiner Bio-One) were coated with 10 μg/ml fibronectin. A total of 20,000 cells were suspended in 100 μl serum-free medium and added to the upper chamber of each Transwell. The lower chamber was filled with 600 μl complete medium and incubated in a CO_2 incubator at 37°C for 6 h, after which fixation and staining occurred. For clonogenicity assay, 200 cells were cultured in each well of a six well plate in complete medium for 10 d, and after cells were fixed and stained. Imaging was performed using EVOS M7000 inverted microscope (Thermo Fisher Scientific). Quantitation was performed by manual counting. For MTT assay, 1,000 cells were seeded in a 96-well plate for 24 h, then a final concentration of 1 mM MTT was added. The plates were incubated in a 37°C incubator for 2.5 h, and DMSO was added to dissolve the formazan crystals. Absorbance was measured using a Synergy HT plate reader at 570 nm.

2.4.7 CELL DENSITY ASSAY

Low cell density was achieved in seeding 35,000 cells per well in a six-well plate. High density was achieved in seeding 210,000 cells per well in a 24-well plate.

2.4.8 HYPOXIA ASSAY

A hypoxia chamber was used to regulate the oxygen in the incubator to 0.2%. A total of 20,000 cells were seeded in 24 well plates for 24 h under hypoxia or normaxia.

2.4.9 MATRIX STIFFNESS ASSAY

Easy Coat hydrogels Softwell plates with 0.5 and 8 kPa were obtained from Matrigen (SW6-EC-0.5 EA, SW6-EC-8 EA) and regular six-well plates were coated with 10 μg/ml fibronectin before use. Cells were seeded at a density of 100,000 in a six-well plate and incubated for 24 h.

2.4.10 IC50 DETERMINATION

SK-OV3 and ID8-IP2-luc cells were cultured in 96-well plates at a density of 2,500 cells per well for 24 h. Then the medium was replaced with fresh medium containing Doxorubicin. After 72 h incubation with drugs, Sulforhodamine B (SRB, A14769-14, Alfa Aesar) assay was performed as previously described [168]. IC50 was calculated using IC50 calculator in Graph Pad Prism.

2.4.11 RNA FISH AND IMMUNOFLUORESCENCE

PVT1 visualization and localization were performed using a View-RNA cell plus assay probe for PVT1 (VA4-3082274-VCP; Thermo Fisher Scientific). The probe set per manufacturer covers region 423–1,392 and is designed to hybridize with human PVT1 specifically. Cells were seeded onto a NUNC eight-well chamber slide. DapB was used as a negative control, whereas GAPDH was used as a positive control. The procedure was performed as described by the manufacturer with no modifications. Images were acquired with a ZEISS LSM 800 confocal.

For immunofluorescence, cells were fixed in 4% paraformaldehyde for 15 min and permeabilized with 0.3% Triton X for 10 min at room temperature. Blocking was performed with 5% BSA, and cells were then incubated with a 1:100 dilution of anti-YAP1 overnight at 4°C. Then, the secondary antibody conjugated to Alexa 488 was used, at

1:200, for 1 h at room temperature in the dark. For actin, cells were stained for 20 min after fixation and permeabilization as above with Alexa 488 Phalloidin. Images were obtained using an EVOS M7000 microscope. Image J was used to perform the quantification.

2.4.12 ANIMAL STUDIES

All mouse studies were performed in accordance with the Institutional Animal Care and Use Committee at the University of Alabama Birmingham. Female C57BL/6J mice were obtained from the Jackson laboratory. Five million ID8-Trp53 -/- shCtrl and shPvt1 were intraperitoneally injected in mice (n=12 per group). Mice were monitored daily with girth and weight measurement taken weekly. Animals were sacrificed after either 4 weeks (n=6) or 8 weeks (n=6). At necropsy, ascites, if present, were collected and volumes measured, tumor weights in the omentum and other organs were recorded and collected when possible. For microscopic analysis of tissues, formalin-fixed tissues were processed, paraffin-embedded, and sectioned at 5 μm thickness and H&E stained at UAB's histology core.

2.4.13 RNA SEQUENCING

Library preparation was performed on purified, extracted RNA using a KAPA mRNA HyperPrep Kit (Kapa, Biosystems, Wilmington, MA) according to the manufacturer's protocol. High throughput sequencing with 75-bp single-end reads was performed on an Illumina NextSeq 550 using an Illumina NextSeq 500/550 High Output Kit. Reads were aligned to the human transcriptome GENCODE v35 (GRCh38.p13) using STAR and counted using Salmon [169, 170]. Normalization and differential expression analysis were performed using the R package DESeq2 v1.34 [171]. Genes where there were fewer than three samples with normalized counts less than or equal to five were

filtered out of the final data set. Benjamini-Hochberg-adjusted p-value of $p < 0.05$ and $\log_2$ fold change of ±1 were the thresholds used to identify differentially expressed genes between treatment conditions. Pathway enrichment analysis was performed with GSEA [172, 173].

2.4.14 STATISTICAL ANALYSIS

Xenograft data were analyzed using parametric statistics. All real time PCR's are relative quantitative RT-PCR's (hereby referred to as RT-qPCR) and are a combined quantitation of independent biological trials (indicated in legends) assayed in triplicate. All statistical analyses were conducted with GraphPad Prism Software and utilized test are referred in the figure's legend.

2.5 DATA AVAILABILITY

The authors confirm that all data supporting the findings of this study are available within the paper and supplementary data. RNA-seq data have been deposited in the NCBI-Gene Expression Omnibus (GEO) database under the accession ID GSE185933.

2.6 SUPPLEMENTARY INFORMATION

Supplementary Information is available at https://doi.org/10.26508/lsa.202201370.

2.7 AUTHOR CONTRIBUTIONS

K Tabury: conceptualization, resources, data curation, formal analysis, funding acquisition, validation, visualization, methodology, and writing—original draft, review, and editing. M Monavarian: formal analysis, validation, investigation, visualization, methodology, and writing—review and editing. E Listik: formal analysis and writing—review and editing. AK Shelton: formal analysis, methodology, and writing, review and

editing. AS Choi: methodology and manuscript editing. R Quintens: conceptualization, methodology, and writing, review and editing. RC Arend: resources. N Hempel: funding acquisition, methodology, and writing, review and editing. CR Miller: software, validation, investigation, methodology, and writing—review and editing. B Györrfy: formal analysis and writing, review and editing. K Mythreye: conceptualization, formal analysis, supervision, funding acquisition, investigation, visualization, methodology, project administration, and writing, review and editing.

2.8 ACKNOWLEDGEMENTS

Funding for this work was provided partially by NIH R01CA230628 to K Mythreye and N Hempel. B Györffy was supported by the FIEK_16-1-2016-0005 and 2020-4.1.1.-TKP2020 grants of the Ministry for Innovation and Technology in Hungary. We also thank Antonis Kourtidis for generous guidance on the FISH methodology, Jill K Slack-Davis, Iain McNeish, Amir Jazaeri, Susan K Murphy, and the Canadian Ovarian Tissue Bank for the gift of cell lines.

CHAPTER 3

LNCRNA PVT1 AS POTENTIAL BIOMARKER OF SURVIVAL AND TREATMENT RESPONSE IN UCEC PATIENTS[2]

Gynecological cancers are still leading cause of cancer related death in women worldwide. Early detection methods as well as treatment resistance remain challenging. Long non-coding RNAs PVT1 is an emerging therapeutic target with diagnostic and prognostic potential. We observed that high PVT1 RNA expression without copy number alteration has the most favorable patient survival outcome in Uterine Corpus Endometrial Carcinoma (UCEC). Favorable patient survival outcome is followed by PVT1 diploid with low RNA expression, which is enriched with estrogen signaling pathway. This sub-group of patients could positively respond to hormonal therapy. On the other hand, PVT1 Amplification with high RNA expression has the most unfavorable patient survival in UCEC and is enriched in cell cycle progression most probably through MYC and E2F target genes. Altogether, PVT1 is a potential biomarker of survival and treatment response in UCEC patients

[2] Kevin Tabury, Jürgen Claesen, Tarek Shazly, Karthikeyan Mythreye, Sarah Baatout, Roel Quintens. To be submitted

3.1 INTRODUCTION

The female reproductive system is complex and includes the ovaries, fallopian tubes, uterus, cervix, vagina and vulva. Cancers in these tissues, generally called gynecological cancers, accounted for over a million cases worldwide in 2020, of which more than six hundred thousand did not survive [174]. Each of these tissues have distinct genomic landscapes and functions. Consequently, a wide variety of cancer types can arise. In the USA, most frequently occurring gynecological cancers are: uterine corpus (also known as endometrial ~57 %), ovarian (~17 %), cervical (~12 %) and to a lesser extent, vagina (~7 %) and vulvar (~5 %) cancers. Despite endometrial cancer being the most diagnosed gynecological cancer, it is only ranked as the sixth leading cause of cancer related death in women worldwide while ovarian cancer is ranked fifth [43]. However, this distribution varies in the world due to several disparities between developed and developing countries [174].

Treatment strategies are cancer type-dependent. Yet, surgery is often the first line of treatment for gynecological cancers followed by chemotherapy [175], radiotherapy [176], targeted therapy [177] and immunotherapy [178]. Even though advancements in each of these treatments have been made, the lack of early diagnosis and treatment resistance continue to be challenging.

Long non-coding RNAs (lncRNAs) (RNA transcripts > 200 nucleotides that are not translated into functional proteins) have important roles in gene regulation [179], are implicated in tumorigenesis [180, 181] and are emerging as therapeutic targets with diagnostic and prognostic potential in, among others, gynecological cancers [182-184]. One of these lncRNAs of interest is plasmacytoma variant translocation 1 (PVT1). PVT1

is located within the well-known cancer risk region 8q24 and only 53 kb downstream from the key oncogene MYC [139]. PVT1 dysregulation and oncogenic function has been observed in multiple cancers, such as plasmacytomas, breast and prostate cancer amongst others [37, 185]. Furthermore, PVT1 transcript encompasses multiple miRNAs [42], expresses different splice variants [186] as well as different circular transcripts [153, 187]. Yet, little is known about PVT1 in gynecological cancers.

PVT1 function in gynecological cancers appears to be independent of the cancer type (Table A.1). PVT1 is involved in promoting cell proliferation, migration, invasion, cell cycle progression, apoptosis resistance, sphere formation, colony formation, epithelial-mesenchymal transition (EMT) and chemo resistance (Table A.1). An overview of function profiles linked to PVT1 per cancer type (endometrial, ovarian and cervical) can be found in Figure B. 4. In regards to vulvar and vaginal cancers, no studies on PVT1 have been published to the authors knowledge. However, PVT1 mechanistic seems to be cancer type dependent (Table A.1) and act mainly epigenetically through EZH2 or as a competitive endogenous RNA. It should be noted though that PVT1 has also been reported to have an anticancer activity [77]. Differences between PVT1 copy number amplification and RNA expression was first described in ovarian cancer [78]. PVT1 copy number and RNA expression are often studied in parallel with the oncogene MYC due to their proximity. However, the complete understanding of their interaction and correlation remains unclear. MYC and PVT1 correlation as well as their individual copy number versus RNA expression seem to be histopathological subtype and tissue reference dependent [79, 80]. Consequently, conclusions on the prognostic potential of PVT1 are contradictory [79, 81,

82], emphasizing the need of novel studies tackling the differences between copy number alteration and RNA expression.

This study summarizes the current knowledge on PVT1 in the main gynecological cancers (endometrial, cervical and ovarian) (Table A.1). To further understand PVT1's role in these cancers, a multi-platform analysis was performed on the corresponding TCGA data. We found that PVT1 is most clinically relevant in Uterine Corpus Endometrial Carcinoma and implicate PVT1 as a potential biomarker of survival and treatment response.

3.2 RESULTS

3.2.1 DESCRIPTIVE ANALYSIS OF THE SELECTED DATA

As all three-cancer types exhibited similar PVT1 functional profiles (Figure B. 4), we investigated if a common transcriptomic signature between these cancers and PVT1 exists. We also investigated the impact of PVT1 alterations and RNA expression on patient survival rates. PVT1 alterations and RNA expression were investigated in four gynecological tumor types: Uterine Corpus Endometrial Carcinoma (UCEC), Uterine Carcinosarcoma (UCS), Cervical Squamous Cell Carcinoma / Endocervical Adenocarcinoma (CESC) and Ovarian Serous Cystadenocarcinoma (OV) (sample size per tumor type can be found in Materials and Method). Genes mapping within amplicons are candidate oncogenes [188] and as PVT1 has been described as an oncogene [37], this study focuses on gain and amplification as alterations. Samples containing deep deletion and shallow deletion were discarded.

PVT1 alterations frequency per tumor type indicated that PVT1 is mostly altered in OV and UCS with gain as main alteration followed by amplification and to a lesser

extent diploid (no cna) (Figure 3. 1A). UCEC and CESC were mostly composed of PVT1 diploid followed by gain and to a lesser extent amplification as alterations (Figure 3. 1A). PVT1 RNA expression per tumor type showed no differences between UCEC and UCS but a significant increase of expression in CESC and OV compared to UCEC (Figure 3. 1B). After subdividing the samples per PVT1 alterations (Diploid, Gain and Amplification) for each tumor type, we also subdivided the sample per PVT1 RNA expression (high and low) (see Materials and Methods). An arbitrary 30% top – 30% bottom approach was adopted to derive the PVT1 RNA expression subgroups. Although the mean expression of PVT1 is highest in Amplification when compared to Diploid samples, similar PVT1 expression can be found across all alterations in each tumor type (Figure 3. 1C). Likewise, when subdividing the samples by PVT1 RNA expression (high versus low), all alterations are found in each subgroup for each tumor type except in CESC, for which PVT1 amplification is only present in the high PVT1 RNA expression subgroup (Figure 3. 1D). This indicates that observations based on PVT1 alteration might not necessarily correlate with observations based on PVT1 RNA expression. Hence the interest to investigate the differences between copy number alteration and RNA expression of PVT1.

3.2.2 PVT1 COPY NUMBER ALTERATIONS IS UNFAVORABLE TO PATIENT SURVIVAL IN UCEC

Kaplan-Meier survival curves for overall, disease-free and progression-free survival was performed based on PVT1 alterations per tumor type. OV and UCS survival rates were not significantly impacted by PVT1 alterations (Figure B. 5A and Figure B. 5B, respectively). Similarly, CESC survival rates were not affected except for PVT1 gain

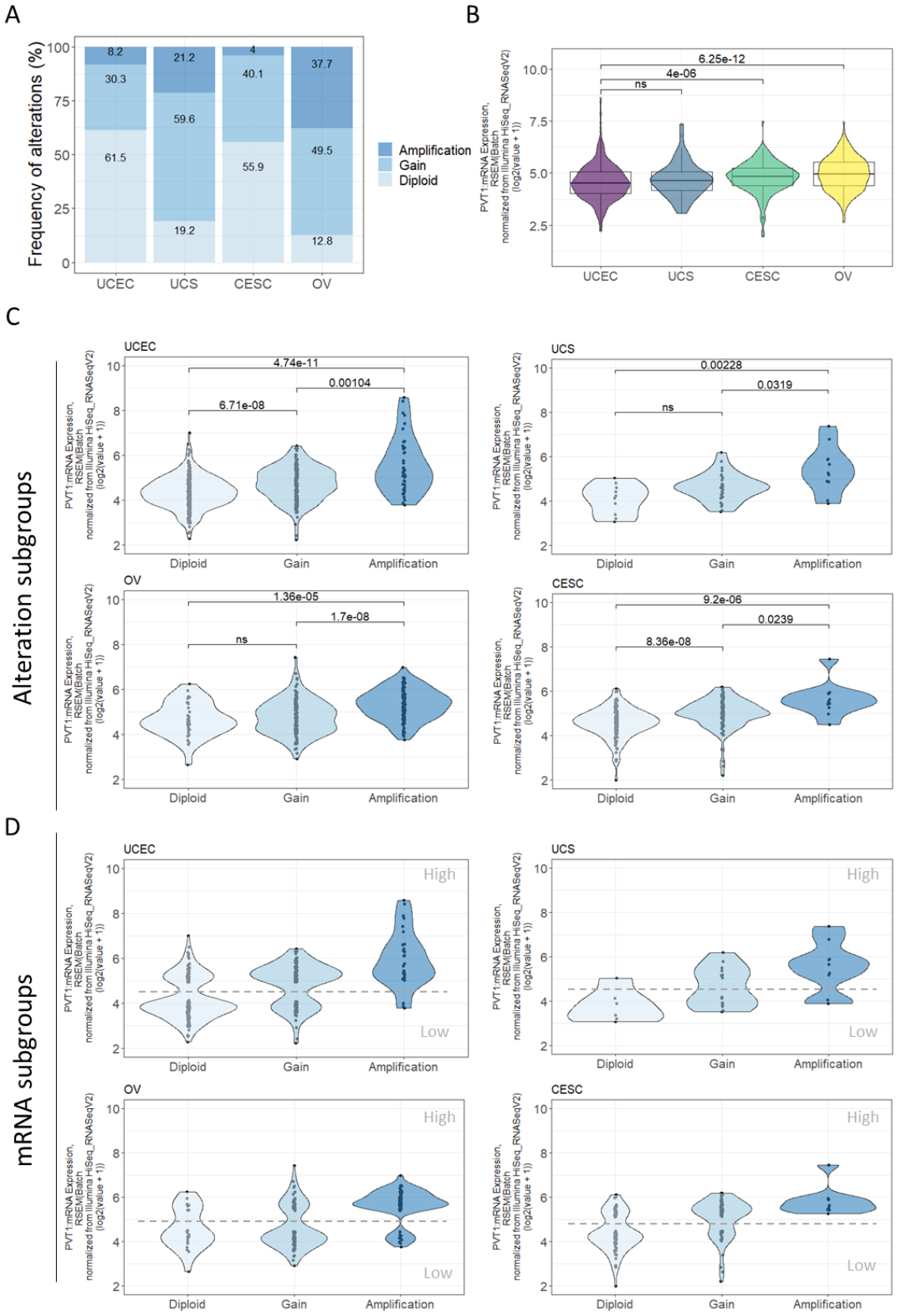
A
Frequency of alterations (%)
100
75
50
25
0
8.2
30.3
61.5
21.2
59.6
19.2
4
40.1
55.9
37.7
49.5
12.8
UCEC
UCS
CESC
OV
Amplification
Gain
Diploid
B
PVT1:mRNA Expression, RSEM(Batch normalized from Illumina HiSeq_RNASeqV2) (log2(value + 1))
6.25e-12
4e-06
ns
10.0
7.5
5.0
2.5
UCEC
UCS
CESC
OV
C
Alteration subgroups
UCEC
4.74e-11
0.00104
6.71e-08
UCS
0.00228
0.0319
ns
OV
1.36e-05
1.7e-08
ns
CESC
9.2e-06
0.0239
8.36e-08
Diploid
Gain
Amplification
D
mRNA subgroups
High
Low

Figure 3. 1: Descriptive analysis of selected data.(A) PVT1 alteration frequency per tumor type.
(B) PVT1 RNA expression per tumor type (Kruskal Wallis test followed by post-hoc Dunn test with Benjamini-Hochberg correction). (C) PVT1 RNA expression per alteration subgroups for each tumor type (Kruskal Wallis test followed by post-hoc Dunn test with Benjamini-Hochberg correction). (D) PVT1 RNA expression per RNA subgroups (30% top – 30% bottom sample selection) for each tumor type. ns = p-value: >0.05.

subgroup, which negatively affected progression-free survival (p-value = 0.030) (Figure B. 6). On the contrary, PVT1 alterations, both Gain and Amplification, reduced overall, disease-free and progression-free survival in UCEC (Figure 3. 2). PVT1 Amplification had a more significant negative impact on overall, disease-free and progression-free survival (Figure 3. 2 – p-value: 6.07e-06; p-value: <0.001; p-value: 3.03e-06, respectively) than PVT1 Gain (Figure 3. 2– p-value: 0.003; p-value: 0.036; p-value: <0.001, respectively).

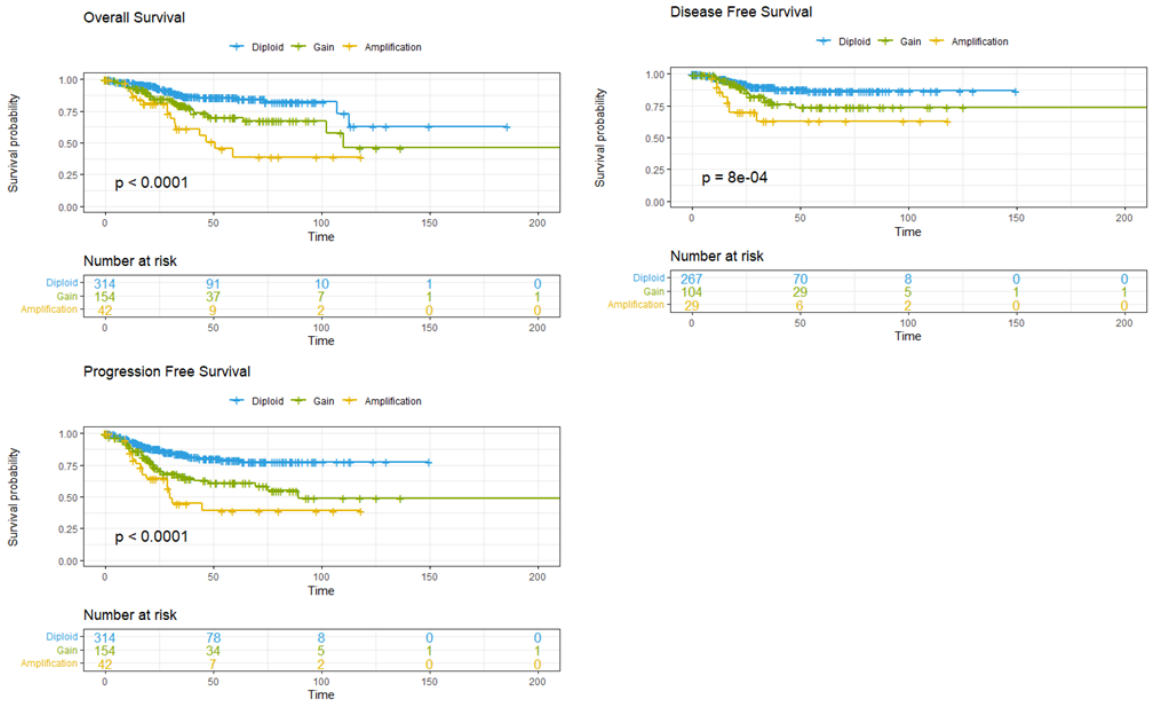

Figure 3. 2: PVT1 alterations is unfavorable to patient survival in UCEC.
Kaplan-Meier survival curves per alterations subgroups. Global log rank p-value are shown.

As cox proportional hazard model was used to compute significance in the survival curves, we verified the model assumptions using the Schoenfeld residuals (Figure B. 7).

Cox proportional hazard model was further used to investigate the effect of PVT1 alterations (denoted here as AMP_Status) and clinical parameters such as age, stage, grade and radiotherapy on patient survival in UCEC. For overall survival, multivariate analysis did not show any significant impact of PVT1 Amplification but showed that age (>60 years), stage (III and IV) and radiation therapy (no treatment) negatively influenced survival (Figure 3. 3A). Grade was discarded as Schoenfeld residuals were statistically significant (p-value < 0.05). Multivariate analysis did not show any significance of PVT1 Amplification for progression-free survival but showed significant negative impact of stage (III and IV) (Figure 3. 3B). Radiation therapy was discarded as Schoenfeld residuals were statistically significant. However, PVT1 Amplification stayed significant in multivariate analysis for disease-free survival together with stage (III) (Figure 3. 3C). As stage had the most significant effect, interaction between PVT1 Amplification and stage was evaluated. Although not statistically significant, an association between PVT1 amplification and stage III appeared to be possible (Figure 3. 3D). Schoenfeld residuals are available in Figure B. 7B.

Based on the above analysis, PVT1 copy number alterations are most clinically relevant in UCEC and that even few additional copies of PVT1 (=Gain) are sufficient to negatively affect patient survival rates. The lack of statistical significance of PVT1 copy number alterations in multivariate analysis indicates that the prediction capability of PVT1 copy number alterations is most probably associated with other predictors.

3.2.3 PVT1 AMPLIFICATION SUBGROUP IS ASSOCIATED WITH TYPE II ENDOMETRIAL CANCERS

To investigate differences between the tumor types and possibly understand why PVT1 is most clinically relevant in UCEC, we performed transcriptomic analysis. First, we investigated overlaps between significant down- and up-regulated genes per copy number alterations as well as per tumor types. We found that these overlaps are minimal (Figure B. 8). PVT1 Amplification subgroups showed PVT1 upregulation in UCEC, UCS and CESC but not OV because of the selected cutoff (see Materials and Methods - PVT1 in OV has a log2 fold change of 0.93 with an adjusted p-value of 1.2e-4) and SQLE was the only common upregulated gene (Figure B. 8A). PVT1 Gain subgroup did not show common down- or up-regulated genes between the tumor types (Figure B. 8B). In addition, PVT1 was not differentially expressed in the Gain subgroup (Figure B. 8B). We also investigated genes which were common to CESC, OV and UCS but not to UCEC. However, no such genes were found in PVT1 Amplification subgroup and only PKHD1L1 was upregulated in CESC, OV and UCS, but not in UCEC when considering PVT1 Gain subgroup (Figure B. 8B). Second, a pathway enrichment analysis on the unique differently expressed genes per tumor types showed distinct pathway enrichments for each tumor type (Figure B. 9 and Figure B. 10). Amongst the most significantly downregulated pathways in UCEC (PVT1 Amplification subgroup) was the estrogen signaling pathway (p-value: 2.043e-6). Estrogen signaling plays a central role in gynecological cancers and it is generally accepted that estrogen and progesterone receptor expression is associated with favorable outcome in ovarian [189], cervical [190] and endometrial cancer [191].

A

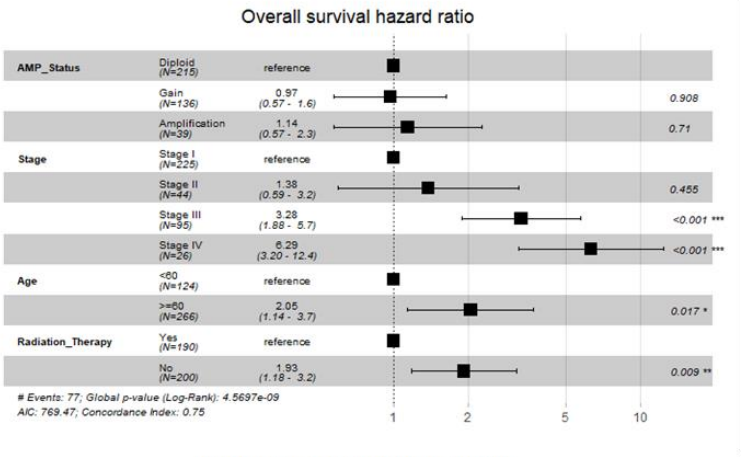

B

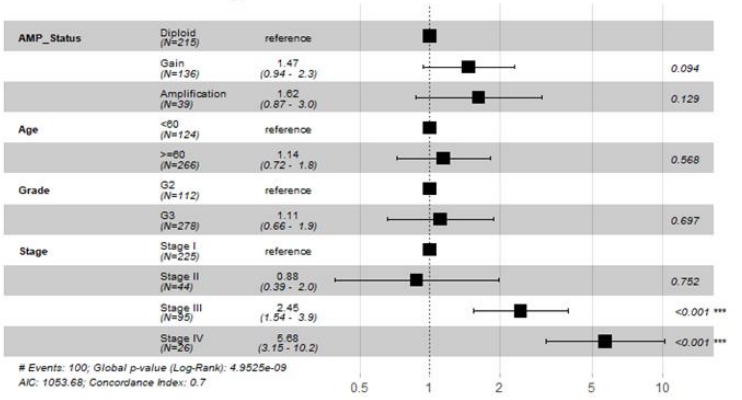

C

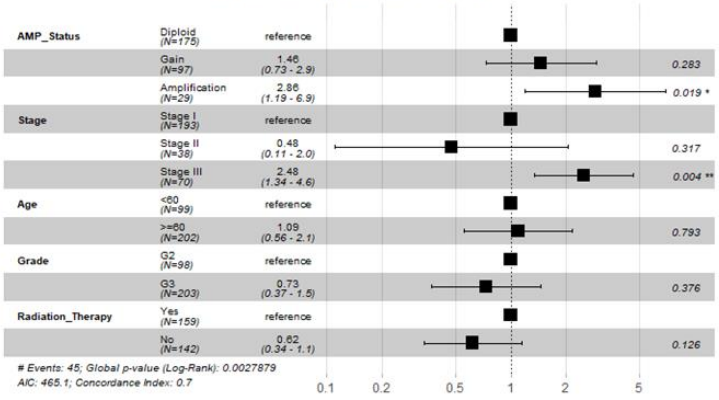

D

Survival	AMP_Status	pvalue
Overall survival	Amplification:StageIII	0.106
Overall survival	Amplification:StageIV	0.1637
Progression free survival	Amplification:StageIII	0.0688
Progression free survival	Amplification:StageIV	0.4612
Disease free survival	Amplification:StageIII	0.0508
Disease free survival	Amplification:StageIV	NA

Figure 3. 3: Effect of clinical parameters on survival curves.
(A) Multivariate analysis of PVT1 alterations, stage, age and radiotherapy on overall survival. (B) Multivariate analysis of PVT1 alterations, grade, age and stage on progression-free survival. (C) Multivariate analysis of PVT1 alterations, stage, age, grade and radiotherapy on disease-free survival. (D) Interaction between PVT1 amplification and stage in overall, progression-free and disease-free survival.

Both estrogen receptor alpha (encoded by ESR1 gene) and progesterone receptor (encoded by PGR gene) were downregulated in UCEC (PVT1 Amplification subgroup only) but not in the other tumor types at the RNA level (both p-value: <0.0001) (Figure 3. 4A) and at the protein level for ESR1 (p-value: 1.6e-5) but only slightly for PGR (p-value: 0.06) (Figure 3. 4B) (Figure B. 11). Because differential expressed genes (DEG) analysis depends on significant cutoffs and the statistical test used, we extended our analysis using gene set enrichment analysis (GSEA), an unbiased, threshold-free procedure [172]. GSEA also showed a downregulation of estrogen response pathway (early and late) in PVT1 Amplification subgroup in UCEC (Figure 3. 4C) but not in the other tumor type. An overview of GSEA analysis per subgroup and tumor type can be found in Figure B. 12 and Figure B. 13. Besides the downregulation of estrogen response pathways, PVT1 amplification subgroup in UCEC showed an upregulation of cell cycle progression (Figure B. 12) and cell cycle related cancer hallmarks such as E2F targets, G2M checkpoint, MYC targets V1 and V2 as well as mitotic spindle (Figure B. 12). Therefore, UCEC tumors harboring amplified PVT1 appears to drive cell cycle independently of estrogen receptor alpha, indicative that hormonal therapy would be inefficient to these patients [191]. Furthermore, loss of estrogen receptor alpha has been correlated with the more aggressive and poorer survival outcome non-endometrioid endometrial cancer subtype (NEEC - type II endometrial cancers) [191]. NEEC has been characterized by O'Mara et al. [192]. Using their 145 genes, we found that PVT1 Amplification subgroup corresponded to NEEC while

PVT1 Diploid subgroup corresponded to EEC (endometrioid endometrial cancer) (Figure 3. 4D). PVT1 Gain subgroup resulted in a similar association to NEEC (Figure B. 14A). This might indicate that PVT1 Gain and Amplification is potentially sufficient to identify type II endometrial cancer patients in UCEC.

Third, we compared the DEG to favorable and unfavorable prognostic markers of each cancer type (cervical, endometrial and ovarian cancer) and observed that overlaps were only occurring in UCEC (Figure B. 14B and Figure B. 15A). In PVT1 Amplification subgroup, 182 favorable prognostic markers were downregulated while 138 unfavorable prognostic markers were upregulated (Figure B. 14B). GSEA further confirmed our observation (Figure 3. 4E). In PVT1 Gain subgroup 48 favorable prognostic markers were downregulated while 94 unfavorable prognostic markers were upregulated (Figure B. 15A) which was also observed with GSEA (Figure B. 15B).

Altogether, we suggest that PVT1 Amplification subgroup in UCEC corresponds to NEEC, combines the highest number of unfavorable prognostic markers with the lowest number of favorable prognostic markers and drives cell cycle independently of estrogen receptor alpha resulting in patient poor survival. However, the exact role and mechanism of PVT1 warrants further investigation.

3.2.4 PVT1 HIGH RNA EXPRESSION IS UNFAVORABLE TO PATIENT SURVIVAL IN UCEC

Kaplan-Meier survival curves for overall, disease-free and progression-free survival were performed based on PVT1 RNA expressions per tumor type (30% top – 30% bottom sample selection). OV and CESC survival rates were not significantly impacted by PVT1 alterations (Figure B. 16A and B). High PVT1 expression was significantly reducing

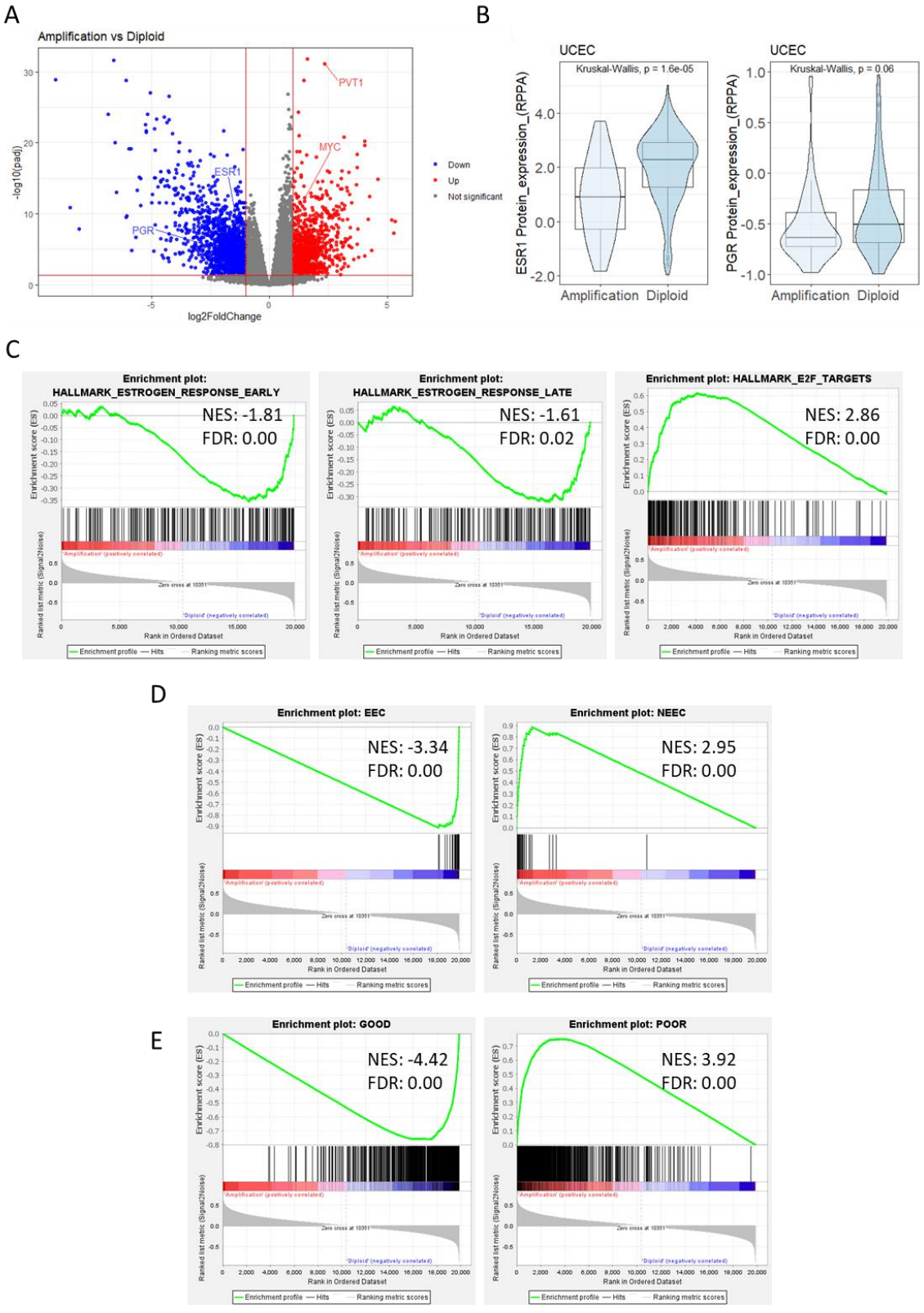
A
Amplification vs Diploid
PVT1
MYC
ESR1
PGR
Down
Up
Not significant
-log10(padj)
log2FoldChange
B
UCEC
Kruskal-Wallis, p = 1.6e-05
ESR1 Protein_expression_(RPPA)
Amplification
Diploid
UCEC
Kruskal-Wallis, p = 0.06
PGR Protein_expression_(RPPA)
Amplification
Diploid
C
Enrichment plot: HALLMARK_ESTROGEN_RESPONSE_EARLY
NES: -1.81
FDR: 0.00
Enrichment plot: HALLMARK_ESTROGEN_RESPONSE_LATE
NES: -1.61
FDR: 0.02
Enrichment plot: HALLMARK_E2F_TARGETS
NES: 2.86
FDR: 0.00
Enrichment score (ES)
Ranked list metric (Signal2Noise)
Rank in Ordered Dataset
Enrichment profile
Hits
Ranking metric scores
D
Enrichment plot: EEC
NES: -3.34
FDR: 0.00
Enrichment plot: NEEC
NES: 2.95
FDR: 0.00
E
Enrichment plot: GOOD
NES: -4.42
FDR: 0.00
Enrichment plot: POOR
NES: 3.92
FDR: 0.00

Figure 3. 4: Estrogen receptor alpha is downregulated in PVT1 amplification subgroup in UCEC.
(A) Volcano plot of DEG for PVT1 amplification versus diploid subgroup in UCEC. (B) ESR1 and PGR protein expression of PVT1 amplification versus diploid subgroup in UCEC (Kruskal Wallis test). (C) GSEA for estrogen response signatures and E2F targets signature in PVT1 amplification versus diploid subgroup in UCEC. (D) GSEA of endometrioid endometrial cancer (EEC) and non-endometrioid endometrial cancer (NEEC) for PVT1 amplification versus diploid subgroup in UCEC. (E) GSEA for favorable (GOOD) and unfavorable (POOR) prognostic markers in PVT1 amplification versus diploid subgroup in UCEC.

disease-free survival in USC patients (p-value = 0.034; (Figure B. 17). An indication of unfavorable impact on patient survival rate in UCEC for high PVT1 RNA was seen, although not statistically significant (Figure 3. 5). Schoenfeld residuals to verify cox proportional hazards model assumption can be found in Figure B. 18A.

The impact of the used threshold method was investigated and a 20% top – 20% bottom approach was also tested. Under this condition, PVT1 high RNA was unfavorable for disease-free and progression-free survival in UCEC but not overall survival (Figure 3. *6* - p-value: 0.048; p-value: 0.0077; p-value: 0.31 respectively). Schoenfeld residuals to verify cox proportional hazards model assumption can be found in Figure B. 18B. No significant changes were observed in CESC (Figure B. 19A) and OV (Figure B. 19B). Yet, PVT1 high RNA became unfavorable for progression-free survival in UCS (Figure B. 19C). This indicates that our observation is threshold dependent.

Cox proportional hazard model was further used to investigate the effect of PVT1 RNA expression (denoted here as PVT1_status) and clinical parameters such as age, stage, grade and radiotherapy on survival in UCEC. For overall survival, multivariate analysis did not show any significance of PVT1 status, but showed that age (>60 years), radiation therapy (no treatment) and stage (III and IV) negatively influenced survival curves (Figure 9A). Grade was discarded as Schoenfeld residuals were statistically significant.

Multivariate analysis showed significant negative impact of high PVT1 high RNA expression and stage (III and IV) for progression-free survival (Figure 9B). Age was discarded as Schoenfeld

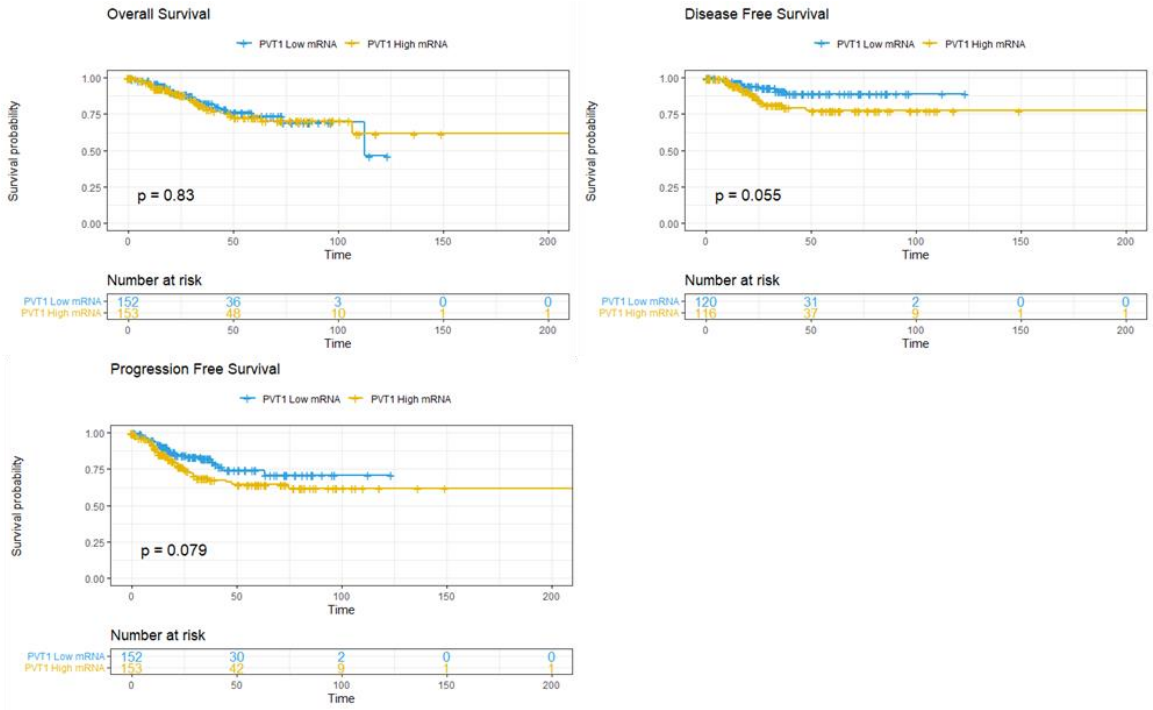

Figure 3. 5: Kaplan-Meier survival curves per RNA subgroup in UCEC (30% top – 30% bottom sample selection).
Global log rank p-value are shown.

residuals were statistically significant. PVT1 high RNA expression as well as stage (III) stayed significant in multivariate analysis for disease-free survival (Figure 9C). However, interaction between PVT1 high RNA expression and stage was not statistically significant. Schoenfeld residuals are available in Figure B. 20.

In summary, our analysis indicates that PVT1 high RNA expression is unfavorable to patient survival in UCEC. However, this observation is threshold dependent.

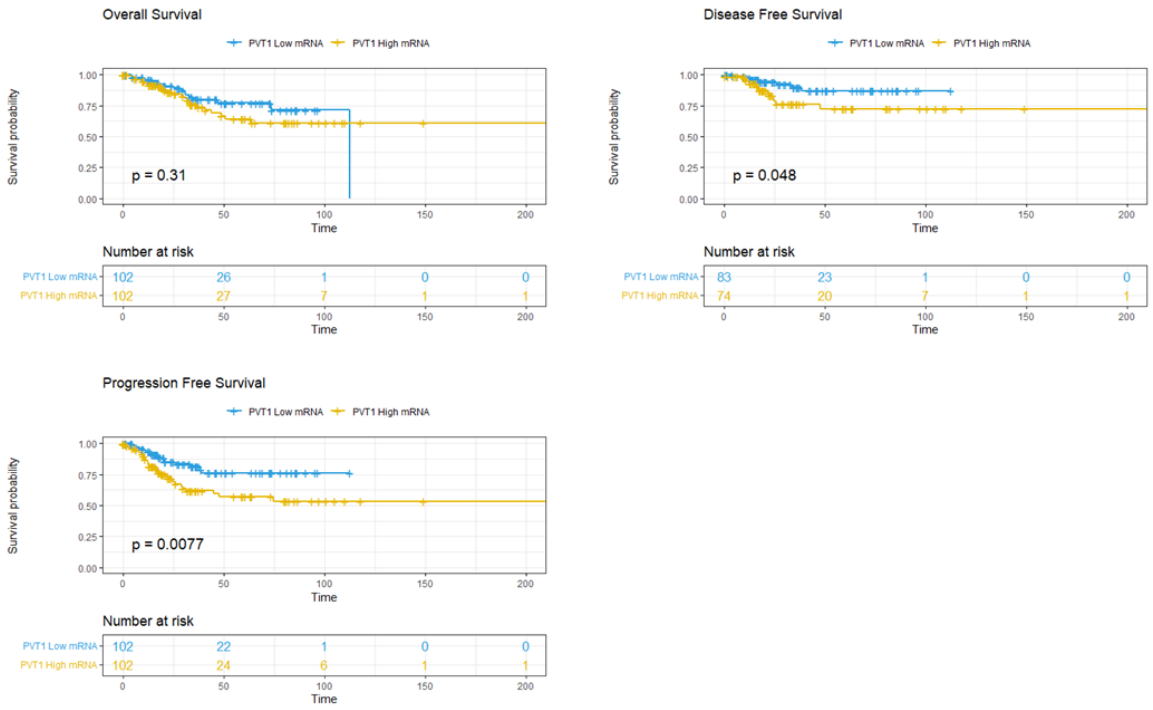

Figure 3. 6: PVT1 high RNA expression is unfavorable to patient survival in UCEC. Kaplan-Meier survival curves per RNA subgroup in UCEC (20% top – 20% bottom sample selection). Global log rank p-value are shown.

3.2.5 HIGH PVT1 RNA SUBGROUP HAS A LESS PRONOUNCED ASSOCIATION WITH TYPE II ENDOMETRIAL CANCERS

To further investigate the role of PVT1 RNA expression, we performed a transcriptomic analysis per PVT1 RNA subgroups. As the 30% top – 30% bottom sample selection did not reveal significant impact on the survival curves, we continued with the 20% top – 20% bottom sample selection (Figure 3. 8A). First, we investigated overlaps between significant down- and up-regulated genes per RNA subgroup as well as per tumor types. We found that 4 genes (PVT1, TOP1MT, MYC, GLI4) were commonly upregulated and 2 genes (GALNT5, ZPLD1) were commonly downregulated in high PVT1 RNA subgroup (Figure B. 21). Furthermore, 5 genes (RPL8, NDUFB9, RPL36, EEF1D, MYBPHL) were commonly upregulated and 7 genes (VCAN, ALOX15, MMP10, GDA,

CYP1B1, MFAP3L, INHBA) were commonly downregulated in all tumor types except in UCEC for the high PVT1 RNA subgroup (Figure B. 21).

Second, a pathway enrichment analysis on the unique differently expressed genes per tumor type, was performed (Figure B. 22). No upregulated estrogen signaling pathway was observed in low PVT1 RNA subgroup in UCEC and ESR1 was also not differentially expressed at the RNA level (p-value: 0.96) (Figure 3. 8B). Although ESR1 expression is strongly associated to single sample GSEA scores of both hallmarks for estrogen response pathway [193], GSEA did show upregulation of the estrogen response pathway (early and late) in low PVT1 RNA subgroup unique to UCEC (Figure 3. 8C). An overview of GSEA analysis per subgroup and tumor type can be found in Figure B. 23 and Figure B. 24.

We also investigated the association between PVT1 RNA subgroup with the endometrial subtypes. We found that, similarly to PVT1 Amplification subgroup, PVT1 high RNA subgroup is associated with NEEC (Figure 3. 8D). Yet, the association is less pronounced.

Third, we compared the DEG to favorable and unfavorable prognostic markers of each cancer type (cervical, endometrial and ovarian cancer) and observed that overlaps were mostly occurring in UCEC and UCS (Figure B. 25). More precisely, in PVT1 high RNA subgroup, 15 favorable prognostic markers were downregulated while 16 unfavorable prognostic markers were upregulated in UCEC. However, GSEA did not show significant enrichment in these prognostic signatures.

Altogether, our analysis might suggest that PVT1 high RNA subgroup in UCEC corresponds to NEEC in combination with some upregulated unfavorable prognostic markers and some downregulated favorable prognostic markers. Yet, this observation is

A

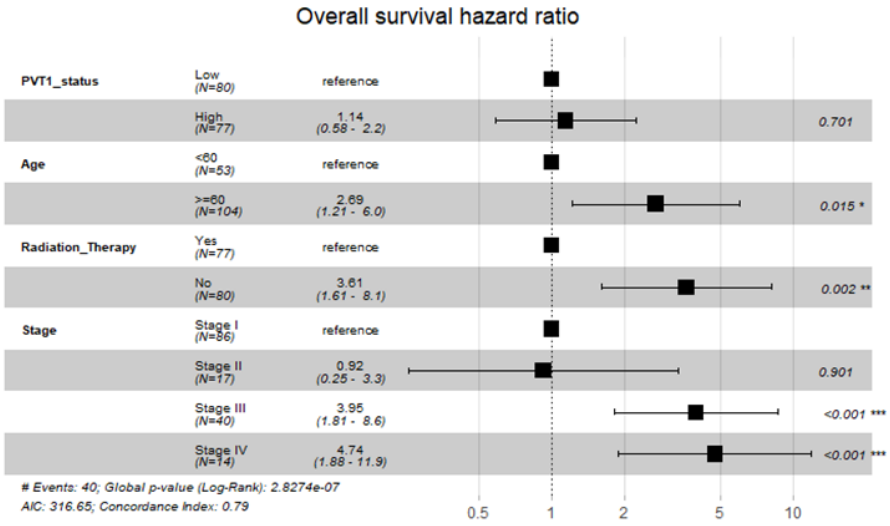
Overall survival hazard ratio
PVT1_status
Low (N=80)
reference
High (N=77)
1.14 (0.58 - 2.2)
0.701
Age
<60 (N=53)
reference
>=60 (N=104)
2.69 (1.21 - 6.0)
0.015 *
Radiation_Therapy
Yes (N=77)
reference
No (N=80)
3.61 (1.61 - 8.1)
0.002 **
Stage
Stage I (N=86)
reference
Stage II (N=17)
0.92 (0.25 - 3.3)
0.901
Stage III (N=40)
3.95 (1.81 - 8.6)
<0.001 ***
Stage IV (N=14)
4.74 (1.88 - 11.9)
<0.001 ***
Events: 40; Global p-value (Log-Rank): 2.8274e-07
AIC: 316.65; Concordance Index: 0.79
0.5
1
2
5
10

B

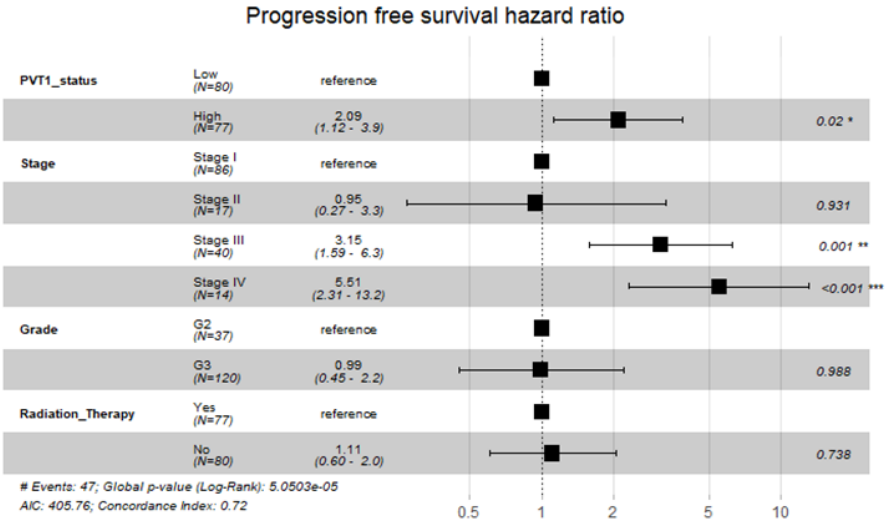
Progression free survival hazard ratio
PVT1_status
Low (N=80)
reference
High (N=77)
2.09 (1.12 - 3.9)
0.02 *
Stage
Stage I (N=86)
reference
Stage II (N=17)
0.95 (0.27 - 3.3)
0.931
Stage III (N=40)
3.15 (1.59 - 6.3)
0.001 **
Stage IV (N=14)
5.51 (2.31 - 13.2)
<0.001 ***
Grade
G2 (N=37)
reference
G3 (N=120)
0.99 (0.45 - 2.2)
0.988
Radiation_Therapy
Yes (N=77)
reference
No (N=80)
1.11 (0.60 - 2.0)
0.738
Events: 47; Global p-value (Log-Rank): 5.0503e-05
AIC: 405.76; Concordance Index: 0.72
0.5
1
2
5
10

C

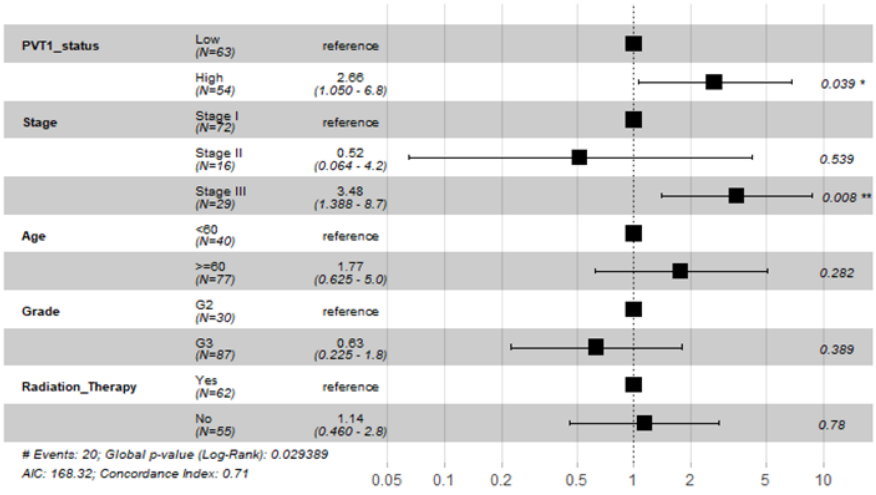
Disease free survival hazard ratio
PVT1_status
Low (N=63)
reference
High (N=54)
2.66 (1.050 - 6.8)
0.039 *
Stage
Stage I (N=72)
reference
Stage II (N=16)
0.52 (0.064 - 4.2)
0.539
Stage III (N=29)
3.48 (1.388 - 8.7)
0.008 **
Age
<60 (N=40)
reference
>=60 (N=77)
1.77 (0.625 - 5.0)
0.282
Grade
G2 (N=30)
reference
G3 (N=87)
0.63 (0.225 - 1.8)
0.389
Radiation_Therapy
Yes (N=62)
reference
No (N=55)
1.14 (0.460 - 2.8)
0.78
Events: 20; Global p-value (Log-Rank): 0.029389
AIC: 168.32; Concordance Index: 0.71
0.05
0.1
0.2
0.5
1
2
5
10

Figure 3. 7: Effect of clinical parameters on survival curves.
(A) Multivariate analysis of PVT1 RNA expression, age, radiotherapy and stage, on overall survival. (B) Multivariate analysis of PVT1 RNA expression, stage, grade and radiotherapy on progression-free survival. (C) Multivariate analysis of PVT1 RNA expression, stage, age, grade and radiotherapy on disease-free survival.

threshold dependent and less pronounced than with PVT1 Amplification subgroup. This also suggest that differences exist between the PVT1 Amplification and high RNA expression group. The exact role and mechanism of PVT1 warrants further investigation.

3.2.6 HIGH PVT1 EXPRESSION COMBINED WITH AMPLIFICATION IS THE MOST UNFAVORABLE TO PATIENT SURVIVAL IN UCEC

Looking at the sample distribution (Figure 3. 9A), we also wanted to investigate the impact of the observed sample grouping (Low Diploid, High Diploid, Low Gain, High Gain and High Amplification) on the patient survival curves. Low Amplification subgroup was discarded, as this group only contained 2 samples.

We found that, compared to Low Diploid and High Diploid, High Amplification negatively impacted overall survival (p-value: 0.0034 and 0.0070 respectively) (Figure 3. 9B), progression-free survival (p-value: 7.27e-5 and 0.0020 respectively) (Figure 3. 9C) and disease-free survival (p-value: 0.0016 and 0.0242 respectively) (Figure 3. 9D). Schoenfeld residuals to verify cox proportional hazards model assumption can be found in Figure B. 26A. This indicates that high PVT1 expression alone (High Diploid) is not sufficient to unfavorably impact patient survival curves in UCEC but that PVT1 Amplification is needed (High Amplification).

Cox proportional hazard model was further used to investigate the effect of PVT1 subgroups (denoted here as PVT1_AMP) and clinical parameters such as age, stage, grade and radiotherapy on survival in UCEC. For overall survival, multivariate analysis did not show any significance of PVT1_AMP, but showed that Stage (III) negatively influenced

survival curves (Figure B. 26B). Multivariate analysis showed significant negative impact of PVT1 High Gain and High Amplification for disease-free survival (Figure 3. 9E). Similarly, PVT1 High Gain and High Amplification as well as stage (III) stayed significant in multivariate analysis for progression-free survival (Figure 3. 9F). Age was discarded as Schoenfeld residuals were statistically significant. However, interaction between PVT1 High Gain or High Amplification and stage was not statistically significant. Schoenfeld residuals are available in Figure B. 26C.

To summarize, the analysis suggests that PVT1 high RNA expression is not sufficient to contribute to unfavorable patient survival in UCEC and that PVT1 Amplification is needed. This indicates that PVT1 alone might not be the main driver of poor patient survival. However, the exact mechanism remains unclear and needs further investigation.

3.2.7 PVT1 HIGH EXPRESSION COMBINED WITH AMPLIFICATION HAS AN UPREGULATED CELL CYCLE THROUGH MYC AND E2F TARGET GENES

To further investigate why PVT1 Low Diploid (denoted as LD) and High Diploid (denoted as HD) subgroups have favorable survival curves compared to PVT1 High Amplification (denoted as HA) subgroup (which is the most unfavorable for patient survival) (Figure 3. 9B, C and D), we performed a transcriptomic analysis between the different combination of subgroups. We investigated overlaps between significant down- and up-regulated genes and found that while each subgroup share common genes, each subset of comparison between the group is characterized by unique DEG indicating that HA, HD and LD subgroups have also unique transcriptomes (Figure B. 27).

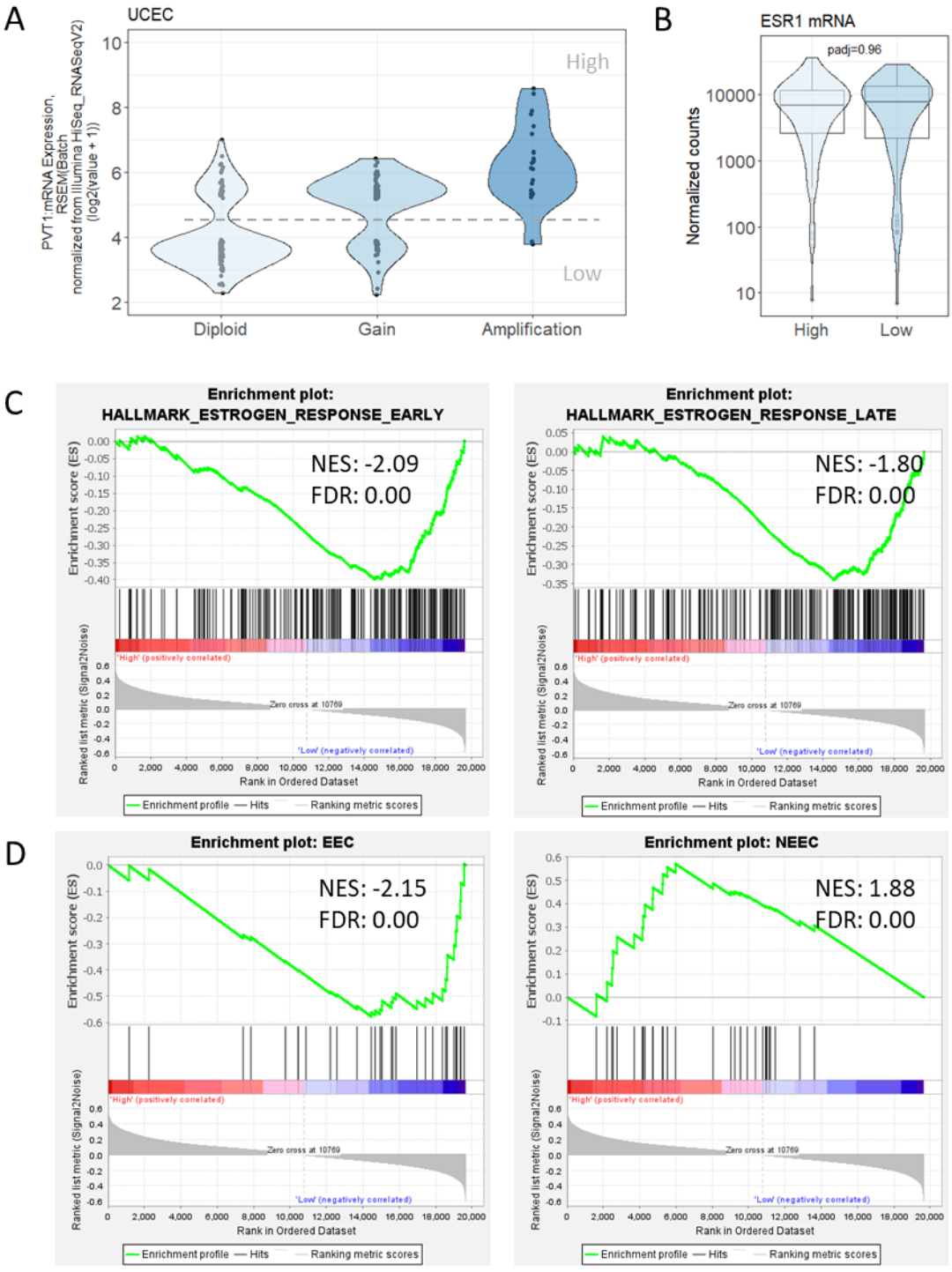

Figure 3. 8: High PVT1 RNA subgroup is associated with type II endometrial cancers. (A) PVT1 RNA expression per RNA subgroups (20% top – 20% bottom sample selection) for UCEC. (B) ESR1 mRNA expression per PVT1 RNA subgroups (20% top – 20% bottom sample selection). (C) GSEA for estrogen response signatures for PVT1 high versus low RNA subgroup (20% top -20% bottom). (D) GSEA of endometrioid endometrial

cancer (EEC) and non-endometrioid endometrial cancer (NEEC) for PVT1 high versus low RNA subgroup (20% top -20% bottom).

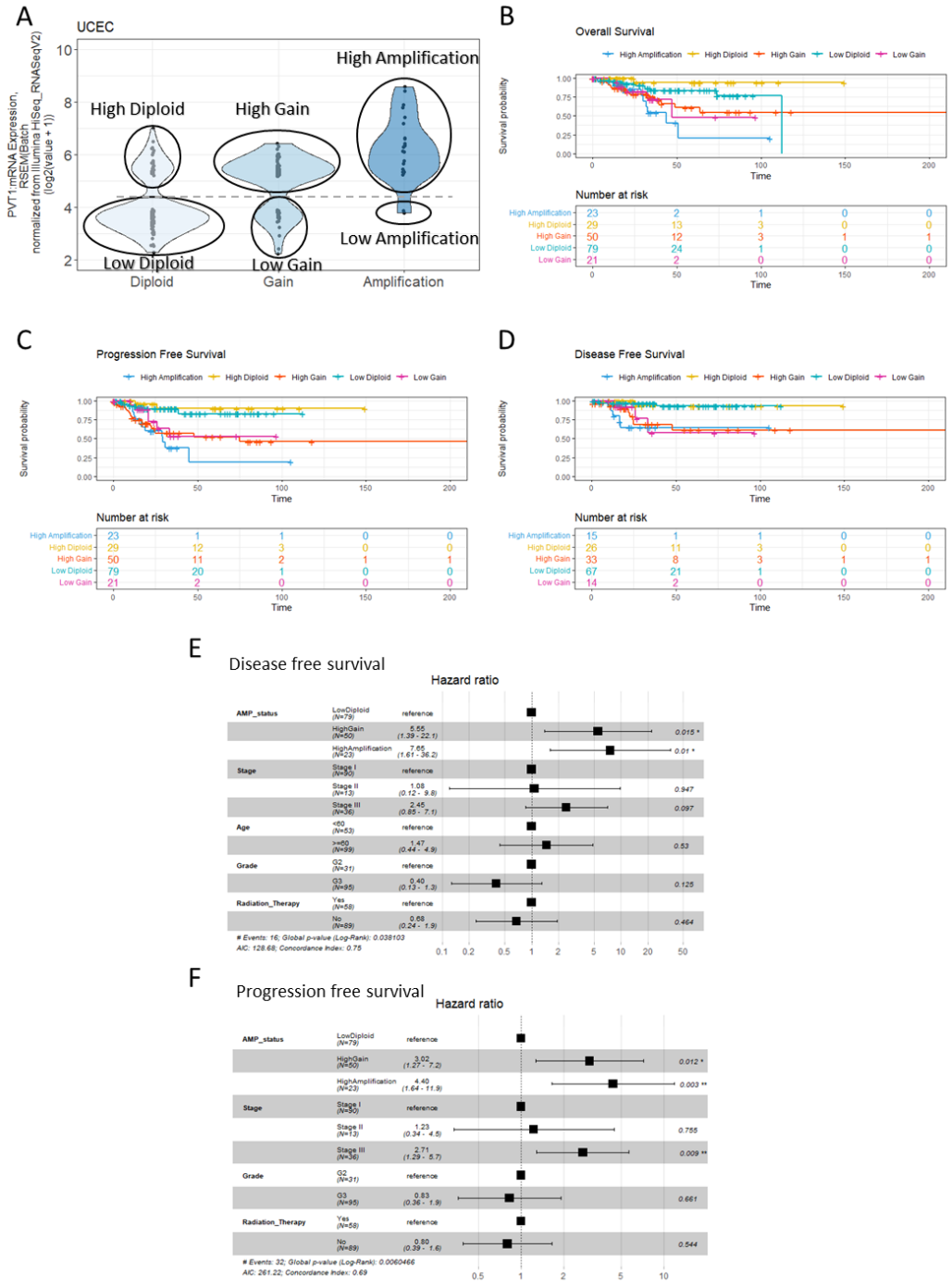

Figure 3. 9: High PVT1 expression combined with PVT1 Amplification is the most unfavorable to patient survival in UCEC.
(A) PVT1 RNA expression and alteration subgroups (20% top – 20% bottom sample selection) for UCEC. (B) Kaplan-Meier survival curves for overall survival per RNA and

alteration subgroup in UCEC (20% top – 20% bottom sample selection). (C) Kaplan-Meier survival curves for progression-free survival per RNA and alteration subgroup in UCEC (20% top – 20% bottom sample selection). (D) Kaplan-Meier survival curves for disease-free survival per RNA and alteration subgroup in UCEC (20% top – 20% bottom sample selection). (E) Multivariate analysis of PVT1 RNA and alterations, stage, grade and radiotherapy on progression-free survival. (F) Multivariate analysis of PVT1 RNA and alterations, stage, grade and radiotherapy on disease-free survival.

Second, a pathway enrichment analysis on the DEG per combination was performed (Figure B. 28). In short, it appears that HA is driven by an upregulated cell cycle progression and that LD is driven by an active estrogen signaling pathway. Volcano plots of the DEG between the different comparison indicated that MYC is mostly upregulated in HA and that ESR1 is mostly upregulated in the LD and HD subgroups (Figure 3. 10A) which was also observed at the protein level (only for ESR1) (Figure B. 29). To corroborate this observation, we performed GSEA and found that HA is indeed driven by upregulated cell cycle pathways (GSEA hallmarks, KEGG cell cycle and GOBP linked to DNA replication and transcription) most probably through MYC (V1 and V2) and E2F hallmarks target genes when compared to LD (Figure 3. 10B and Figure B. 30) and HD (Figure B. 32). Although, no differences in ESR1 mRNA and protein expression were observed between HD and LD, we also found that LD is driven by an active estrogen signaling pathway (hallmarks) when compared to HA and HD (and KEGG when only comparing to HA) (Figure B. 30 and Figure B. 32). GSEA hallmarks, KEGG and GOBP pathway enrichment indicated that LD has an upregulation cell cycle when compared to HD (Figure B. 31). This observation might suggest that the differences seen in the survival curves between HD and LD could result from a more proliferative capacity of cancer cells [194] in LD subgroup through possibly estrogen signaling pathway [195].

We also investigated the association between the different subgroups with the endometrial subtypes and found that, similarly to PVT1 Amplification subgroup, HA subgroup is associated with NEEC while LD (Figure 3. *10*C) or HD (Figure B. 33A) are associated with EEC. Endometrial cancers have previously been classified into four categories: POLE ultramutated, microsatellite instability hypermutated, copy-number low, and copy-number high [196]. Comparing with our subgroups, only HA appears to be corresponding to the copy-number high category while the other categories are mixed within our subgroups (HD and LD) (Figure B. 33B).

Finally, we investigated the association of the subgroups with the prognostic markers and found that HA is associated with unfavorable prognostic markers while LD is associated with favorable prognostic markers (Figure 3. 10D). Yet, when compared to HD, HD had a more pronounced association with favorable prognostic markers (Figure B. 33C). Altogether, our observations are indicating that HA is driven by an upregulated cell cycle progression, most probably through MYC and E2F target genes while LD is driven by an active estrogen signaling pathway. HA also corresponds with type 2 endometrial cancers resulting in the most unfavorable patient survival. However, the exact role and mechanism of PVT1 warrants further experimental investigation.

3.2.8 A RNA CLASSIFIER FOR PVT1 LOW DIPLOID

We observed that PVT1 (RNA expression and copy number alteration) is a potential biomarker of patient survival and that 2 particular subgroups, Low diploid and High Amplification, have the potential to predict treatment response (hormone therapy and cell cycle inhibitor therapy, respectively). We therefore investigated the prediction

potential of these subgroups based on transcriptomic analysis. To do so, we used random forest (RF) classification.

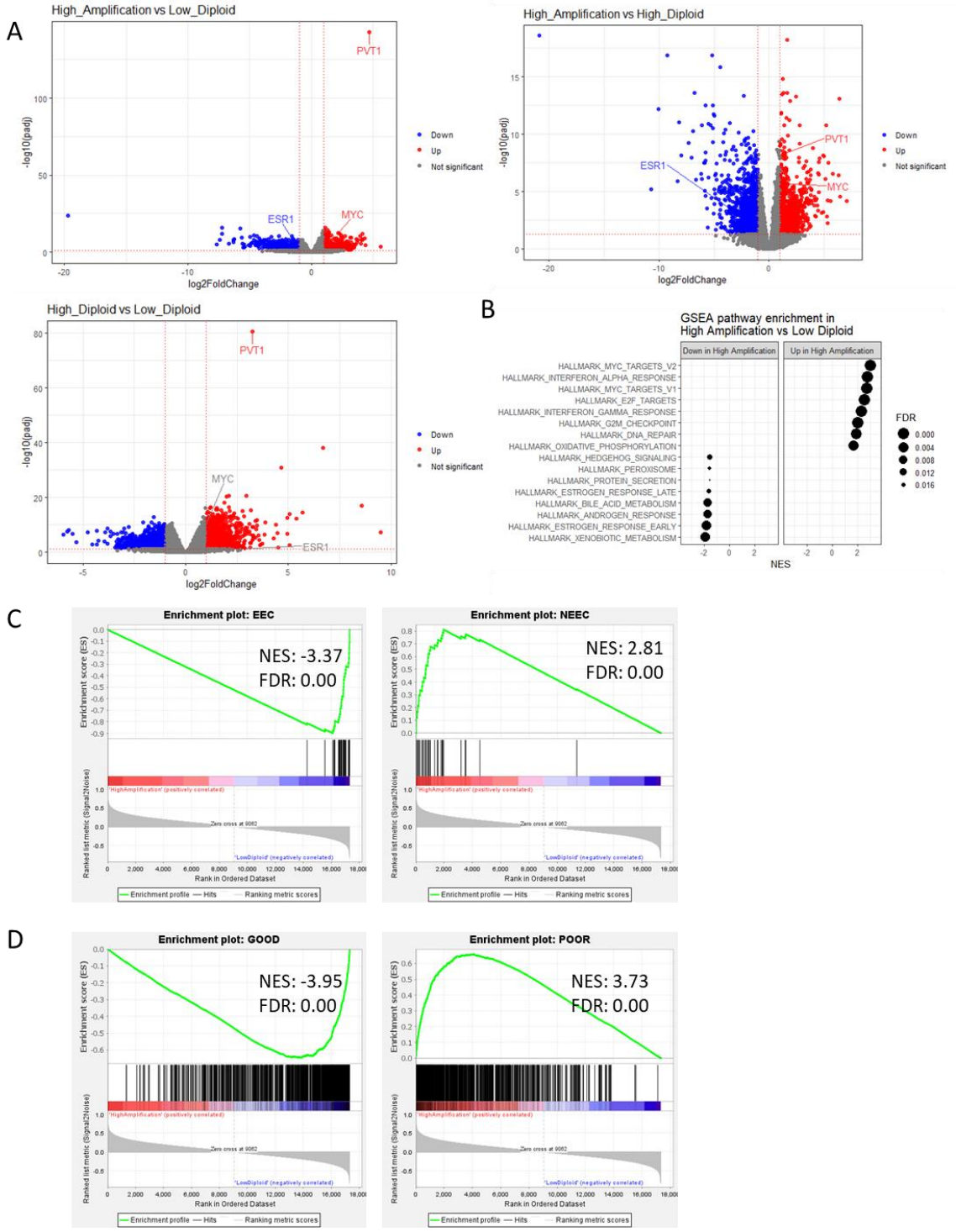

Figure 3. 10: PVT1 high expression combined with Amplification has an upregulated cell cycle through MYC and E2F target genes in UCEC.

(A) Volcano of DEG between the different combination of comparison between high amplification, low diploid and high diploid subgroup. (B) GSEA of cancer hallmarks for high amplification versus low diploid. (C) GSEA of endometrioid endometrial cancer (EEC) and non-endometrioid endometrial cancer (NEEC) for high amplification versus low diploid. (D) GSEA of prognostic markers for high amplification versus low diploid.

RF classification yields a measure of variable importance, which can be used to determine which gene expression values are the most important for predicting the different subgroups. In this case mean decrease accuracy was used to identify these variables of importance. We found that only PVT1 Low Diploid subgroup was accurately identified with a 6.4 % classification error using the top 3 genes (PVT1, DCAF13 and NSMCE2) of importance or 4.3 % classification error using the top 10 genes of importance (when including PVT1) (Figure 3. 11A). As samples were already partially classified through PVT1, we also investigated the prediction potential without PVT1 as a variable of importance. PVT1 Low Diploid subgroup was accurately identified with a 4.3 % classification error using the top 10 genes of importance (Figure 3. 11B). Other subgroups were however classified with classification errors superior to 20%. Therefore, it appears that PVT1 High Amplification subgroup is best identified using information from both copy number alteration and RNA expression.

Altogether, we found that RNA expression of PVT1, DCAF13 and NSMCE2 could be sufficient to identify LD patients, which could benefit from hormone therapy. Yet, the underlying mechanisms of action, being multiple and complex, remain elusive. PVT1 has a linear and circular form acting independently from each other [41].

A

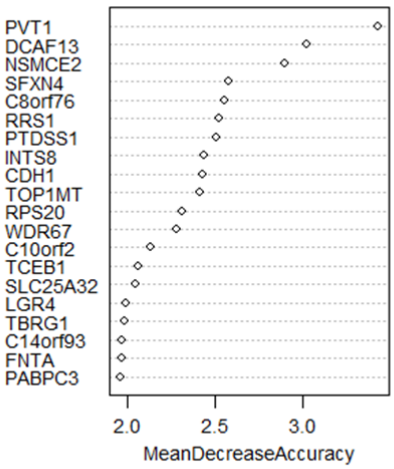

Confusion matrix Top 3: OOB estimate of error rate: 22.5%

	LD	HD	LG	HG	LA	HA	classification error
LD	44	0	3	0	0	0	0.0638
HD	0	14	0	2	0	1	0.1764
LG	3	0	9	0	0	0	0.25
HG	0	5	0	21	0	4	0.3
LA	1	0	0	0	0	0	1
HA	0	1	0	7	0	5	0.6153

Confusion matrix Top 10: OOB estimate of error rate: 19.17%

	LD	HD	LG	HG	LA	HA	classification error
LD	45	0	2	0	0	0	0.0425
HD	0	15	0	2	0	0	0.1176
LG	4	0	8	0	0	0	0.3333
HG	0	2	0	26	0	2	0.1333
LA	1	0	0	0	0	0	1
HA	0	1	0	9	0	3	0.7692

B

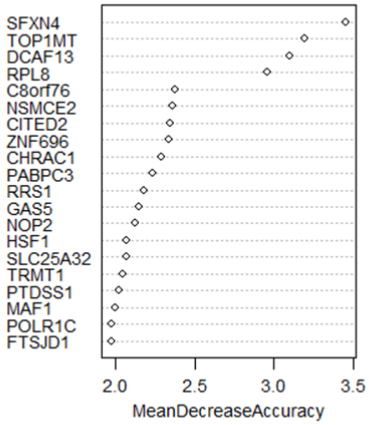

Confusion matrix Top 5: OOB estimate of error rate: 35%

	LD	HD	LG	HG	LA	HA	classification error
LD	40	3	4	0	0	0	0.148936
HD	4	10	0	3	0	0	0.411765
LG	5	0	5	1	0	1	0.583333
HG	1	4	0	20	0	5	0.333333
LA	1	0	0	0	0	0	1
HA	1	1	0	8	0	3	0.769231

Confusion matrix Top 10: OOB estimate of error rate: 30%

	LD	HD	LG	HG	LA	HA	classification error
LD	45	0	2	0	0	0	0.042553
HD	4	11	0	2	0	0	0.352941
LG	4	0	4	2	0	2	0.666667
HG	1	3	2	23	0	1	0.233333
LA	1	0	0	0	0	0	1
HA	2	1	1	8	0	1	0.923077

Figure 3. 11: Random Forest prediction to classify PVT1 RNA combined with alteration subgroups.
(A) Random forest prediction including PVT1. (B) Random forest prediction excluding PVT1. LD: low diploid, HD: high diploid, LG: High Gain, HG: High Gain, LA: Low Amplification and HA: high amplification.

PVT1 encompasses six miRNAs [42] which function in gynecological cancers have not been investigated yet. So far, in gynecological cancers, PVT1 is shown to act as a

competitive endogenous RNA or on the epigenetic machinery by binding to EZH2. Furthermore, upstream mechanisms of activation are unclear and numerous. First indications point towards a stress responsive lncRNA with multiple activators such as FOXM1 [154], P53 [157, 197], MYC [139] and STAT3 [155]. Functionally, PVT1 plays a role in cell proliferation, migration, invasion, cell cycle progression, apoptosis resistance, sphere-forming and chemo resistance in gynecological as well as other cancer [185]. Finally, PVT1 has a great potential to be used as a biomarker of detection, due to its presence in different body fluids, as well as therapeutic target.

Genes targeted by somatic copy number alterations play central roles in oncogenesis and cancer therapy [198]. Although, PVT1 amplification has been mostly linked to poor prognosis [37], the contrary has also been shown in ovarian cancer [79]. Consequently, we wondered on the implications of PVT1 copy number alterations versus RNA expression. Furthermore, as similar functional profiles of PVT1 were observed in gynecological cancers, we also investigated whether similarities exist between the major cancers that are part of the female reproductive system (endometrial, ovarian and cervical cancer).

Our findings indicate, for the first time, that PVT1 is most clinically relevant in UCEC and not in the other three studied tumor types (OV, CESC and UCS). Which is in contradiction to the studies reported in the literature (Table A.1). It is important to mention that out of the 34 studies that have been reported here, only one study performed analysis on RNA sequencing data and found an aberrantly expressed PVT1/miR-612/CENP-H/CDK1 axis [199]. Although this study did not include miRNA analysis, we did not find aberrantly expressed PVT1 in association with CENP-H and CDK1. This might be

explained that most studies compared normal tissue versus cancer tissue, while our study specifically focused on PVT1 differences within the cancer tissue. Also, most studies performed RT-qPCRs on cell lines or patient samples. Although, RT-qPCR is used to confirm RNA-sequencing data, variable outcomes can be observed depending on the selected reference genes as well as the primer sequences [200]. Furthermore, we only focused on the linear form of PVT1. We were not able to corroborate findings related to PVT1 upregulation associated with Talin 1 [201] or FGFR1/FGF2 [102], most probably due to the aforementioned differences in the study concept.

Investigation and comparison of gynecological Pan-Cancer has been performed elsewhere [202] but to the authors knowledge, this is the first multi-platform analysis that investigates PVT1 copy number alterations and RNA expression in multiple gynecological cancers.

TCGA samples (UCEC, OV, CESC and UCS) were divided and described per PVT1 copy number alteration and RNA expression as well as per tumor type. Subsequently, survival curves for overall, disease-free and progression-free were investigated. For the first time, we observed that PVT1 Gain and Amplification subgroups are unfavorable to patient survival while the negative impact on survival of PVT1 high RNA expression subgroup is threshold dependent in UCEC only (except for UCS for disease-free survival when PVT1 RNA expression subgroups are divided based on the 20% bottom – 20% top sample selection method). One study, in early-stage epithelial ovarian cancer, focused on the impact of PVT1 amplification and RNA expression on patient survival [203]. Their findings indicate that low copy number of MYC or PVT1 is associated with favorable patient overall survival, which contradicts our observations. Besides the fact

that our observations are in different tumor types (ovarian versus endometrial cancer) and based on different method of copy number quantification (RT-qPCR versus GISTIC2.0), we performed all the different stages in our analysis. Though cox proportional hazard analysis did not indicate a correlation between PVT1 copy number alteration and stage in multivariate analysis.

As the survival curves were most impacted in UCEC, we investigated enrichment pathways in the different subgroups (PVT1 copy number alterations and RNA expression) in that particular tumor type. Our investigation revealed two prominent subgroups (PVT1 Low Diploid and PVT1 High Amplification) that are potential candidates for treatment response. Also, we observed that PVT1 high Diploid subgroup had the most favorable patient survival curves indicating that high PVT1 RNA expression alone is not sufficient for poor survival prognosis. The underlying causes could, however, not be clarified.

PVT1 High Amplification subgroup is enriched in cell cycle progression, potentially driven through MYC and E2F target genes. Our observation of cell growth and proliferation support from MYC in UCEC is consistent with a previous Pan-cancer study [204]. A complex interplay between MYC and PVT1 has been observed so far [139]. Tseng et al. showed that a positive feedback loop between MYC and PVT1 is needed for high tumorigenic potency [119]. Yet, promoter-enhancer competition between PVT1 and MYC has also been observed, but only in breast cancer so far [140]. PVT1 participation in MYC downstream related signaling pathway is described by Jin et al. [139]. PVT1 has been shown to regulate P15 and P16 through binding to EZH2 in gastric cancer [205]. Downregulation of CDKN2A (P16) is inconsistent with our observation as CDKN2A was upregulated in PVT1 High Amplification subgroup. PVT1 has also been shown to

downregulate P15 and P21 expression in non-small cell lung cancer. Downregulation of CDKN1A (P21) is however consistent in PVT1 High Amplification subgroup. Upregulation of CDK4 or cyclin D1 as described by Wang et al. [206], was also not observed in PVT1 High Amplification subgroup. Finally, Chen et al. showed that circPVT1 can enhance the expression of the transcription factor E2Fs in gastric cancer [207]. Altogether, our observation might indicate that PVT1 contributes to the cell cycle progression driven by MYC and E2F target genes. Nevertheless, a Pan-cancer analysis on lncRNAs reported in the literature, showed that PVT1 was not directly linked to the hallmarks of MYC or E2F target genes in UCEC [208] despite the finding that PVT1 acts as decoy, as cofactor, guide or as molecular switch to alter transcription factor or RNA binding protein activity. Furthermore, PVT1 High Amplification is also characterized by a downregulation of estrogen receptor alpha. Loss of estrogen receptor alpha alone [209] or in combination with other hormone receptors [202, 210] have been proposed to be correlated with advanced stage, more aggressive cancer and consequently with poorer survival. As hormonal therapy is inefficient in these tumors [211], novel therapeutic targets are needed. Therefore, identifying patients with PVT1 amplification and high RNA expression might help in the treatment selection. Whether cell cycle inhibitors [212], E2F inhibitor [213] or PVT1 inhibitors (e.g., siRNAs) would be the best treatment, remains to be elucidated.

For instance, PVT1 Low Diploid is enriched in estrogen signaling pathway indicating a potential good response to hormonal therapy. Yet, most of our understanding about estrogen signaling comes from breast cancer and some aspects of this signaling differ in endometrial cancer resulting in a knowledge gap [191]. PVT1 Low Diploid subgroup

could be predicted using the RNA expression of 3 genes (PVT1, DCAF13 and NSMCE2) with an error rate of ~0.06%. DCAF13 enables nuclear estrogen receptor binding activity (Alliance of Genome Resources) and NSMCE2 is involved in maintaining telomeres length in cancer cell lines to prevent cell cycle arrest [214].

Our sample classification appears to be different from the one proposed by Levine et al. in particular for PVT1 Low diploid and High Diploid subgroups [196]. Yet, one might consider that PVT1 High Amplification corresponds to the C1 cluster and PVT1 Low diploid to the C4 cluster, proposed by Berger et al. [202]. Further investigation is needed for confirmation though.

In summary, this study revealed for the first time differences between PVT1 amplification and RNA expression in UCEC and identified PVT1 as a potential biomarker of survival and treatment response in UCEC patients.

This study should be considered as a hypothesis yielding clues to be tested and validated in follow-up studies (which is beyond the intended scope of this study). Several limitations are linked to our study. First, to better correlate the RNA sequencing data with the published RT-qPCR data, our study would benefit from investigating PVT1 alternative splicing in the various cancer studies, which might indicate cancer dependency for certain transcripts. The circular form of PVT1 has also not been investigated here. Second, lack of experimental evidence diminishes the clinical relevance of our suggested observation. Third, we did not validate our suggested observation in an independent dataset as datasets combining copy number alterations, RNA and protein expression levels are very limited. Lastly, this study would benefit from additional integration of miRNA and methylation data.

3.3 MATERIAL AND METHODS

3.4.1. LITERATURE RESEARCH

We searched the terms PVT1 and gynecological cancer, endometrial cancer, cervical cancer as well as ovarian cancer in PubMed, PubMed central, Google scholar and web of science. Duplicates and retracted publications were eliminated.

3.4.2. TCGA DATA – SAMPLE SLECTION AND GROUPING

The following tumor types: TCGA Uterine Corpus Endometrial Carcinoma (UCEC TCGA), Uterine Carcinosarcoma (UCS TCGA); TCGA Cervical Squamous Cell Carcinoma and Endocervical Adenocarcinoma (CESC TCGA) and TCGA Ovarian Serous Cystadenocarcinoma (OV TCGA) were investigated using cBioportal [215, 216]. Further exploration was completed on samples with RNA Expression "RSEM" (Batch normalized from Illumina HiSeq_RNASeqV2) and log2 copy-number data (1162 samples). Samples with deep and shallow deletion were discarded (46 samples in total – 18 in CESC, 14 in OV, 4 in UCS, 10 in UCEC).

The remaining samples (1116 samples) were subdivided per tumor type. UCEC (511 samples in total) was subdivided based on PVT1 GISTIC alteration (diploid (314 samples) versus gain (155 samples) and amplification (42 samples) and RNA expression (high RNA (30% top samples – 153 samples) versus low RNA (30% bottom samples – 153 samples) as well as high RNA (20% top samples – 102 samples) versus low RNA (20% bottom samples – 102 samples). UCS (52 samples in total) was subdivided based on PVT1 GISTIC alteration (diploid (10 samples) versus gain (31 samples) and amplification (11 samples)) and RNA expression (high RNA (30% top samples – 15 samples) versus low RNA (30% bottom samples – 15 samples) as well as high RNA (20% top samples – 10 samples) versus low RNA (20% bottom samples – 10 samples). CESC (272 samples in

total) was subdivided based on PVT1 GISTIC alteration (diploid (152 samples) versus gain (109 samples) and amplification (11 samples)) and RNA expression (high RNA (30% top samples – 81 samples) versus low RNA (30% bottom samples – 81 samples) as well as high RNA (20% top samples – 54 samples) versus low RNA (20% bottom samples – 54 samples). OV (281 samples in total) was subdivided based on PVT1 GISTIC alteration (diploid (36 samples) versus gain (138 samples) and amplification (106 samples)) and RNA expression (high RNA (30% top samples – 84 samples) versus low RNA (30% bottom samples – 83 samples) as well as high RNA (20% top samples – 56 samples) versus low RNA (20% bottom samples – 55 samples).

Sample distribution of PVT1 RNA expression combined with alteration in UCEC (204 samples) was as follows: High Amplification (23 samples), Low amplification (2 samples), Low Diploid (79 samples), High Diploid (29 samples), High Gain (50 samples) and Low Gain (21 samples).

Amplification is defined as having a high number of DNA copies and often seen as focal, while gain is defined as having a few additional DNA copies and often seen as broad. TCGA data were used for their uniform clinical elements, consistent processing and normalization of mutations, copy number, mRNA data, miRNA data, protein data and methylation data. They are as such ideally processed for comparative analyses.

3.4.3. TCGA DATA – SURVIVAL CURVES

Clinical data for the corresponding TCGA samples was retrieved from firebrowse (http://gdac.broadinstitute.org). Survival curves were performed in R with the packages “survminer” and “survival”. Verification of Cox proportional hazards model assumption was performed by calculating Schoenfeld residuals. To note, due to missing data, sample sized dropped from 511 to 390 patients for overall survival and progression-free survival,

disease-free survival had a sample size of 301 patients when performing multivariate analysis with clinical parameters.

3.4.4. TCGA DATA – MRNAS ANALYSIS

Level 3 gene expression RNA sequencing data for UCEC, OV, CESC and UCS were retrieved from firebrowse (http://gdac.broadinstitute.org) as gene-level raw expression values, produced by RSEM [217] (.uncv2.mRNAseq_raw_counts.txt). Differential gene expression was performed in R with the package "DESeq2" based on the aforementioned subgroups. Genes with row sum below 10 counts were discarded. Differentially expressed genes with log2 fold change >1 and adjusted p-value <0.05 were regarded as significantly upregulated. Differentially expressed genes with log2 fold change <-1 and adjusted p-value <0.05 were regarded as significantly downregulated. Adjusted p-value refers to corrected for multiple testing with an FDR alpha = 0.1.

R package "VennDiagram" was used to generate Venn diagrams. Prognostic markers for each cancer types were retrieved from The Human Protein Atlas (https://www.proteinatlas.org/).

3.4.5 TCGA DATA – PROTEIN ANALYSIS

Protein expression profiles (RPPA) were retrieved from cBioportal [215, 216].

3.4.6. TCGA DATA – PATHWAY ENRICHMENT ANALYSIS

To investigate pathway enrichment in differentially expressed genes, we used the web tool gProfiler [218] with default settings for GO and KEGG pathways. To investigate pathway enrichment at the whole gene expression level, we extracted the normalized counts from DESEQ2 ("counts(dds, normalized = T)") and used GSEA [172] with default settings and "gene_set" as permutation type. GSEA for PVT1 alterations, "equalize and

balance" was used as randomization mode. Statistical significance was achieved when FWER< 0.1.

3.4.7. RANDOM FOREST CLASSIFICATION

To predict the different subgroups in UCEC samples, we used the R package RandomForest. Samples were first split into training and test sets (60:40 – set seed = 100) and subjected to differential gene expression using DESeq2 in R (as described in section 5.3). RandomForest package was used with default settings and mean decrease accuracy was used to define the variables of importance.

3.4.8. STATISTICAL ANALYSIS

Selection of statistical test was performed after identifying the data distribution, using the shapiro-wilk test as well as for variance homogeneity using the levene test, included in the R package "rstatix". Kruskal Wallis test followed by post-hoc Dunn test with Benjamini & Hochberg correction was used for Figure 9C and Figure B.29. Kruskal Wallis test was used for Figure 12B; 16B, as well as Figure B.11.

CHAPTER 4

GENERAL DISCUSSION AND PERSPECTIVES

Worldwide, an age shifting distribution of the population is observed (World Health Organization). With a growing ageing, populations come along higher health risks, such as the development of cancer [43]. Cancer therefore has become a major public health and economic burden. For women, gynecological cancers, mainly including ovarian, cervical and endometrial cancers, are still the leading cause of cancer related death worldwide [43].

All these gynecological cancers, when progressed to an advanced stage, have poor prognosis. This is due to the lack of effective treatment for refractory, recurrent and drug-resistance cancers. Yet, targeted therapies are emerging as promising treatment strategies [219]. Targeted therapy uses mostly small molecule drugs or monoclonal antibodies to target proteins that promote cell growth, division, and spreading specifically of cancer cells or tumor environment, leaving normal cells untouched [220]. Examples of promising targeted therapies are PARP inhibitors in ovarian cancer, hormone-dependent histological type and POLE/MSI molecular subtypes in endometrial cancer [219]. However, to further develop targeted therapies, mechanistic insights and discovery of novel therapeutic targets are key steps.

LncRNAs play important roles in gene regulation [179]. They are implicated in tumorigenesis [180, 181] and are emerging as therapeutic targets with diagnostic and prognostic potential, among others, in gynecological cancers [182-184]. The most studied

lncRNAs, and relevant in gynecological cancers are lncRNAs H19, HOTAIR and MALAT1 [221]. H19 is one of the first lncRNAs to be linked with genomic imprinting and involved in the fetal development [222]. More recently, H19 was found to be involved in a variety of pathological processes including cancer [223]. Targeting H19 can be done through BC-819, a plasmid containing the promoter of H19 and coding sequence of diphtheria toxin, which has been used in clinical trial for ovarian cancer (NCT00826150). HOTAIR is involved in chromatin silencing [28] and has also been found to play a role in cancer [224]. MALTA1 was first identified as being overexpressed in human lung cancer and is associated with a higher risk of metastasis [225]. Although no clinical trial has been made yet for HOTAIR and MALAT1, other targeting strategies are being investigated such as small interfering RNAs (RNAi), antisense oligonucleotides (ASO), clustered regularly interspaced short palindromic repeats (CRISPR) and small molecules [226]. Challenges, however, remain in specificity, efficacy and delivery of these strategies for clinical implementation [227].

LncRNA PVT1 has received growing attention [37] with therapeutic target potential [228]. PVT1 dysregulation and oncogenic function has been observed in multiple cancers, such as plasmacytomas, breast and prostate cancer [37, 185]. Furthermore, PVT1 transcript encompasses multiple miRNAs [42], expresses different splice variants [186] as well as different circular transcripts [153, 187]. However, little is known about PVT1 in gynecological cancers.

This PhD sought to bring insights in the regulatory mechanisms of lncRNA PVT1 in ovarian cancer and to investigate the potential implications of lncRNA PVT1 copy

number alteration and RNA expression in endometrial cancer, envisioning PVT1 as a potential therapeutic target.

In chapter 2, we described PVT1 as a contextual oncogenic lncRNA, amplified along with MYC, and a prognostic indicator in ovarian cancers, that is dynamically altered in expression primarily in response to cellular stressors. Notably, cell density and matrix stiffness changes, both of which converge on pathways associated with YAP1, lead to changes in PVT1. Our study is the first to report such mechanism in ovarian cancer and suggest a potential feedforward relationship between YAP1 and PVT1.

A feature of successful metastasis is the ability of cancer cells to adapt and survive under cellular stress. Metastatic growth of ovarian cancer cells into the peritoneal cavity requires adaptation to various cellular stress factors to facilitate cell survival and growth. Cellular stressors impacting most cancers include changes in oxygen tension (hypoxia), changes in extracellular matrix (ECM) composition and matrix rigidity, alterations in cell-cell contacts (cell density) and changes in anchorage-independent survival capabilities, oxidative, and metabolic stress as well as therapeutic treatments. After evaluating the TCGA ovarian cancer dataset, we observed that 8q24.21 exhibits the highest copy number amplifications. Chromosome 8q24.21 has a cancer risk locus in multiple cancers [141], but also specifically in ovarian cancer [142, 143]. Besides harboring MYC, dysregulation and amplification of which is found in many human cancers [144], the 8q24.21 locus also harbors lncRNA PVT1 which is ~53 kb downstream of MYC. Correlation between PVT1 and MYC in ovarian cancer has been previously documented [119, 139, 140]. Interestingly, copy number alteration frequency of PVT1 is among the highest in ovarian cancer, highlighting the significance and relevance of PVT1 in ovarian cancer.

To evaluate the possible relationship between cellular stress and PVT1 RNA expression, we first evaluated PVT1 expression at baseline using primers spanning PVT1 transcript isoforms containing – exon 1-2, exon 2-3 and exon 6-7 in a panel of human ovarian cancer cells lines, normal immortalized fallopian tube epithelial cells (p211) and surface epithelial cells (IOSE80). SK-OV3 cells exhibited the most robust levels of detectable PVT1 across all three exons of PVT1 consistent with prior reports of high PVT1 levels in this cell line [58, 62, 71].

Second, we exposed SK-OV3 cells to a series of stressors out of which hypoxia, serum starvation, matrix stiffness and cell density altered PVT1 expression. Increases in PVT1 RNA expression under hypoxia have been previously described in non-ovarian cancers [96, 145, 146], but were somewhat modest in our study with SK-OV3. Also in our study, increase in PVT1 RNA under low cell density was reproduced in multiple human and mouse cell lines but seemed to be dependent on their mesenchymal status. Yet, in mouse ID8 cell line alterations were also seen independently of TP53 status. Cell density changes can lead to alterations in the cell cycle and concomitant changes to the Hippo pathway, a key modulator of cell survival in response to cellular stressors [229] and a key negative regulator of YAP1 in various models [129-131]. To directly test if PVT1 expression depended on YAP1 levels, we used shRNAs' to lower YAP1 levels or inhibit the YAP1-TEAD association using the small molecule inhibitor verteporfin [133]. We found that specific reduction of YAP1 or the use of verteporfin significantly reduced PVT1 levels compared to control cells. Furthermore, exposing SK-OV3 to serum starvation or reduced matrix stiffness, both inactivating YAP1 [130, 132], reduced PVT1 RNA expression. Also, modulation of PVT1 RNA expression after exposure to the stressors

followed the RNA expression of YAP1 canonical target genes CTGF and CYR61 [131, 147], indicating a correlation between YAP1 nuclear localization and PVT1 RNA expression. To our knowledge, cell density, serum starvation or matrix stiffness associated PVT1 expression has not been shown elsewhere so far. Our study did not elucidate the exact mechanism behind PVT1 and YAP1. However, association between PVT1 and YAP1 was shown in esophageal adenocarcinoma [230], hepatocellular carcinoma [231], head and neck squamous cell carcinoma [153] and gastric cancer [232]. In esophageal adenocarcinoma, Xu et al. indicated a positive feedback regulation of PVT1 by YAP1. Although they did not detect PVT1 promoter by the ChIP assay using YAP1 antibody, the RNA-immunoprecipitation assay showed that YAP1 was directly associated with PVT1 possibly leading towards PVT1 stabilization by YAP1 [230]. On the other hand, Lan et al. showed that PVT1 regulated YAP1 expression as a competing endogenous RNA for miR-186-5p [231]. In head and neck squamous cell carcinoma, Verduci et al. demonstrated that a YAP1/mutant-p53/TEAD complex was formed specifically at the promoter site of circPVT1 and not to the promoter of the host gene PVT1 regulating as such circPVT1 expression [153]. Finally, Ji et al. suggested that PVT1 positively regulates YAP1, yet without a clear mechanism. Interestingly, Xu et al. exposed a positive feedback loop between PVT1 and FOXM1 in gastric cancer, where FOXM1 directly binds to the promoter of PVT1 [154]. Yet, FOXM1 is a downstream target of YAP1 in ovarian cancer suggesting that YAP1 might regulate PVT1 expression through FOXM1 [156]. Altogether, PVT1 – YAP1 relationship is versatile and complex which remains to be clarified.

Third, functional assays with gain or loss of PVT1 RNA expression demonstrated PVT1's role in promoting survival and chemo resistance in ovarian cancer cell lines and

during intra peritoneal tumor growth, highlighting a pro-metastatic role for Pvt1 in ovarian cancer. This is in accordance to what has been published so far in the literature (Table A.1). Yet, our study revealed a novel contribution of PVT1 in the regulation of aldo-keto reductases including AKR1C, AKR1C2, and AKR1B10. Aldo-keto reductases (AKR) have been demonstrated to regulate the metabolic processing of chemotherapeutic drugs such as doxorubicin, cisplatin, and paclitaxel, among others, and to cause chemo resistance in multiple cancers [159, 160]. The results shown in chapter 2, therefore suggest PVT1 as an attractive therapeutic target in ovarian cancer.

In chapter 3, we sought to investigate the impact of PVT1 copy number alterations (CNA) (diploid, gain and amplification) as well as RNA expression (low and high) in gynecological cancers. After reviewing the literature, we found that PVT1 function appears to be independent of the cancer type (ovarian, cervical and endometrial cancers). PVT1 is commonly described as being involved in promoting cell proliferation, migration, invasion, cell cycle progression, apoptosis resistance, colony formation and chemo resistance. Consequently, we performed a multi-platform analysis on the corresponding TCGA data (Uterine Corpus Endometrial Carcinoma (UCEC), Uterine Carcinosarcoma (UCS); Cervical Squamous Cell Carcinoma and Endocervical Adenocarcinoma (CESC) and Ovarian Serous Cystadenocarcinoma (OV) to investigated if a common transcriptomic signature is present. After subdividing TCGA samples per PVT1 CNA and RNA expression for each tumor type, we explored their impact on patient survival curves. To our surprise, PVT1 was most clinically relevant in UCEC and not in the other three studied tumor types (OV, CESC and UCS). This is in contradiction to the studies reported in the literature (Table A.1). We observed that high PVT1 RNA expression without copy number

alteration had the most favorable patient survival outcome in UCEC. Favorable patient survival outcome is followed by PVT1 diploid with low RNA expression which is enriched with estrogen signaling pathway. This subgroup of patients could positively respond to hormonal therapy. On the other hand, PVT1 Amplification with high RNA expression had the most unfavorable patient survival in UCEC and is enriched in cell cycle progression most probably through MYC and E2F target genes.

While our study investigated the impact of PVT1 CNA and RNA expression within each cancer, it is worthy to note that most of the published data on PVT1 in gynecological cancers investigated PVT1 in these cancers compared to normal tissues. Also, most studies are based on RT-qPCRs analysis on cell lines or patient samples while our analysis is based on RNA sequencing data. Although, RT-qPCR is used to confirm RNA-sequencing data, variable outcomes can be observed depending on the selected reference genes as well as the primer sequences [200]. So far, only one study performed analysis on RNA sequencing data in endometrial cancer and found an aberrantly expressed *PVT1*/miR-612/*CENP-H*/*CDK1* axis (compared to normal tissue) [199]. Although this study did not include miRNA analysis, we did not find aberrantly expressed PVT1 in association with CENP-H and CDK1. Likewise, we were not able to corroborate findings related to PVT1 upregulation associated with Talin 1 [201] as our study only focused on linear PVT1 and not the circular form or FGFR1/FGF2 [102]. Differences in study concept might therefore explain the observed discrepancies.

Investigation and comparison of gynecological Pan-Cancer have been performed elsewhere [202] but to the authors knowledge, this is the first multi-platform analysis that investigates PVT1 CNA and RNA expression in multiple gynecological cancers. Although

we showed that PVT1 CNA and high expression (threshold dependent) negatively impacted patient survival in UCEC, our investigation revealed two prominent subgroups (PVT1 Low Diploid and PVT1 High Amplification) that are potential candidates for treatment response. In addition, we observed that PVT1 high Diploid had the most favorable patient survival curves indicating that high PVT1 RNA expression alone is not sufficient for poor survival prognosis. Clarification on the underlying causes was however not identified.

PVT1 High Amplification subgroup is enriched in cell cycle progression, potentially driven through MYC and E2F target genes. Our observation of cell growth and proliferation support from MYC in UCEC is consistent with a previous Pan-cancer study [204]. A complex interplay between MYC and PVT1 has been observed so far [139]. Tseng et al. showed that a positive feedback loop between MYC and PVT1 is needed for high tumorigenic potency [119]. Yet, promoter-enhancer competition between PVT1 and MYC has also been observed but only in breast cancer so far [140]. PVT1 participation in MYC downstream related signaling pathway is described by Jin et al. [139]. PVT1 has been shown to regulate P15 and P16 through biding to EZH2 in gastric cancer [205]. Downregulation of CDKN2A (P16) is inconsistent with our observation as CDKN2A was upregulated in PVT1 High Amplification subgroup. PVT1 has also been shown to downregulate P15 and P21 expression in non-small cell lung cancer [233]. Downregulation of CDKN1A (P21) is however consistent in PVT1 High Amplification subgroup. Upregulation of CDK4 or cyclin D1 were also not observed in PVT1 High Amplification subgroup as described by Wang et al. [206]. Finally, Chen et al. showed that circPVT1 can enhance the expression of the transcription factor E2Fs in gastric cancer [207]. Altogether,

our observation might indicate that PVT1 contributes to the cell cycle progression driven by MYC and E2F target genes. Interestingly, enrichment of MYC target genes were found in all subgroups with PVT1 amplification regardless of the tumor type, which might suggest that the common functional observation on increased cell proliferation, cell cycle progression, invasion and apoptosis resistance arise from MYC regulation of cancer hallmarks [234]. We previously exposed the existing link between MYC and PVT1, yet the role of PVTA remains to be determined. It is noteworthy that Chiu et al. performed a Pan-cancer analysis on lncRNAs, PVT1 was not directly linked to the hallmarks of MYC or E2F target genes in UCEC [208], despite the finding that PVT1 acts as decoy, as cofactor, guide or as molecular switch to alter transcription factor or RNA binding protein activity. Therefore, further investigation on PVT1's role in UCEC is needed.

Endometrial cancers have previously been classified into four categories: POLE ultramutated, microsatellite instability hypermutated, copy-number low, and copy-number high [196]. Comparing with our subgroups, only PVT1 High Amplification appears to be mostly corresponding to the copy number high category while the other categories are mixed within our subgroups (PVT1 High Diploid and Low Diploid). Our sample classification appears to be different from the one proposed by Levine et al. in particular for PVT1 Low diploid and High Diploid subgroups [196]. Yet, one might consider that PVT1 High Amplification correspond to C1 cluster and PVT1 Low diploid to C4 cluster proposed by Berger et al. [202].

Since experimental evidence is essential for clinical relevance, care should be taken when interpreting this chapter as the suggested observation should be tested and validated in follow-up studies. To better correlate our observation with the published RT-qPCR data,

our study would benefit from investigating PVT1 alternative splicing in the various cancer studies as it might indicate cancer dependency for certain transcripts. The addition of miRNAs as well as methylation data might bring more insight into the potential mechanism of PVT1 in UCEC.

Future work should focus on confirming the hypothesis that PVT1 response to cellular stressor in a YAP1 depended manner through FOXM1 in ovarian cancer. Also, the exact mechanism on how PVT1 appears to contribute to the regulation of aldo-keto reductases should be investigated. Finally, the exploratory study that we performed on the TCGA data should be further explored to include miRNAs and network analysis and validated through experimental data.

In conclusion, the broad impact of PVT1 on multiple pathways suggest that blocking PVT1 may be an attractive target to simultaneously suppress multiple pathways. Few tools to silence lncRNAs are currently available (RNA interference, antisense oligonucleotides and genome editing (CRISPR/Cas9 system) but none have been clinically employed for PVT1 [164] and warrant further investigation. This work is an important step forward towards a better understanding of lncRNA PVT1 in ovarian and endometrial cancer, crucial for developing novel therapeutic treatment of cancer patients.

REFERENCES

1. Cobb, M., *60 years ago, Francis Crick changed the logic of biology.* PLoS biology, 2017. **15**(9): p. e2003243-e2003243.
2. Crick, F., *Central Dogma of Molecular Biology.* Nature, 1970. **227**(5258): p. 561-563.
3. Venter, J.C., et al., *The sequence of the human genome.* Science, 2001. **291**(5507): p. 1304-51.
4. Mattick, J.S. and I.V. Makunin, *Non-coding RNA.* Hum Mol Genet, 2006. **15 Spec No 1**: p. R17-29.
5. Mattick, J.S., *Challenging the dogma: the hidden layer of non-protein-coding RNAs in complex organisms.* Bioessays, 2003. **25**(10): p. 930-9.
6. Dunham, I., et al., *An integrated encyclopedia of DNA elements in the human genome.* Nature, 2012. **489**(7414): p. 57-74.
7. He, L. and G.J. Hannon, *MicroRNAs: small RNAs with a big role in gene regulation.* Nature Reviews Genetics, 2004. **5**(7): p. 522-531.
8. Pauli, A., J.L. Rinn, and A.F. Schier, *Non-coding RNAs as regulators of embryogenesis.* Nature Reviews Genetics, 2011. **12**(2): p. 136-149.
9. Esteller, M., *Non-coding RNAs in human disease.* Nature Reviews Genetics, 2011. **12**(12): p. 861-874.
10. Ozata, D.M., et al., *PIWI-interacting RNAs: small RNAs with big functions.* Nature Reviews Genetics, 2019. **20**(2): p. 89-108.
11. Kiss, T., *Small Nucleolar RNAs: An Abundant Group of Noncoding RNAs with Diverse Cellular Functions.* Cell, 2002. **109**(2): p. 145-148.
12. Hezroni, H., et al., *Principles of long noncoding RNA evolution derived from direct comparison of transcriptomes in 17 species.* Cell Rep, 2015. **11**(7): p. 1110-22.
13. Djebali, S., et al., *Landscape of transcription in human cells.* Nature, 2012. **489**(7414): p. 101-108.
14. Dinger, M.E., et al., *Differentiating protein-coding and noncoding RNA: challenges and ambiguities.* PLoS computational biology, 2008. **4**(11): p. e1000176-e1000176.
15. Hartford, C.C.R. and A. Lal, *When Long Noncoding Becomes Protein Coding.* Molecular and Cellular Biology, 2020. **40**(6): p. e00528-19.
16. Guttman, M., et al., *Chromatin signature reveals over a thousand highly conserved large non-coding RNAs in mammals.* Nature, 2009. **458**(7235): p. 223-227.
17. Smith, M.A., et al., *Widespread purifying selection on RNA structure in mammals.* Nucleic Acids Res, 2013. **41**(17): p. 8220-36.
18. Statello, L., et al., *Gene regulation by long non-coding RNAs and its biological functions.* Nature Reviews Molecular Cell Biology, 2021. **22**(2): p. 96-118.
19. Derrien, T., et al., *The GENCODE v7 catalog of human long noncoding RNAs: analysis of their gene structure, evolution, and expression.* Genome research, 2012. **22**(9): p. 1775-1789.
20. Carlevaro-Fita, J. and R. Johnson, *Global Positioning System: Understanding Long Noncoding RNAs through Subcellular Localization.* Molecular Cell, 2019. **73**(5): p. 869-883.

21. Geng, X., et al., *Circular RNA: biogenesis, degradation, functions and potential roles in mediating resistance to anticarcinogens.* Epigenomics, 2020. **12**(3): p. 267-283.
22. Kopp, F. and J.T. Mendell, *Functional Classification and Experimental Dissection of Long Noncoding RNAs.* Cell, 2018. **172**(3): p. 393-407.
23. Quinn, J.J. and H.Y. Chang, *Unique features of long non-coding RNA biogenesis and function.* Nature Reviews Genetics, 2016. **17**(1): p. 47-62.
24. Melé, M., et al., *Chromatin environment, transcriptional regulation, and splicing distinguish lincRNAs and mRNAs.* Genome Res, 2017. **27**(1): p. 27-37.
25. Li, L. and H.Y. Chang, *Physiological roles of long noncoding RNAs: insight from knockout mice.* Trends in cell biology, 2014. **24**(10): p. 594-602.
26. Wapinski, O. and H.Y. Chang, *Long noncoding RNAs and human disease.* Trends in Cell Biology, 2011. **21**(6): p. 354-361.
27. Furlan, G. and C. Rougeulle, *Function and evolution of the long noncoding RNA circuitry orchestrating X-chromosome inactivation in mammals.* WIREs RNA, 2016. **7**(5): p. 702-722.
28. Rinn, J.L., et al., *Functional Demarcation of Active and Silent Chromatin Domains in Human HOX Loci by Noncoding RNAs.* Cell, 2007. **129**(7): p. 1311-1323.
29. Taiana, E., et al., *LncRNA NEAT1 in Paraspeckles: A Structural Scaffold for Cellular DNA Damage Response Systems?* Non-coding RNA, 2020. **6**(3): p. 26.
30. Tripathi, V., et al., *The nuclear-retained noncoding RNA MALAT1 regulates alternative splicing by modulating SR splicing factor phosphorylation.* Molecular cell, 2010. **39**(6): p. 925-938.
31. Giovarelli, M., et al., *H19 long noncoding RNA controls the mRNA decay promoting function of KSRP.* Proceedings of the National Academy of Sciences, 2014. **111**(47): p. E5023-E5028.
32. Yoon, J.-H., K. Abdelmohsen, and M. Gorospe, *Functional interactions among microRNAs and long noncoding RNAs.* Seminars in Cell & Developmental Biology, 2014. **34**: p. 9-14.
33. Krause, H.M., *New and Prospective Roles for lncRNAs in Organelle Formation and Function.* Trends in Genetics, 2018. **34**(10): p. 736-745.
34. Webb, E., J.M. Adams, and S. Cory, *Variant (6 ; 15) translocation in a murine plasmacytoma occurs near an immunoglobulin κ gene but far from the myc oncogene.* Nature, 1984. **312**(5996): p. 777-779.
35. Graham, M. and J.M. Adams, *Chromosome 8 breakpoint far 3' of the c-myc oncogene in a Burkitt's lymphoma 2;8 variant translocation is equivalent to the murine pvt-1 locus.* The EMBO journal, 1986. **5**(11): p. 2845-2851.
36. Graham, M., J.M. Adams, and S. Cory, *Murine T lymphomas with retroviral inserts in the chromosomal 15 locus for plasmacytoma variant translocations.* Nature, 1985. **314**(6013): p. 740-3.
37. Colombo, T., et al., *PVT1: A Rising Star among Oncogenic Long Noncoding RNAs.* BioMed Research International, 2015. **2015**: p. 304208.
38. Ghafouri-Fard, S., M.D. Omrani, and M. Taheri, *Long noncoding RNA PVT1: A highly dysregulated gene in malignancy.* Journal of Cellular Physiology, 2020. **235**(2): p. 818-835.
39. Traversa, D., et al., *Unravelling similarities and differences in the role of circular and linear PVT1 in cancer and human disease.* British journal of cancer, 2022. **126**(6): p. 835-850.
40. Olivero, C.E., et al., *p53 Activates the Long Noncoding RNA Pvt1b to Inhibit Myc and Suppress Tumorigenesis.* Mol Cell, 2020. **77**(4): p. 761-774 e8.
41. Li, X., L. Yang, and L.L. Chen, *The Biogenesis, Functions, and Challenges of Circular RNAs.* Mol Cell, 2018. **71**(3): p. 428-442.

42. Huppi, K., et al., *The 8q24 gene desert: an oasis of non-coding transcriptional activity.* Frontiers in genetics, 2012. **3**: p. 69-69.
43. Siegel, R.L., et al., *Cancer statistics, 2022.* CA: A Cancer Journal for Clinicians, 2022. **72**(1): p. 7-33.
44. Momenimovahed, Z., et al., *Ovarian cancer in the world: epidemiology and risk factors.* International journal of women's health, 2019. **11**: p. 287-299.
45. Berek, J.S., et al., *Cancer of the ovary, fallopian tube, and peritoneum: 2021 update.* International Journal of Gynecology & Obstetrics, 2021. **155**(S1): p. 61-85.
46. Pignata, S., et al., *Treatment of recurrent epithelial ovarian cancer.* Cancer, 2019. **125**(S24): p. 4609-4615.
47. Cohen, P.A., et al., *Cervical cancer.* The Lancet, 2019. **393**(10167): p. 169-182.
48. Bhatla, N., et al., *Cancer of the cervix uteri: 2021 update.* International Journal of Gynecology & Obstetrics, 2021. **155**(S1): p. 28-44.
49. Dion, L., et al., *The Landscape and Therapeutic Implications of Molecular Profiles in Epithelial Ovarian Cancer.* Journal of clinical medicine, 2020. **9**(7): p. 2239.
50. Bowtell, D.D.L., *The genesis and evolution of high-grade serous ovarian cancer.* Nature Reviews Cancer, 2010. **10**(11): p. 803-808.
51. Hollis, R.L. and C. Gourley, *Genetic and molecular changes in ovarian cancer.* Cancer biology & medicine, 2016. **13**(2): p. 236-247.
52. Shih, I.-M., Y. Wang, and T.-L. Wang, *The Origin of Ovarian Cancer Species and Precancerous Landscape.* The American Journal of Pathology, 2021. **191**(1): p. 26-39.
53. Cortez, A.J., et al., *Advances in ovarian cancer therapy.* Cancer chemotherapy and pharmacology, 2018. **81**(1): p. 17-38.
54. Meijer, C.J.L.M. and R.D.M. Steenbergen, *Novel molecular subtypes of cervical cancer — potential clinical consequences.* Nature Reviews Clinical Oncology, 2017. **14**(7): p. 397-398.
55. Bell, D.W. and L.H. Ellenson, *Molecular Genetics of Endometrial Carcinoma.* Annual Review of Pathology: Mechanisms of Disease, 2019. **14**(1): p. 339-367.
56. Talhouk, A. and J.N. McAlpine, *New classification of endometrial cancers: the development and potential applications of genomic-based classification in research and clinical care.* Gynecologic Oncology Research and Practice, 2016. **3**(1): p. 14.
57. Yang, H.P., et al., *Endometrial cancer risk factors by 2 main histologic subtypes: the NIH-AARP Diet and Health Study.* American journal of epidemiology, 2013. **177**(2): p. 142-151.
58. Yang, Q., et al., *Long non-coding RNA PVT1 promotes cell proliferation and invasion through regulating miR-133a in ovarian cancer.* Biomedicine & pharmacotherapy = Biomedecine & pharmacotherapie, 2018. **106**: p. 61-67.
59. Ding, Y., et al., *Amplification of lncRNA PVT1 promotes ovarian cancer proliferation by binding to miR-140.* Mammalian Genome, 2019. **30**(7): p. 217-225.
60. Liu, G., et al., *lncRNA PVT1/MicroRNA-17-5p/PTEN Axis Regulates Secretion of E2 and P4, Proliferation, and Apoptosis of Ovarian Granulosa Cells in PCOS.* Molecular Therapy - Nucleic Acids, 2020. **20**: p. 205-216.
61. Qu, C., et al., *Long non-coding RNA PVT1-mediated miR-543/SERPINI1 axis plays a key role in the regulatory mechanism of ovarian cancer.* Bioscience Reports, 2020. **40**(6).
62. Yi, K., et al., *LncRNA PVT1 epigenetically stabilizes and post-transcriptionally regulates FOXM1 by acting as a microRNA sponge and thus promotes malignant behaviors of ovarian cancer cells.* American journal of translational research, 2020. **12**(6): p. 2860-2874.
63. Sun, X., L. Luo, and Y. Gao, *Circular RNA PVT1 enhances cell proliferation but inhibits apoptosis through sponging microRNA-149 in epithelial ovarian cancer.* J Obstet Gynaecol Res, 2020. **46**(4): p. 625-635.

64. Chen, Y., et al., *LncRNA PVT1 promotes ovarian cancer progression by silencing miR-214.* Cancer biology & medicine, 2018. **15**(3): p. 238-250.
65. Guo, J., et al., *miR-133a suppresses ovarian cancer cell proliferation by directly targeting insulin-like growth factor 1 receptor.* Tumour Biol, 2014. **35**(2): p. 1557-64.
66. Lan, H., et al., *miR-140-5p inhibits ovarian cancer growth partially by repression of PDGFRA.* Biomedicine & Pharmacotherapy, 2015. **75**: p. 117-122.
67. Wang, J., et al., *MiR-140-3p inhibits natural killer cytotoxicity to human ovarian cancer via targeting MAPK1.* J Biosci, 2020. **45**.
68. Fang, Y., C. Xu, and Y. Fu, *MicroRNA-17-5p induces drug resistance and invasion of ovarian carcinoma cells by targeting PTEN signaling.* Journal of biological research (Thessalonike, Greece), 2015. **22**: p. 12-12.
69. Michael Iv, T., Dan Feng, Nicholas, Samantha J Holdsworth, Kristen W Yeom & Heike E Daldrup-Link, *Clinical applications of iron oxide nanoparticles for magnetic resonance imaging of brain tumors.* Future Medicine, 2015.
70. Yu, Q., et al., *MiR-543 functions as tumor suppressor in ovarian cancer by targeting TWIST1.* J Biol Regul Homeost Agents, 2020. **34**(1): p. 101-110.
71. Sun, L., et al., *MicroRNA-149 suppresses the proliferation and increases the sensitivity of ovarian cancer cells to cisplatin by targeting X-linked inhibitor of apoptosis.* Oncology letters, 2018. **15**(5): p. 7328-7334.
72. Liu, J., et al., *miR-214 targets the PTEN-mediated PI3K/Akt signaling pathway and regulates cell proliferation and apoptosis in ovarian cancer.* Oncol Lett, 2017. **14**(5): p. 5711-5718.
73. Zhang, Q. and S. Zhang, *miR-214 promotes radioresistance in human ovarian cancer cells by targeting PETN.* Bioscience reports, 2017. **37**(4): p. BSR20170327.
74. Farhan, M., et al., *Role of FOXO Transcription Factors in Cancer Metabolism and Angiogenesis.* Cells, 2020. **9**(7): p. 1586.
75. Liu, E., et al., *Overexpression of long non-coding RNA PVT1 in ovarian cancer cells promotes cisplatin resistance by regulating apoptotic pathways.* International journal of clinical and experimental medicine, 2015. **8**(11): p. 20565-20572.
76. El-Khazragy, N., et al., *Tissue-based long non-coding RNAs "PVT1, TUG1 and MEG3" signature predicts Cisplatin resistance in ovarian Cancer.* Genomics, 2020. **112**(6): p. 4640-4646.
77. Liu, E., Z. Liu, and Y. Zhou, *Carboplatin-docetaxel-induced activity against ovarian cancer is dependent on up-regulated lncRNA PVT1.* International journal of clinical and experimental pathology, 2015. **8**(4): p. 3803-3810.
78. Guan, Y., et al., *Amplification of PVT1 Contributes to the Pathophysiology of Ovarian and Breast Cancer.* Clinical Cancer Research, 2007. **13**(19): p. 5745-5755.
79. Yamamoto, A., et al., *High amplification of PVT1 and MYC predict favorable prognosis in early ovarian carcinoma.* Pathology - Research and Practice, 2020. **216**(11): p. 153175.
80. Haverty, P.M., et al., *High-resolution analysis of copy number alterations and associated expression changes in ovarian tumors.* BMC Medical Genomics, 2009. **2**(1): p. 21.
81. Martini, P., et al., *lncRNAs as Novel Indicators of Patients' Prognosis in Stage I Epithelial Ovarian Cancer: A Retrospective and Multicentric Study.* Clinical Cancer Research, 2017. **23**(9): p. 2356-2366.
82. Filippov-Levy, N., et al., *Expression and clinical role of long non-coding RNA in high-grade serous carcinoma.* Gynecologic Oncology, 2018. **148**(3): p. 559-566.
83. Gao, Y.-L., et al., *Long Noncoding RNA PVT1 Facilitates Cervical Cancer Progression via Negative Regulating of miR-424.* Oncology research, 2017. **25**(8): p. 1391-1398.

84. Chang, Q.-Q., et al., *LncRNA PVT1 promotes proliferation and invasion through enhancing Smad3 expression by sponging miR-140-5p in cervical cancer.* Radiology and oncology, 2019. **53**(4): p. 443-452.
85. Wang, C., et al., *C-Myc-activated long non-coding RNA PVT1 enhances the proliferation of cervical cancer cells by sponging miR-486-3p.* The Journal of Biochemistry, 2020. **167**(6): p. 565-575.
86. Zhang, S., G. Zhang, and J. Liu, *Long noncoding RNA PVT1 promotes cervical cancer progression through epigenetically silencing miR-200b.* APMIS, 2016. **124**(8): p. 649-658.
87. Shen, C.-J., Y.-M. Cheng, and C.-L. Wang, *LncRNA PVT1 epigenetically silences miR-195 and modulates EMT and chemoresistance in cervical cancer cells.* Journal of Drug Targeting, 2017. **25**(7): p. 637-644.
88. Wang, X., et al., *miR-424 acts as a tumor radiosensitizer by targeting aprataxin in cervical cancer.* Oncotarget, 2016. **7**(47).
89. Zhou, Y., et al., *miR424-5p functions as an anti-oncogene in cervical cancer cell growth by targeting KDM5B via the Notch signaling pathway.* Life Sci, 2017. **171**: p. 9-15.
90. Guo, H., et al., *LncRNA SNHG20 promotes cell proliferation and invasion via miR-140-5p-ADAM10 axis in cervical cancer.* Biomedicine & Pharmacotherapy, 2018. **102**: p. 749-757.
91. Ye, H., et al., *MiR-486-3p targeting ECM1 represses cell proliferation and metastasis in cervical cancer.* Biomedicine & Pharmacotherapy, 2016. **80**: p. 109-114.
92. He, L., et al., *Effect of miRNA-200b on the proliferation and apoptosis of cervical cancer cells by targeting RhoA.* Open Medicine, 2020. **15**(1): p. 1019-1027.
93. Li, Z., et al., *MiR-195 inhibits the proliferation of human cervical cancer cells by directly targeting cyclin D1.* Tumor Biology, 2016. **37**(5): p. 6457-6463.
94. Zhong, J., et al., *MicroRNA-195 inhibits cell proliferation, migration and invasion by targeting defective in cullin neddylation 1 domain containing 1 in cervical cancer.* Int J Mol Med, 2018. **42**(2): p. 779-788.
95. Liu, X., et al., *MiR-195-5p Inhibits Malignant Progression of Cervical Cancer by Targeting YAP1.* Onco Targets Ther, 2020. **13**: p. 931-944.
96. Iden, M., et al., *The lncRNA PVT1 Contributes to the Cervical Cancer Phenotype and Associates with Poor Patient Prognosis.* PLOS ONE, 2016. **11**(5): p. e0156274.
97. Wang, H., et al., *Circular RNA circ_PVT1 induces epithelial-mesenchymal transition to promote metastasis of cervical cancer.* Aging, 2020. **12**(20): p. 20139-20151.
98. Yang, J.P., et al., *Long noncoding RNA PVT1 as a novel serum biomarker for detection of cervical cancer.* Eur Rev Med Pharmacol Sci, 2016. **20**(19): p. 3980-3986.
99. Wang, X., et al., *LncRNA PVT1 promotes the growth of HPV positive and negative cervical squamous cell carcinoma by inhibiting TGF-β1.* Cancer Cell International, 2018. **18**(1): p. 70.
100. Sun, W., et al., *Four Circulating Long Non-Coding RNAs Act as Biomarkers for Predicting Cervical Cancer.* Gynecologic and Obstetric Investigation, 2018. **83**(6): p. 533-539.
101. Kong, F., et al., *Long non-coding RNA PVT1 promotes malignancy in human endometrial carcinoma cells through negative regulation of miR-195-5p.* Biochimica et Biophysica Acta (BBA) - Molecular Cell Research, 2018. **1865**(10): p. 1479-1490.
102. Dong, P., et al., *Long noncoding RNA NEAT1 drives aggressive endometrial cancer progression via miR-361-regulated networks involving STAT3 and tumor microenvironment-related genes.* Journal of experimental & clinical cancer research : CR, 2019. **38**(1): p. 295-295.
103. Xing, T.-R., et al., *UPF1 Participates in the Progression of Endometrial Cancer by Inhibiting the Expression of lncRNA PVT1.* OncoTargets and therapy, 2020. **13**: p. 2103-2114.

104. Deng, J., et al., *MicroRNA-195 inhibits epithelial-mesenchymal transition by targeting G protein-coupled estrogen receptor 1 in endometrial carcinoma.* Mol Med Rep, 2019. **20**(5): p. 4023-4032.
105. Hanahan, D. and R.A. Weinberg, *Hallmarks of cancer: the next generation.* Cell, 2011. **144**(5): p. 646-74.
106. Siegel, R.L., K.D. Miller, and A. Jemal, *Cancer statistics, 2020.* CA: A Cancer Journal for Clinicians, 2020. **70**(1): p. 7-30.
107. Reid, B.M., J.B. Permuth, and T.A. Sellers, *Epidemiology of ovarian cancer: a review.* Cancer biology & medicine, 2017. **14**(1): p. 9-32.
108. Lheureux, S., et al., *Epithelial ovarian cancer.* Lancet, 2019. **393**(10177): p. 1240-1253.
109. Karnezis, A.N., et al., *The disparate origins of ovarian cancers: pathogenesis and prevention strategies.* Nature Reviews Cancer, 2017. **17**(1): p. 65-74.
110. Kumari, A., et al., *TGFβ signaling networks in ovarian cancer progression and plasticity.* Clin Exp Metastasis, 2021. **38**(2): p. 139-161.
111. Klemba, A., et al., *Hypoxia-Mediated Decrease of Ovarian Cancer Cells Reaction to Treatment: Significance for Chemo- and Immunotherapies.* Int J Mol Sci, 2020. **21**(24).
112. Rankin, E.B., J.-M. Nam, and A.J. Giaccia, *Hypoxia: Signaling the Metastatic Cascade.* Trends in cancer, 2016. **2**(6): p. 295-304.
113. Xu, W., et al., *Cell Stiffness Is a Biomarker of the Metastatic Potential of Ovarian Cancer Cells.* PLOS ONE, 2012. **7**(10): p. e46609.
114. Swaminathan, V., et al., *Mechanical stiffness grades metastatic potential in patient tumor cells and in cancer cell lines.* Cancer Res, 2011. **71**(15): p. 5075-80.
115. McKenzie, A.J., et al., *The mechanical microenvironment regulates ovarian cancer cell morphology, migration, and spheroid disaggregation.* Scientific Reports, 2018. **8**(1): p. 7228.
116. Lander, E.S., *Initial impact of the sequencing of the human genome.* Nature, 2011. **470**(7333): p. 187-197.
117. Rupaimoole, R. and F.J. Slack, *MicroRNA therapeutics: towards a new era for the management of cancer and other diseases.* Nature Reviews Drug Discovery, 2017. **16**(3): p. 203-222.
118. Oncul, S., et al., *Long non-coding RNAs in ovarian cancer: expression profile and functional spectrum.* RNA Biology, 2019: p. 1-12.
119. Tseng, Y.-Y., et al., *PVT1 dependence in cancer with MYC copy-number increase.* Nature, 2014. **512**(7512): p. 82-86.
120. Wang, W., et al., *PVT1 Promotes Cancer Progression via MicroRNAs.* Frontiers in Oncology, 2019. **9**(609).
121. Li, T., X.-l. Meng, and W.-q. Yang, *Long Noncoding RNA PVT1 Acts as a "Sponge" to Inhibit microRNA-152 in Gastric Cancer Cells.* Digestive Diseases and Sciences, 2017. **62**(11): p. 3021-3028.
122. Salamini-Montemurri, M., et al., *The Challenges and Opportunities of LncRNAs in Ovarian Cancer Research and Clinical Use.* Cancers, 2020. **12**(4): p. 1020.
123. Cerami, E., et al., *The cBio cancer genomics portal: an open platform for exploring multidimensional cancer genomics data.* Cancer Discov, 2012. **2**(5): p. 401-4.
124. Gao, J., et al., *Integrative analysis of complex cancer genomics and clinical profiles using the cBioPortal.* Sci Signal, 2013. **6**(269): p. pl1.
125. Bell, D., et al., *Integrated genomic analyses of ovarian carcinoma.* Nature, 2011. **474**(7353): p. 609-615.

126. Gyorffy, B., A. Lánczky, and Z. Szállási, *Implementing an online tool for genome-wide validation of survival-associated biomarkers in ovarian-cancer using microarray data from 1287 patients.* Endocr Relat Cancer, 2012. **19**(2): p. 197-208.
127. Nagy, Á., et al., *Validation of miRNA prognostic power in hepatocellular carcinoma using expression data of independent datasets.* Scientific Reports, 2018. **8**(1): p. 9227.
128. Yi, B.R., et al., *Alteration of epithelial-mesenchymal transition markers in human normal ovaries and neoplastic ovarian cancers.* Int J Oncol, 2015. **46**(1): p. 272-80.
129. Kim, W., et al., *Hippo signaling is intrinsically regulated during cell cycle progression by* APC/C^{Cdh1}. Proceedings of the National Academy of Sciences, 2019. **116**(19): p. 9423.
130. Dobrokhotov, O., et al., *Mechanoregulation and pathology of YAP/TAZ via Hippo and non-Hippo mechanisms.* Clin Transl Med, 2018. **7**(1): p. 23.
131. Piccolo, S., S. Dupont, and M. Cordenonsi, *The Biology of YAP/TAZ: Hippo Signaling and Beyond.* Physiological Reviews, 2014. **94**(4): p. 1287-1312.
132. Yu, F.X., et al., *Regulation of the Hippo-YAP pathway by G-protein-coupled receptor signaling.* Cell, 2012. **150**(4): p. 780-91.
133. Liu-Chittenden, Y., et al., *Genetic and pharmacological disruption of the TEAD-YAP complex suppresses the oncogenic activity of YAP.* Genes Dev, 2012. **26**(12): p. 1300-5.
134. Noviello, T.M.R., et al., *Detection of long non–coding RNA homology, a comparative study on alignment and alignment–free metrics.* BMC Bioinformatics, 2018. **19**(1): p. 407.
135. Zampetaki, A., A. Albrecht, and K. Steinhofel, *Long Non-coding RNA Structure and Function: Is There a Link?* Frontiers in Physiology, 2018. **9**(1201).
136. Cai, Q., L. Yan, and Y. Xu, *Anoikis resistance is a critical feature of highly aggressive ovarian cancer cells.* Oncogene, 2015. **34**(25): p. 3315-24.
137. Yaginuma, Y. and H. Westphal, *Abnormal structure and expression of the p53 gene in human ovarian carcinoma cell lines.* Cancer Res, 1992. **52**(15): p. 4196-9.
138. Nakayama, J., et al., *Decreased peritoneal ovarian cancer growth in mice lacking expression of lipid phosphate phosphohydrolase 1.* PLoS One, 2015. **10**(3): p. e0120071.
139. Jin, K., et al., *Long non-coding RNA PVT1 interacts with MYC and its downstream molecules to synergistically promote tumorigenesis.* Cellular and molecular life sciences : CMLS, 2019. **76**(21): p. 4275-4289.
140. Cho, S.W., et al., *Promoter of lncRNA Gene PVT1 Is a Tumor-Suppressor DNA Boundary Element.* Cell, 2018. **173**(6): p. 1398-1412.e22.
141. Sud, A., B. Kinnersley, and R.S. Houlston, *Genome-wide association studies of cancer: current insights and future perspectives.* Nature Reviews Cancer, 2017. **17**(11): p. 692-704.
142. Goode, E.L., et al., *A genome-wide association study identifies susceptibility loci for ovarian cancer at 2q31 and 8q24.* Nat Genet, 2010. **42**(10): p. 874-9.
143. Phelan, C.M., et al., *Identification of 12 new susceptibility loci for different histotypes of epithelial ovarian cancer.* Nature Genetics, 2017. **49**(5): p. 680-691.
144. Dang, Chi V., *MYC on the Path to Cancer.* Cell, 2012. **149**(1): p. 22-35.
145. Yu, F., et al., *Hypoxia induces the activation of hepatic stellate cells through the PVT1-miR-152-ATG14 signaling pathway.* Molecular and Cellular Biochemistry, 2020. **465**(1): p. 115-123.
146. Wang, C., et al., *LncRNA PVT1 regulate expression of HIF1α via functioning as ceRNA for miR-199a-5p in non-small cell lung cancer under hypoxia.* Mol Med Rep, 2018. **17**(1): p. 1105-1110.
147. Zhang, X., et al., *The Hippo pathway transcriptional co-activator, YAP, is an ovarian cancer oncogene.* Oncogene, 2011. **30**(25): p. 2810-22.

148. Xia, Y., et al. *YAP promotes ovarian cancer cell tumorigenesis and is indicative of a poor prognosis for ovarian cancer patients*. PloS one, 2014. **9**, e91770 DOI: 10.1371/journal.pone.0091770.
149. Han, Y., *Analysis of the role of the Hippo pathway in cancer.* Journal of Translational Medicine, 2019. **17**(1): p. 116.
150. Huang, R.Y., et al., *An EMT spectrum defines an anoikis-resistant and spheroidogenic intermediate mesenchymal state that is sensitive to e-cadherin restoration by a src-kinase inhibitor, saracatinib (AZD0530).* Cell Death Dis, 2013. **4**(11): p. e915.
151. Zanconato, F., M. Cordenonsi, and S. Piccolo, *YAP/TAZ at the Roots of Cancer.* Cancer Cell, 2016. **29**(6): p. 783-803.
152. Grannas, K., et al., *Crosstalk between Hippo and TGFβ: Subcellular Localization of YAP/TAZ/Smad Complexes.* Journal of Molecular Biology, 2015. **427**(21): p. 3407-3415.
153. Verduci, L., et al., *The oncogenic role of circPVT1 in head and neck squamous cell carcinoma is mediated through the mutant p53/YAP/TEAD transcription-competent complex.* Genome Biology, 2017. **18**(1): p. 237.
154. Xu, M.-d., et al., *A Positive Feedback Loop of lncRNA-PVT1 and FOXM1 Facilitates Gastric Cancer Growth and Invasion.* Clinical Cancer Research, 2017. **23**(8): p. 2071.
155. Zhao, J., et al., *LncRNA PVT1 promotes angiogenesis via activating the STAT3/VEGFA axis in gastric cancer.* Oncogene, 2018. **37**(30): p. 4094-4109.
156. Fan, Q., Q. Cai, and Y. Xu, *FOXM1 is a downstream target of LPA and YAP oncogenic signaling pathways in high grade serous ovarian cancer.* Oncotarget; Vol 6, No 29, 2015.
157. Barsotti, A.M., et al., *p53-Dependent induction of PVT1 and miR-1204.* The Journal of biological chemistry, 2012. **287**(4): p. 2509-2519.
158. Li, Y., et al., *Pan-cancer characterization of immune-related lncRNAs identifies potential oncogenic biomarkers.* Nat Commun, 2020. **11**(1): p. 1000.
159. Zeng, C.-M., et al., *Aldo–Keto Reductase AKR1C1–AKR1C4: Functions, Regulation, and Intervention for Anti-cancer Therapy.* Frontiers in Pharmacology, 2017. **8**(119).
160. Matsunaga, T., et al., *Aldo-Keto Reductase 1B10 and Its Role in Proliferation Capacity of Drug-Resistant Cancers.* Front Pharmacol, 2012. **3**: p. 5.
161. Heibein, A.D., et al., *Role of aldo-keto reductases and other doxorubicin pharmacokinetic genes in doxorubicin resistance, DNA binding, and subcellular localization.* BMC Cancer, 2012. **12**(1): p. 381.
162. DiStefano, J.K. and B. Davis, *Diagnostic and Prognostic Potential of AKR1B10 in Human Hepatocellular Carcinoma.* Cancers (Basel), 2019. **11**(4).
163. Zhang, S., et al., *Identification of the molecular basis of doxorubicin-induced cardiotoxicity.* Nat Med, 2012. **18**(11): p. 1639-42.
164. Arun, G., S.D. Diermeier, and D.L. Spector, *Therapeutic Targeting of Long Non-Coding RNAs in Cancer.* Trends Mol Med, 2018. **24**(3): p. 257-277.
165. Varadaraj, A., et al., *Epigenetic Regulation of GDF2 Suppresses Anoikis in Ovarian and Breast Epithelia.* Neoplasia, 2015. **17**(11): p. 826-38.
166. Jazaeri, A.A., et al., *Molecular Requirements for Transformation of Fallopian Tube Epithelial Cells into Serous Carcinoma.* Neoplasia, 2011. **13**(10): p. 899-IN16.
167. Mi, H., et al., *PANTHER version 14: more genomes, a new PANTHER GO-slim and improvements in enrichment analysis tools.* Nucleic Acids Res, 2019. **47**(D1): p. D419-d426.
168. Vichai, V. and K. Kirtikara, *Sulforhodamine B colorimetric assay for cytotoxicity screening.* Nat Protoc, 2006. **1**(3): p. 1112-6.
169. Dobin, A., et al., *STAR: ultrafast universal RNA-seq aligner.* Bioinformatics, 2013. **29**(1): p. 15-21.

170. Patro, R., et al., *Salmon provides fast and bias-aware quantification of transcript expression.* Nat Methods, 2017. **14**(4): p. 417-419.
171. Love, M.I., W. Huber, and S. Anders, *Moderated estimation of fold change and dispersion for RNA-seq data with DESeq2.* Genome Biology, 2014. **15**(12): p. 550.
172. Subramanian, A., et al., *Gene set enrichment analysis: A knowledge-based approach for interpreting genome-wide expression profiles.* Proceedings of the National Academy of Sciences, 2005. **102**(43): p. 15545.
173. Mootha, V.K., et al., *PGC-1α-responsive genes involved in oxidative phosphorylation are coordinately downregulated in human diabetes.* Nature Genetics, 2003. **34**(3): p. 267-273.
174. Sung, H., et al., *Global Cancer Statistics 2020: GLOBOCAN Estimates of Incidence and Mortality Worldwide for 36 Cancers in 185 Countries.* CA: A Cancer Journal for Clinicians, 2021. **71**(3): p. 209-249.
175. Reed, N.S. and A.H. Sadozye, *Update on chemotherapy in gynaecological cancers.* The Obstetrician & Gynaecologist, 2016. **18**(3): p. 182-188.
176. Reed, N.S. and A.H. Sadozye, *Update on radiotherapy in gynaecological malignancies.* The Obstetrician & Gynaecologist, 2017. **19**(1): p. 29-36.
177. Basu, P., A. Mukhopadhyay, and I. Konishi, *Targeted therapy for gynecologic cancers: Toward the era of precision medicine.* International Journal of Gynecology & Obstetrics, 2018. **143**(S2): p. 131-136.
178. Lynam, S., A.A. Lugade, and K. Odunsi, *Immunotherapy for Gynecologic Cancer: Current Applications and Future Directions.* Clinical obstetrics and gynecology, 2020. **63**(1): p. 48-63.
179. Statello, L., et al., *Gene regulation by long non-coding RNAs and its biological functions.* Nature Reviews Molecular Cell Biology, 2020.
180. Carlevaro-Fita, J., et al., *Cancer LncRNA Census reveals evidence for deep functional conservation of long noncoding RNAs in tumorigenesis.* Communications Biology, 2020. **3**(1): p. 56.
181. Anastasiadou, E., L.S. Jacob, and F.J. Slack, *Non-coding RNA networks in cancer.* Nature Reviews Cancer, 2018. **18**(1): p. 5-18.
182. He, J., et al., *Long non-coding RNA in cervical cancer: From biology to therapeutic opportunity.* Biomedicine & Pharmacotherapy, 2020. **127**: p. 110209.
183. Liu, H., J. Wan, and J. Chu, *Long non-coding RNAs and endometrial cancer.* Biomedicine & Pharmacotherapy, 2019. **119**: p. 109396.
184. Calanca, N., et al., *The Interplay between Long Noncoding RNAs and Proteins of the Epigenetic Machinery in Ovarian Cancer.* Cancers (Basel), 2020. **12**(9).
185. Onagoruwa, O.T., et al., *Oncogenic Role of PVT1 and Therapeutic Implications.* Frontiers in Oncology, 2020. **10**(17).
186. Yang, T., et al., *lncRNA PVT1 and its splicing variant function as competing endogenous RNA to regulate clear cell renal cell carcinoma progression.* Oncotarget, 2017. **8**(49): p. 85353-85367.
187. Chen, J., et al., *Circular RNA profile identifies circPVT1 as a proliferative factor and prognostic marker in gastric cancer.* Cancer Letters, 2017. **388**: p. 208-219.
188. Albertson, D.G., *Gene amplification in cancer.* Trends in Genetics, 2006. **22**(8): p. 447-455.
189. Sieh, W., et al., *Hormone-receptor expression and ovarian cancer survival: an Ovarian Tumor Tissue Analysis consortium study.* The Lancet. Oncology, 2013. **14**(9): p. 853-862.
190. Zhai, Y., et al., *Loss of estrogen receptor 1 enhances cervical cancer invasion.* The American journal of pathology, 2010. **177**(2): p. 884-895.

191. Rodriguez, A.C., et al., *Estrogen Signaling in Endometrial Cancer: a Key Oncogenic Pathway with Several Open Questions.* Hormones & cancer, 2019. **10**(2-3): p. 51-63.
192. O'Mara, T.A., M. Zhao, and A.B. Spurdle, *Meta-analysis of gene expression studies in endometrial cancer identifies gene expression profiles associated with aggressive disease and patient outcome.* Scientific reports, 2016. **6**: p. 36677-36677.
193. Liberzon, A., et al., *The Molecular Signatures Database (MSigDB) hallmark gene set collection.* Cell systems, 2015. **1**(6): p. 417-425.
194. Williams, G.H. and K. Stoeber, *The cell cycle and cancer.* The Journal of Pathology, 2012. **226**(2): p. 352-364.
195. Yu, K., et al., *Estrogen Receptor Function: Impact on the Human Endometrium.* Frontiers in Endocrinology, 2022. **13**.
196. Levine, D.A., et al., *Integrated genomic characterization of endometrial carcinoma.* Nature, 2013. **497**(7447): p. 67-73.
197. Olivero, C.E., et al., *p53 Activates the Long Noncoding RNA Pvt1b to Inhibit Myc and Suppress Tumorigenesis.* Molecular Cell, 2020. **77**(4): p. 761-774.e8.
198. Santarius, T., et al., *A census of amplified and overexpressed human cancer genes.* Nature Reviews Cancer, 2010. **10**(1): p. 59-64.
199. Cong, R., et al., *The PVT1/miR-612/CENP-H/CDK1 axis promotes malignant progression of advanced endometrial cancer.* American journal of cancer research, 2021. **11**(4): p. 1480-1502.
200. Derveaux, S., J. Vandesompele, and J. Hellemans, *How to do successful gene expression analysis using real-time PCR.* Methods, 2010. **50**(4): p. 227-230.
201. Wang, Y.-Y., et al., *Elevated Circular RNA PVT1 Promotes Eutopic Endometrial Cell Proliferation and Invasion of Adenomyosis via miR-145/Talin1 Axis.* BioMed research international, 2021. **2021**: p. 8868700-8868700.
202. Berger, A.C., et al., *A Comprehensive Pan-Cancer Molecular Study of Gynecologic and Breast Cancers.* Cancer Cell, 2018. **33**(4): p. 690-705.e9.
203. Yamamoto, A., et al., *High amplification of PVT1 and MYC predict favorable prognosis in early ovarian carcinoma.* Pathol Res Pract, 2020. **216**(11): p. 153175.
204. Schaub, F.X., et al., *Pan-cancer Alterations of the MYC Oncogene and Its Proximal Network across the Cancer Genome Atlas.* Cell Systems, 2018. **6**(3): p. 282-300.e2.
205. Kong, R., et al., *Long noncoding RNA PVT1 indicates a poor prognosis of gastric cancer and promotes cell proliferation through epigenetically regulating p15 and p16.* Mol Cancer, 2015. **14**: p. 82.
206. Wang, C., et al., *Upregulated plasmacytoma variant translocation 1 promotes cell proliferation, invasion and metastasis in colorectal cancer.* Molecular medicine reports, 2018. **17**(5): p. 6598-6604.
207. Chen, J., et al., *Circular RNA profile identifies circPVT1 as a proliferative factor and prognostic marker in gastric cancer.* Cancer Lett, 2017. **388**: p. 208-219.
208. Chiu, H.-S., et al., *Pan-Cancer Analysis of lncRNA Regulation Supports Their Targeting of Cancer Genes in Each Tumor Context.* Cell Reports, 2018. **23**(1): p. 297-312.e12.
209. Backes, F.J., et al., *Estrogen receptor-alpha as a predictive biomarker in endometrioid endometrial cancer.* Gynecologic oncology, 2016. **141**(2): p. 312-317.
210. Smith, D., et al., *ER and PR expression and survival after endometrial cancer.* Gynecologic Oncology, 2018. **148**(2): p. 258-266.
211. Ethier, J.L., et al., *Is hormonal therapy effective in advanced endometrial cancer? A systematic review and meta-analysis.* Gynecol Oncol, 2017. **147**(1): p. 158-166.

212. Giannone, G., et al., *Role of Cyclin-Dependent Kinase Inhibitors in Endometrial Cancer.* International journal of molecular sciences, 2019. **20**(9): p. 2353.
213. Hu, J., J. Shen, and J. Sun, *CDK4/RB/E2Fs axis as potential therapeutic target of endometrial cancer.* Biomed Pharmacother, 2020. **125**: p. 109870.
214. Potts, P.R. and H. Yu, *The SMC5/6 complex maintains telomere length in ALT cancer cells through SUMOylation of telomere-binding proteins.* Nature Structural & Molecular Biology, 2007. **14**(7): p. 581-590.
215. Cerami, E., et al., *The cBio cancer genomics portal: an open platform for exploring multidimensional cancer genomics data.* Cancer discovery, 2012. **2**(5): p. 401-404.
216. Gao, J., et al., *Integrative analysis of complex cancer genomics and clinical profiles using the cBioPortal.* Science signaling, 2013. **6**(269): p. pl1-pl1.
217. Li, B. and C.N. Dewey, *RSEM: accurate transcript quantification from RNA-Seq data with or without a reference genome.* BMC Bioinformatics, 2011. **12**(1): p. 323.
218. Raudvere, U., et al., *g:Profiler: a web server for functional enrichment analysis and conversions of gene lists (2019 update).* Nucleic Acids Res, 2019. **47**(W1): p. W191-w198.
219. Wang, Q., et al., *Targeted therapies in gynecological cancers: a comprehensive review of clinical evidence.* Signal Transduction and Targeted Therapy, 2020. **5**(1): p. 137.
220. Gerber, D.E., *Targeted therapies: a new generation of cancer treatments.* Am Fam Physician, 2008. **77**(3): p. 311-9.
221. Zhao, M., et al., *Long non-coding RNAs involved in gynecological cancer.* Int J Gynecol Cancer, 2014. **24**(7): p. 1140-5.
222. Gabory, A., et al., *The H19 gene: regulation and function of a non-coding RNA.* Cytogenetic and Genome Research, 2006. **113**(1-4): p. 188-193.
223. Yang, J., et al., *LncRNA H19: A novel oncogene in multiple cancers.* International journal of biological sciences, 2021. **17**(12): p. 3188-3208.
224. Yuan, C., Y. Ning, and Y. Pan, *Emerging roles of HOTAIR in human cancer.* Journal of Cellular Biochemistry, 2020. **121**(5-6): p. 3235-3247.
225. Ji, P., et al., *MALAT-1, a novel noncoding RNA, and thymosin β4 predict metastasis and survival in early-stage non-small cell lung cancer.* Oncogene, 2003. **22**(39): p. 8031-8041.
226. Chen, Y., et al., *Long non-coding RNAs: From disease code to drug role.* Acta Pharmaceutica Sinica B, 2021. **11**(2): p. 340-354.
227. Winkle, M., et al., *Noncoding RNA therapeutics — challenges and potential solutions.* Nature Reviews Drug Discovery, 2021. **20**(8): p. 629-651.
228. Pan, X., G. Zheng, and C. Gao, *LncRNA PVT1: a Novel Therapeutic Target for Cancers.* Clin Lab, 2018. **64**(5): p. 655-662.
229. Mao, B., et al., *Hippo signaling in stress response and homeostasis maintenance.* Acta Biochimica et Biophysica Sinica, 2014. **47**(1): p. 2-9.
230. Xu, Y., et al., *LncRNA PVT1 up-regulation is a poor prognosticator and serves as a therapeutic target in esophageal adenocarcinoma.* Molecular Cancer, 2019. **18**(1): p. 141.
231. Lan, T., et al., *Long non-coding RNA PVT1 serves as a competing endogenous RNA for miR-186-5p to promote the tumorigenesis and metastasis of hepatocellular carcinoma.* Tumor Biology, 2017. **39**(6): p. 1010428317705338.
232. Lan, T., et al., *Long non-coding RNA PVT1 serves as a competing endogenous RNA for miR-186-5p to promote the tumorigenesis and metastasis of hepatocellular carcinoma.* Tumour Biol, 2017. **39**(6): p. 1010428317705338.
233. Cui, D., et al., *Long non-coding RNA PVT1 as a novel biomarker for diagnosis and prognosis of non-small cell lung cancer.* Tumour Biol, 2016. **37**(3): p. 4127-34.

234. Llombart, V. and M.R. Mansour, *Therapeutic targeting of “undruggable” MYC.* eBioMedicine, 2022. **75**.
235. Liu, W., D. Yao, and B. Huang, *LncRNA PVT1 promotes cervical cancer progression by sponging miR-503 to upregulate ARL2 expression.* Open life sciences, 2021. **16**(1): p. 1-13.
236. Wu, Y., et al., *LncRNA PVT1 promotes the progression of ovarian cancer by activating TGF-β pathway via miR-148a-3p/AGO1 axis.* J Cell Mol Med, 2021. **25**(17): p. 8229-8243.
237. Chen, Y., et al., *Atezolizumab and blockade of LncRNA PVT1 attenuate cisplatin resistant ovarian cancer cells progression synergistically via JAK2/STAT3/PD-L1 pathway.* Clinical Immunology, 2021. **227**: p. 108728.
238. Li, M., et al., *Circular PVT1 regulates cell proliferation and invasion via miR-149-5p/FOXM1 axis in ovarian cancer.* Journal of Cancer, 2021. **12**(2): p. 611-621.
239. Li, T., et al., *Ketamine Inhibits Ovarian Cancer Cell Growth by Regulating the lncRNA-PVT1/EZH2/p57 Axis.* Frontiers in genetics, 2021. **11**: p. 597467-597467.

APPENDIX A

Literature Summary of PVT1 role in the main gynecological cancers

Table A.1: Summary of PVT1 role in the main gynecological cancers (endometrial, cervical and ovarian)

Sample type	Function	Downstream target	Upstream target	Primer target	Year and reference
Endometrial cancer					
- Adenomyosis patients - Eu_EEC, Eu_ESC cell lines	Proliferation, invasion, colony formation	miR-145/Talin 1/		CircPVT1 (Exon 2)	2021 [201]
- Endometrial cancer tissues - HEC-1A, Ishikawa cell lines	Proliferation, migration, invasion, cell cycle progression, apoptosis resistance	miR-612/CENP-H/CDK1		Exon 2	2021[199]
-Endometrial carcinoma patients -AN3CA, KLE, RL-95, HEC1A, and Ishikawa cell lines	Proliferation, migration	/	UPF1	Exon 6-7	2020 [103]
-HEC-50 cell lines	Invasion, Sphere-formation, chemo resistance	/	/	Microarray	2019 [102]
-Endometrial carcinoma patients -HEC1A, Ishikawa cell lines	Migration, invasion, cell cycle progression, apoptosis resistance	miR-195-5p /FGFR1/FGF2	/	Exon 2	2018 [101]
Cervical cancer					
- Cervical cancer patients - H8, CC HeLa and SIHA cell lines	Proliferation, migration, invasion, apoptosis resistance	miR-503/ARL2	/	Exon 8-9	2021 [235]
- Cervical cancer patients	Proliferation, migration, colony	miR-1286	/	hsa_circ_0009143	2020 [97]

- HUCEC, C33A, HCC-94, HELA, CASKI cell lines	formation, invasion, EMT				
- Cervical cancer patients - HELA, SIHA cell lines	Proliferation	miR-486-3p /ECM1	/	Exon 6-7	2020 [85]
- END1/E6E7, HELA, SIHA cell lines	Proliferation, migration, invasion, colony formation	miR-140-5p /SMAD3	/	Exon 8-9	2019 [84]
- Cervical squamous carcinoma cancer patients / Plasma	Biomarker	/	/	Microarray	2018 [100]
- Cervical squamous cell carcinoma cancer patients / Serum - SIHA, C33A, ECT1/ E6E7, HCVEPC cell lines	Biomarker, proliferation	/	/	Exon 5-6	2018 [99]
- SIHA, HELA, ECT1/ E6E7, C cell lines	Proliferation, migration, invasion,	miR-424	/	Not mentioned	2017 [83]
- Cervical cancer patients - HELA, SIHA cell lines	Proliferation, migration, cell cycle progression	EZH2/miR-200b	/	Exon 6-8	2016 [86]
- Cervical carcinoma patients - HELA, SIHA, DOTC2 4510, ECT1/ E6E7 cell lines	Proliferation, migration, invasion, apoptosis resistance, chemo resistance	Nucleolin	Hypoxia, INF-α	Exon 2-3	2016 [96]
- Cervical carcinoma patients/ Serum	Biomarker	/	/	Exon 6-8	2016 [98]
- CASKI, SIHA cell lines	Chemo resistance, EMT	EZH2/miR-195	/	Exon 6-8	2016 [87]
Ovarian cancer					
-Ovarian cancer patients - SKOV3, A2780, COC1, OVCAR3, CAOV3 cell lines	Proliferation, apoptosis resistance, cell cycle progression	miR-148a-3p/AGO1	/	Exon 2-4	2021 [236]
- Epithelial ovarian cancer patients with cisplatin resistant - A2780cis cell line	Proliferation, invasion, apoptosis resistance, cell cycle progression	JAK/STAT3/PD-L1	/	Exon 5-6	2021 [237]

- SKOV3, A2780 cell lines	Proliferation, migration, invasion	miR-149-5p/FOXM1	/	circPVT1 (Exon 2)	2021 [238]
- OVCAR-3, SKOV3, A2780, 3AO, COC1, OV-90, HOSEpiC cell lines	Proliferation, cell cycle progression, apoptosis resistance, colony formation	EZH2/p57	Ketamine	Exon 5-6	2020 [239]
- FFPE epithelial ovarian cancer patients - OVSAHO cell line	Biomarker	MYC	/	Exon 2	2020 [79]
- FFPE ovarian cancer patients	Biomarker	/	/	Not mentioned	2020 [76]
- SKOV3, OVCAR3, ALST, ES2, IOSE80 cell lines	Proliferation, migration, invasion, cell cycle progression, colony formation, sphere formation	- miR-370-5p/FOXM1 - miR-526-5p	/	Exon 3-4	2020 [62]
- Ovarian cancer patients - OVCAR-3, A2780, TOV-112D, HOSEPIC	Proliferation, migration, invasion, apoptosis resistance	miR-543/SERPINI1	/	Not mentioned	2020 [61]
- Polycystic ovary syndrome patients/Serum - Oocyte-corona radiata cell-cumulus cells	Colony formation, proliferation, apoptosis resistance, cell cycle progression	miR-17-5p/PTEN	/	Exon 5-6	2020 [60]
- AOV3, SKOV3, OVCAR3, SNU119, HOSEPIC cell lines	Proliferation, apoptosis resistance,	miR-149	/	circPVT1	2020 [63]
-TCGA data - A2780, SKOV3 cell lines	Proliferation, cell cycle progression	miR-140	FOXO4	Exon 2-3	2019 [59]
- Epithelial ovarian cancer patients - HO8910, SKOV3, ES2, SW626, A2780 cell lines	Proliferation, migration, invasion	EZH2/miR-214	/	Exon 5-6	2018 [64]
- Ovarian cancer patients - HEY, SKOV-3, OVCAR-3, IOSE80 cell lines	Proliferation, migration, invasion, cell cycle progression	miR-133a	/	Exon 5-6	2018 [58]
- High-grades serous carcinoma patients	Biomarker	/	/	Microarray	2018 [82]

- Ovarian cancer patients - OVCAR3, OVCAR8, A2780, OVCA432, CAOV3 cell lines	Biomarker	/	/	Exon 2	2017 [81]
- Ovarian cancer patients - SKOV3, A2780 cell lines	Chemo resistance	/	/	Not mentioned	2015 [75]
- 3AO cell line	Proliferation	/	/	Exon 2-3	2015 [77]
- Ovarian cancer patients	Biomarker	/	/	Microarray	2009 [80]
- A2780, CAOV3, CAOV4, DOV13, ES2, HEY, OCC1, OV90, OVCA420, OVCA429, OVCA432, OVCA433, OVCAR3, OVCAR5, OVCAR8, PA1, SKOV3, SW626, TOV112D, TOV21G cell lines	Proliferation, apoptosis resistance	/	/	Exon 2-3	2007 [78]

APPENDIX B

Supplementary figures from Chapter 2 and Chapter 3

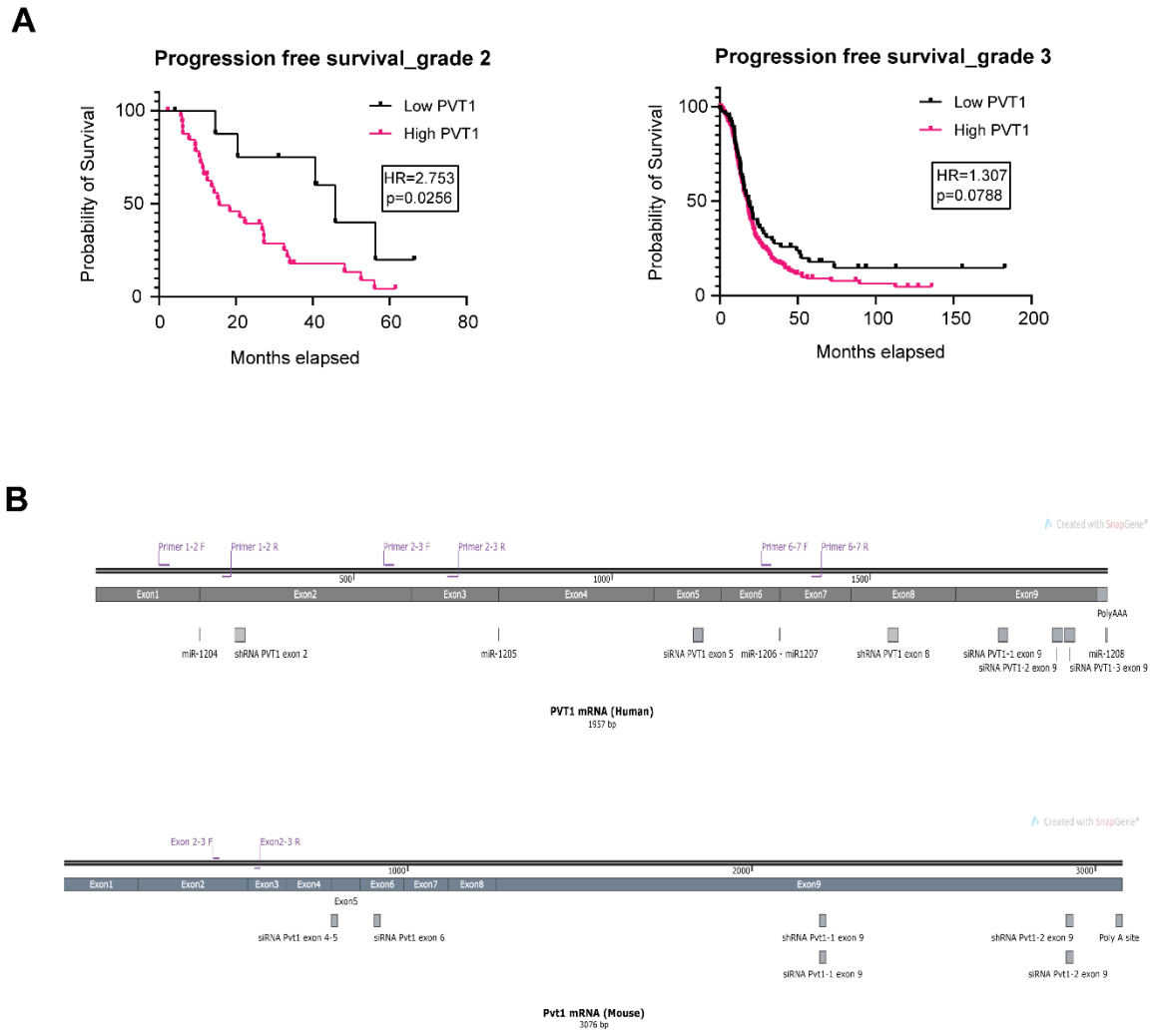

Figure B. 1**:** Progression-free survival per grade as well as PVT1 human and mouse sequences.
(A) Kaplan–Meier analysis for progression-free survival of grades 2 and 3 (log-rank statistics) for ovarian cancer from TCGA. (B) Schematic of PVT1 primer sets and PVT1 shRNAs for human and mouse PVT1 sequence.

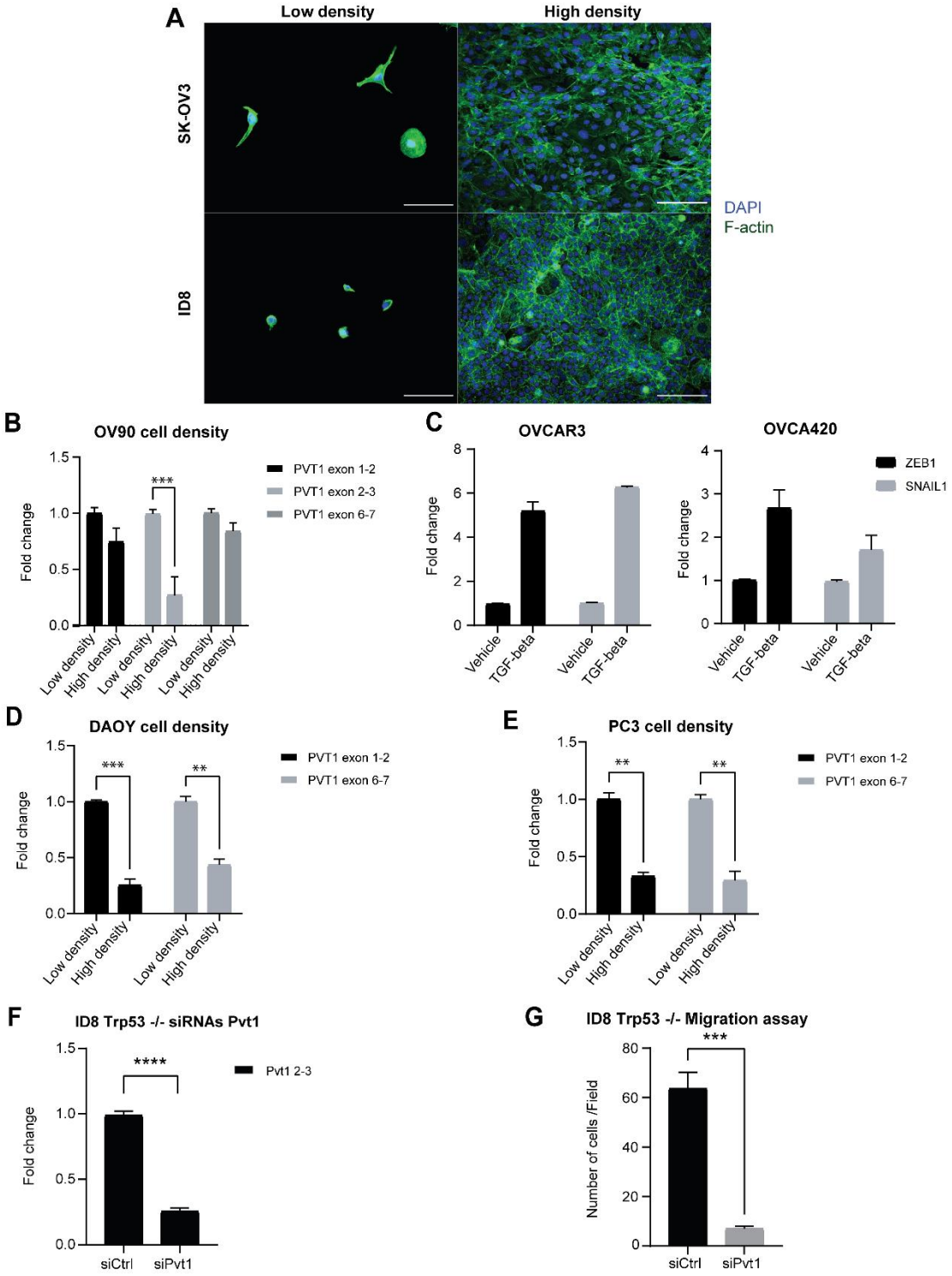

Figure B. 2**:** Cell-cell contact verification and ID8 Trp53 migration assay.
(A) Cell–cell contact staining with F-actin for low and high density SK-OV3 and ID8 cells–scale bar: 100 μm. (B) RT-qPCR analysis of PVT1 RNA at different densities in OV90 cells (two-way ANOVA-Sidak's multiple comparisons test: exon 2–3, P = 0.0005; N = 3) normalized to low density levels. (C) RT-qPCR analysis of indicated genes in OVCAR3

and OVCA420 cells after treatment with 200 pM TGF-β1 for 96 h normalized to vehicle control cells. (D) RT-qPCR analysis of PVT1 RNA at different cell densities in DAOY cells normalized to the low density levels (two-way ANOVA-Sidak multiple comparisons test: exon 1–2, P = 0.0006; exon 6–7, P = 0.0018; N = 2). (E) RT-qPCR analysis of PVT1 RNA at different cell densities in PC3 cells normalized to the low density levels (two-way ANOVA-Sidak multiple comparisons test: exon 1–2, P = 0.0021; exon 6–7, P = 0.0017; N = 2). (F) RT-qPCR of Pvt1 in siPvt1 or siCtrl mouse cells (ID8 Trp53−/−) (unpaired two-tailed t test: P < 0.0001) normalized to levels in siCtrl cells. (G) Transwell migration analysis of siRNA Pvt1 or siCtrl ID8 Trp53−/− cells after 6 h of migration (unpaired two-tailed t test: P = 0.0001; N = 3).

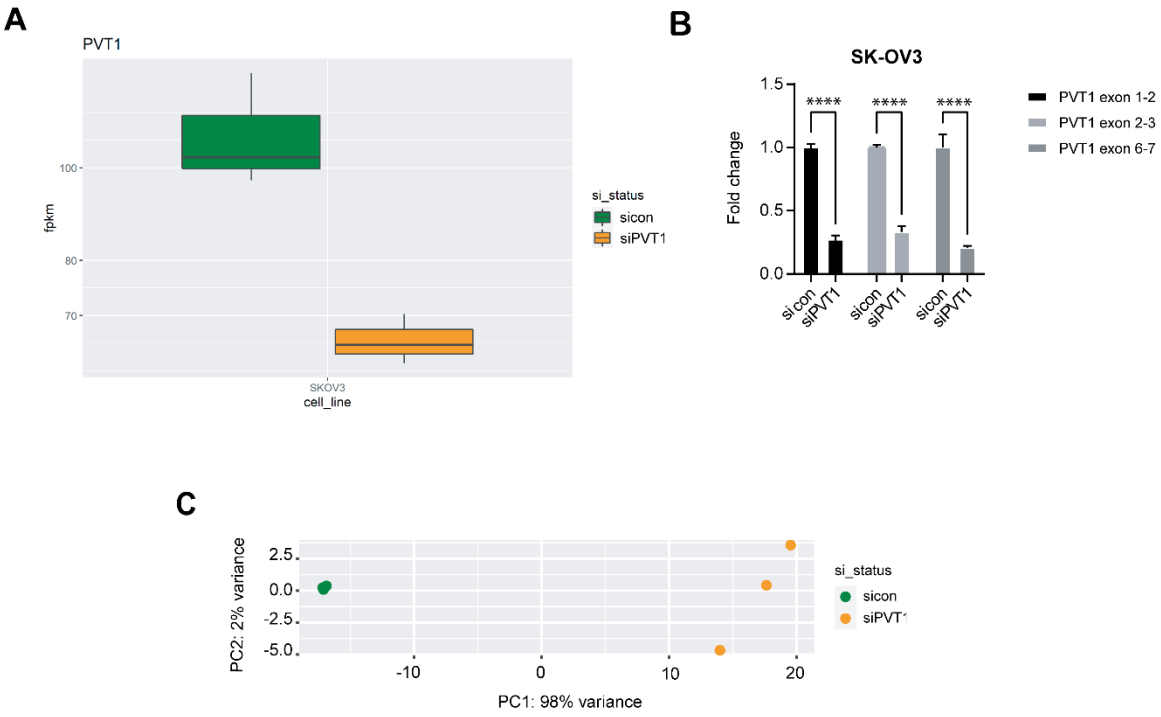

Figure B. 3: PVT1 RNA sequencing verification.
(A) PVT1 expression (RPKM) in sictrl or siPVT1. (B) RT-qPCR analysis of PVT1 in siPVT1 or siCtrl SK-OV3 normalized to values in sicon cells (2way ANOVA – Sidak's multiple testing - exon 1-2 P < 0.0001; exon 2-3 P < 0.0001; exon 6-7 P< 0.0001 – N = 2). (C) Principal component analysis (PCA) plot of sicon versus siPVT1.

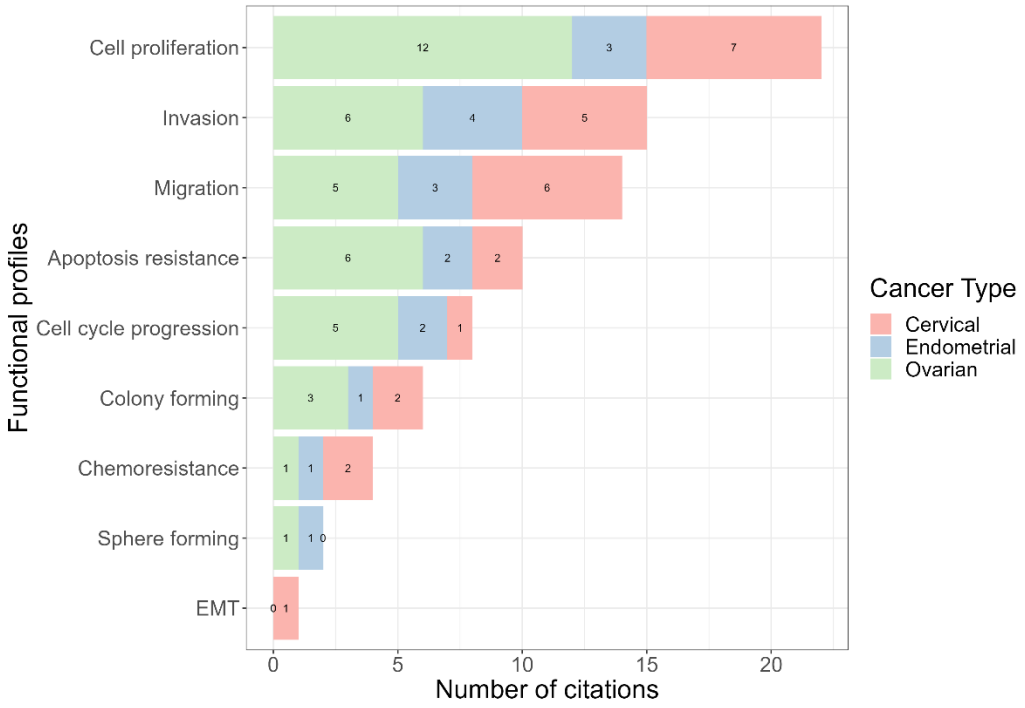

Figure B. 4: Functional profiling of PVT1.
Functional profiling of PVT1 per cancer type based on investigated functions in the literature (Table A.1).

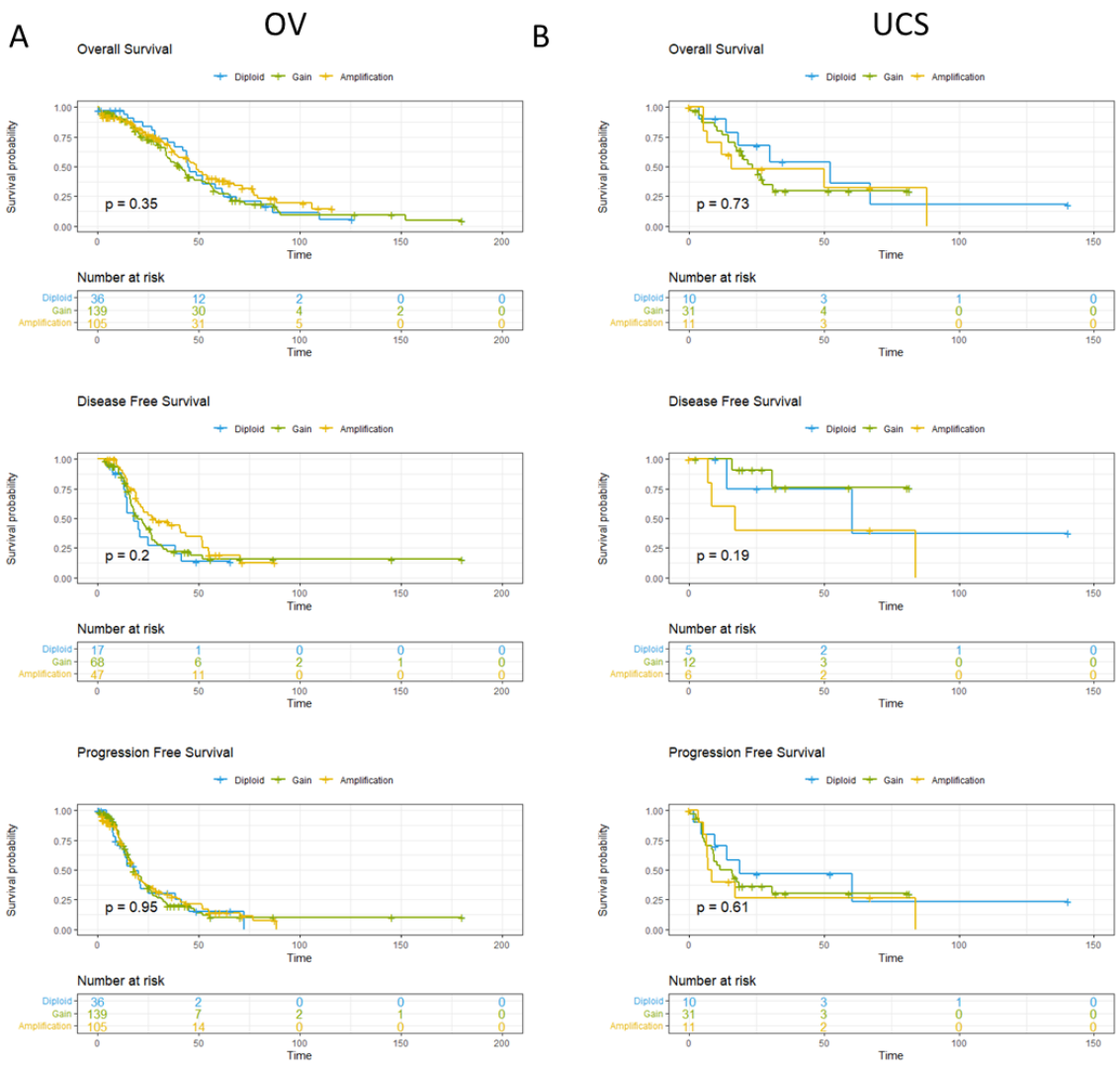

Figure B. 5: Kaplan-Meier survival curves for OV and UCS.
(A) Kaplan-Meir survival curves per PVT1 alteration subgroups. (B) Kaplan-Meir survival curves per PVT1 alteration subgroups. Global log rank p-value are shown.

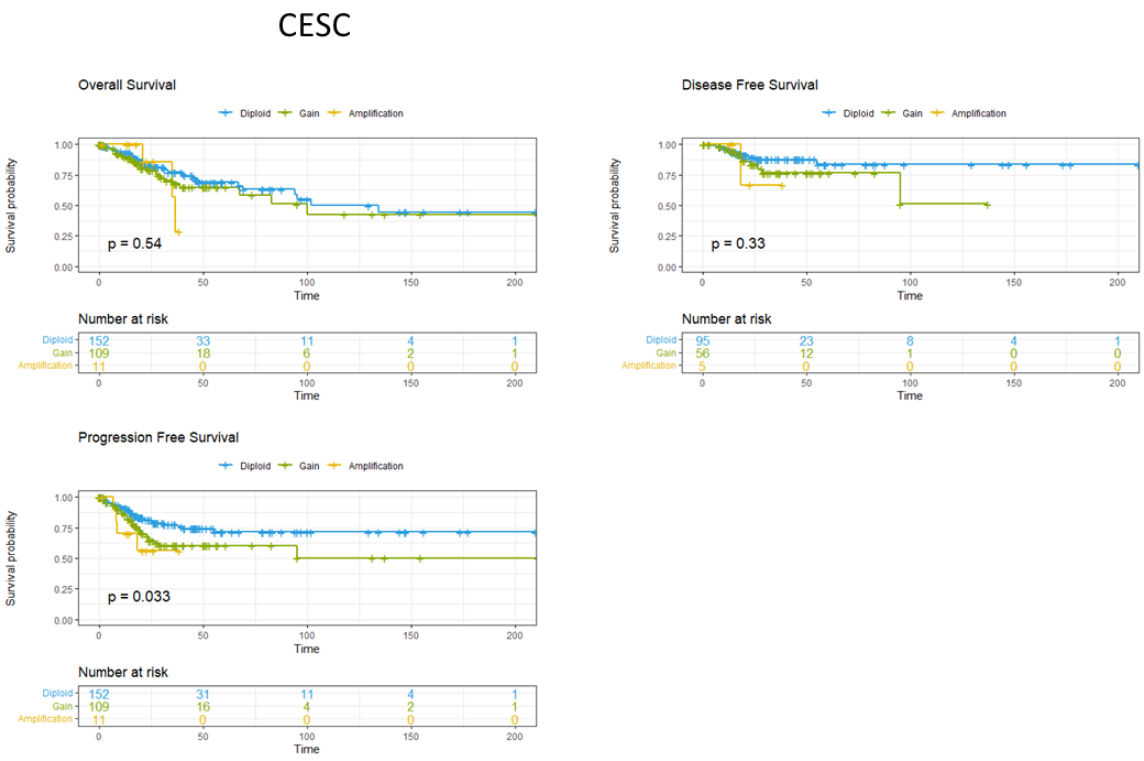

Figure B. 6: Kaplan-Meier survival curves for CESC.
Kaplan-Meir survival curves per PVT1 alteration subgroups. Global log rank p-value are shown.

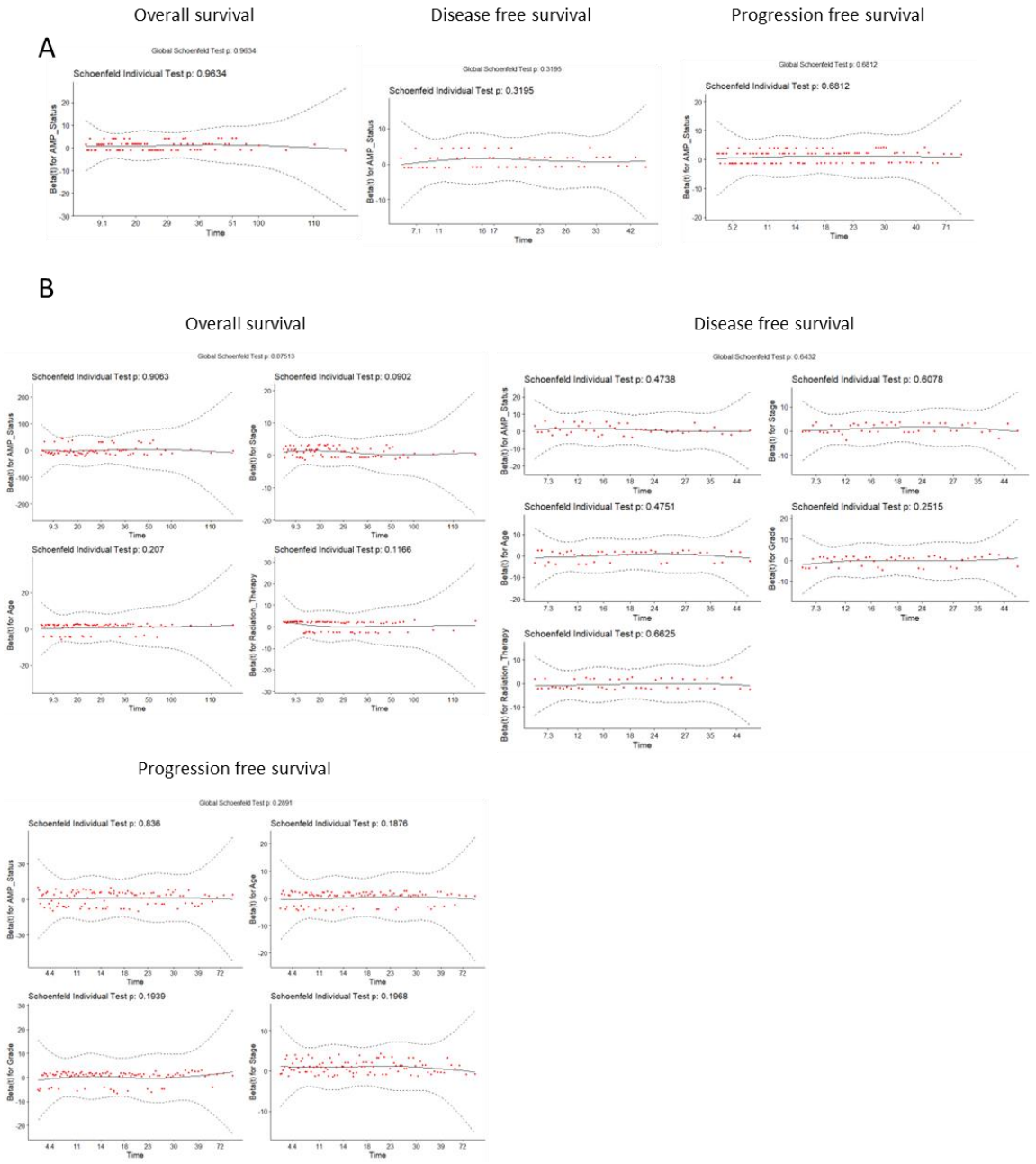

Figure B. 7: Schoenfeld residuals to validate cox proportional hazard model.
(A) Schoenfeld residuals for PVT1 alterations in UCEC. (B) Schoenfeld residuals for multivariate analysis with clinical parameters for PVT1 alterations in UCEC.

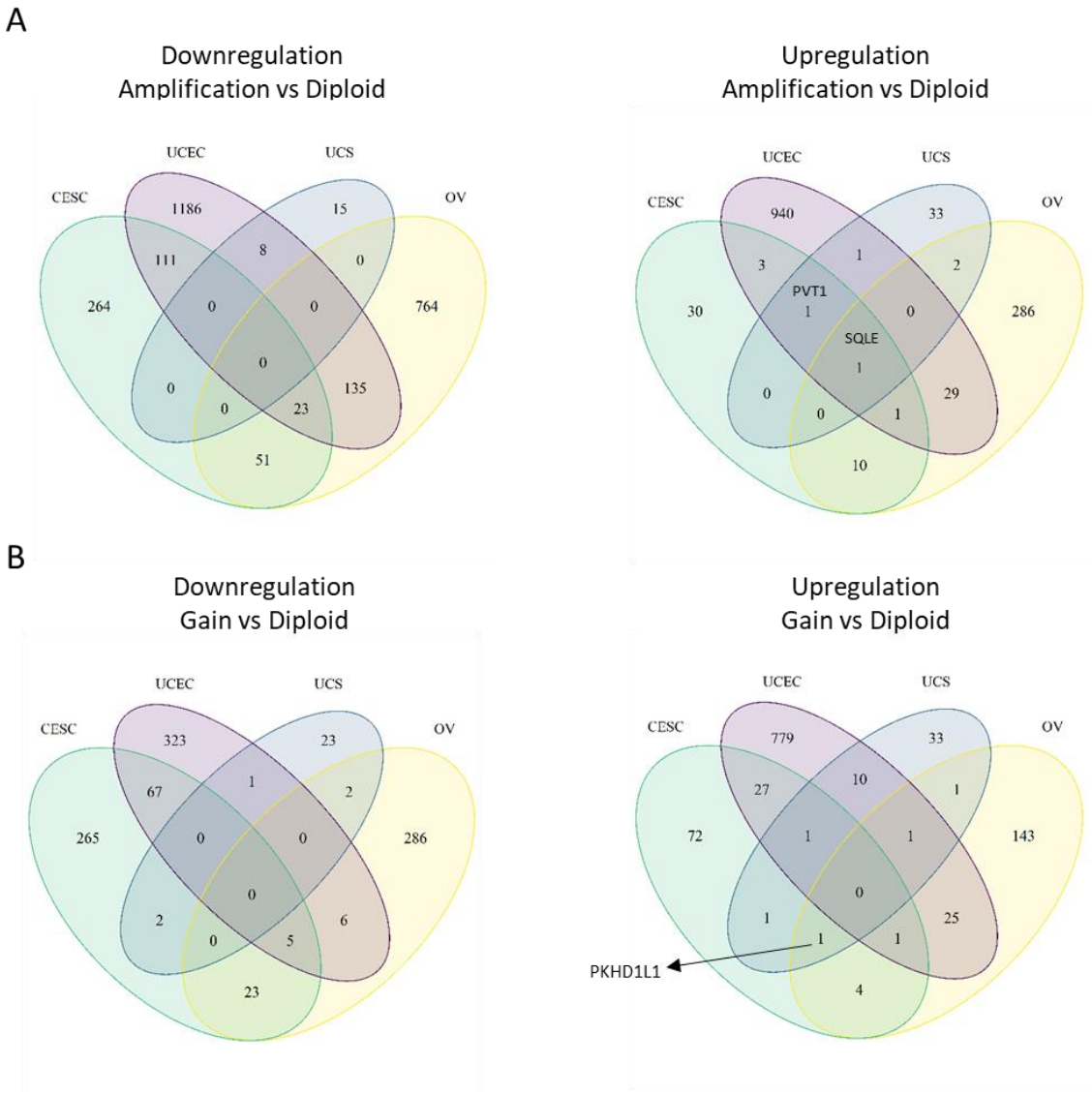

Figure B. 8: Venn diagram of differential gene expression per PVT1 alterations for each tumor type.
(A) Venn diagram of downregulated and upregulated differentially expressed genes between PVT1 amplification and diploid subgroups for each tumor type. (B) Venn diagram of downregulated and upregulated differentially expressed genes between PVT1 gain and diploid subgroup for each cancer study.

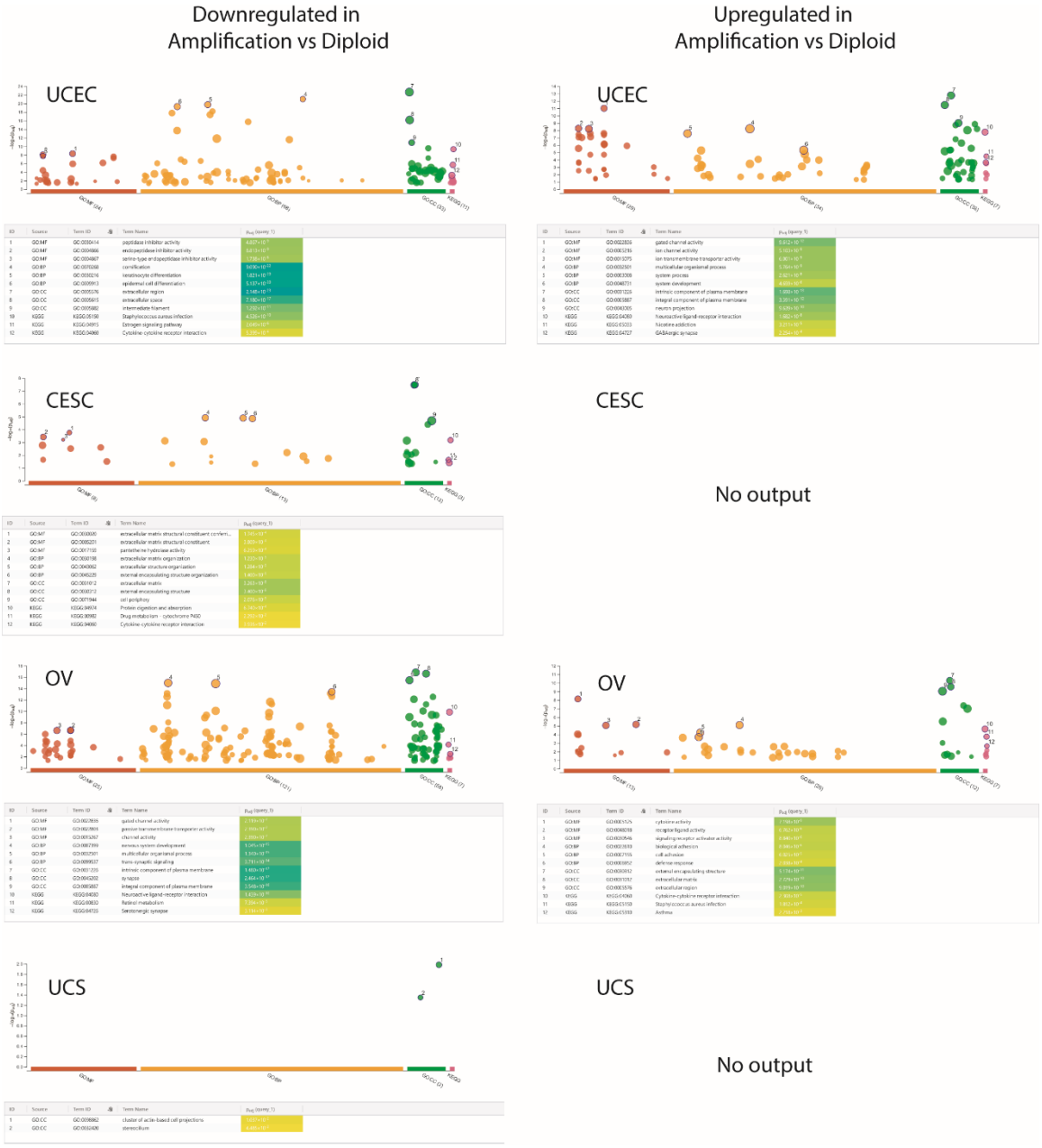

Figure B. 9: gProfiler enrichment analysis on differentially expressed genes between PVT1 amplification and diploid subgroup and unique to each tumor type when available.
(A) gProfiler enrichment analysis on downregulated differentially expressed genes for each caner study (UCEC, CESC, OV and UCS, respectively when available). (B) gProfiler enrichment analysis on upregulated differentially expressed genes (UCEC, CESC, OV and UCS, respectively when available).

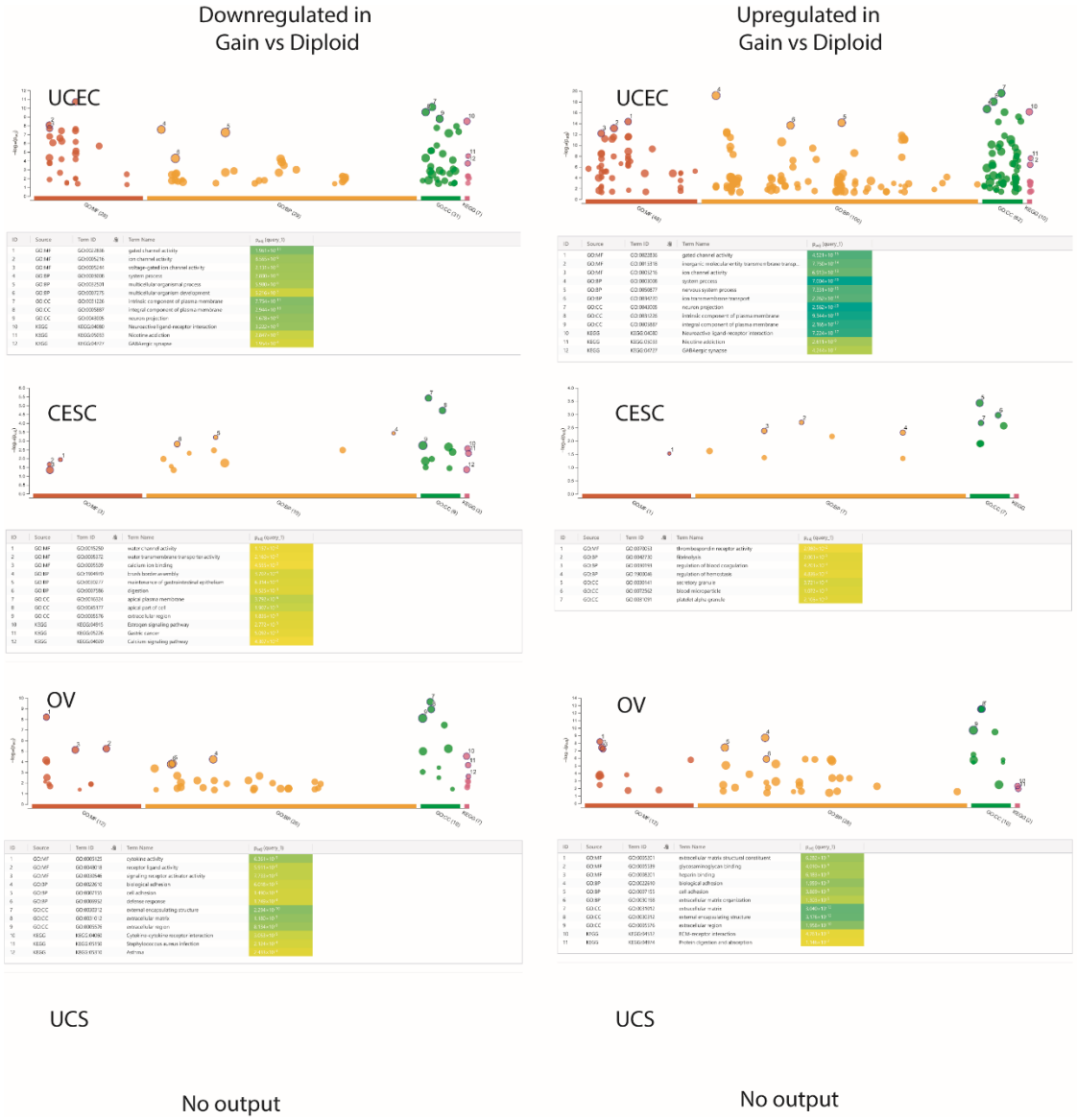

Figure B. 10: gProfiler enrichment analysis on differentially expressed genes between PVT1 gain and diploid subgroup and unique to each tumor type when available.
(A) gProfiler enrichment analysis on downregulated differentially expressed genes (UCEC, CESC, OV and UCS, respectively when available). (B) gProfiler enrichment analysis on upregulated differentially expressed genes (UCEC, CESC, OV and UCS, respectively when available).

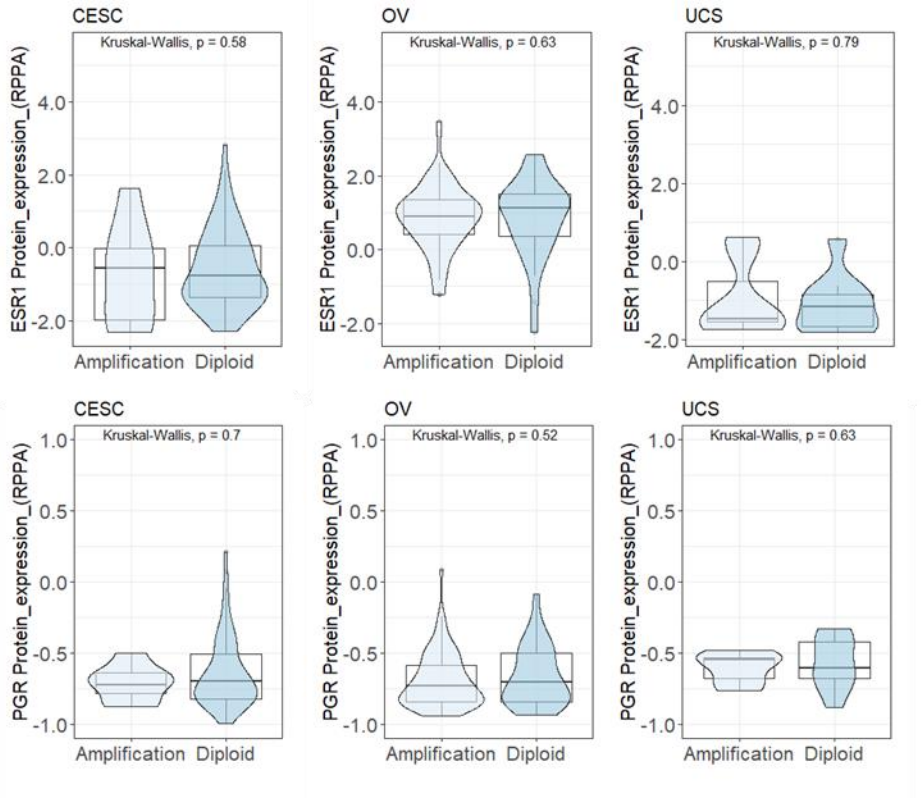

Figure B. 11: ESR1 and PGR protein expression for PVT1 amplification and diploid subgroup per tumor type.
(Kruskal Wallis test).

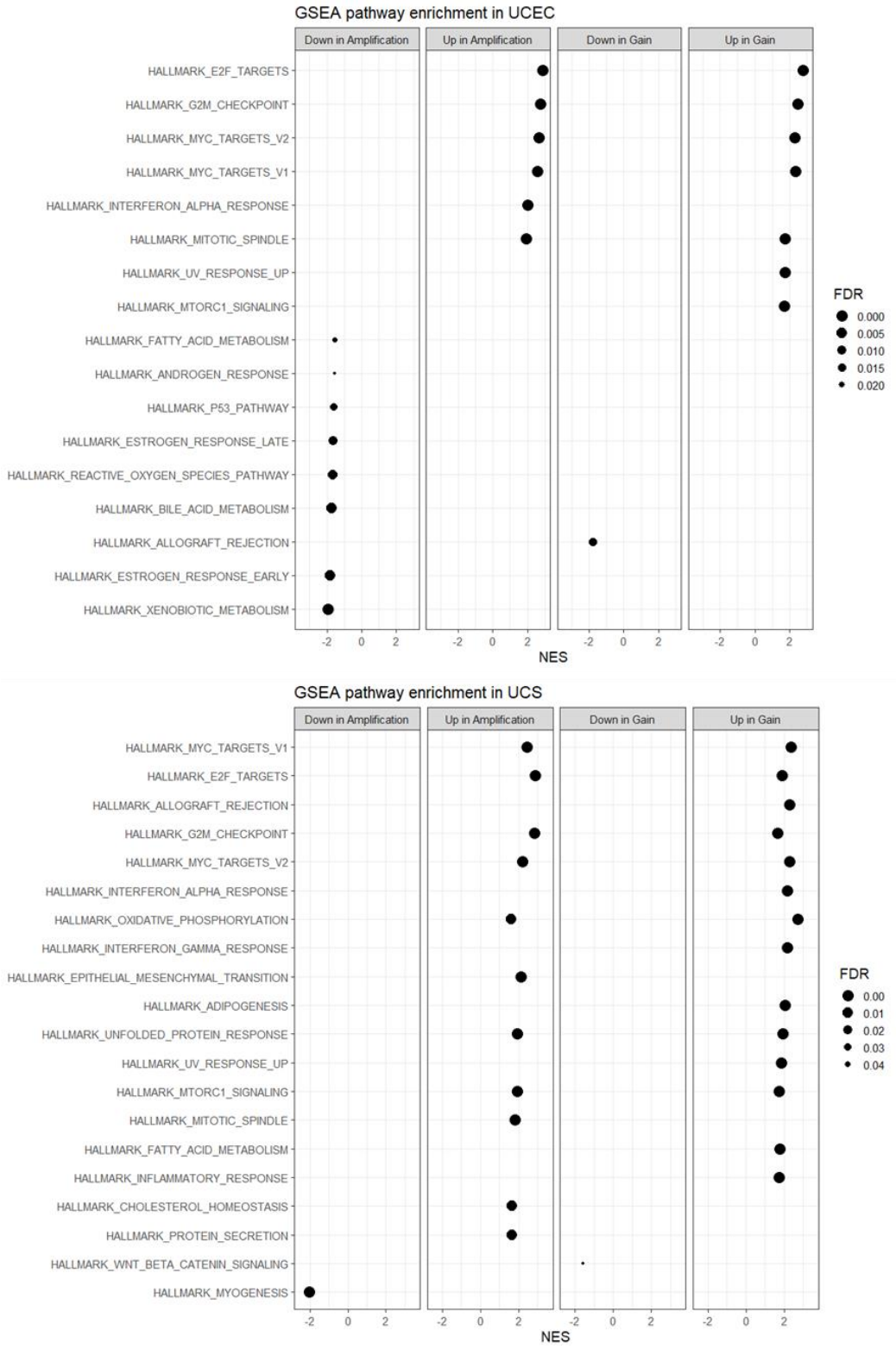

Figure B. 12: Dotplot of GSEA outcome for UCEC and UCS in PVT1 alteration subgroups. Enriched gene signatures are based on FWER<0.1.

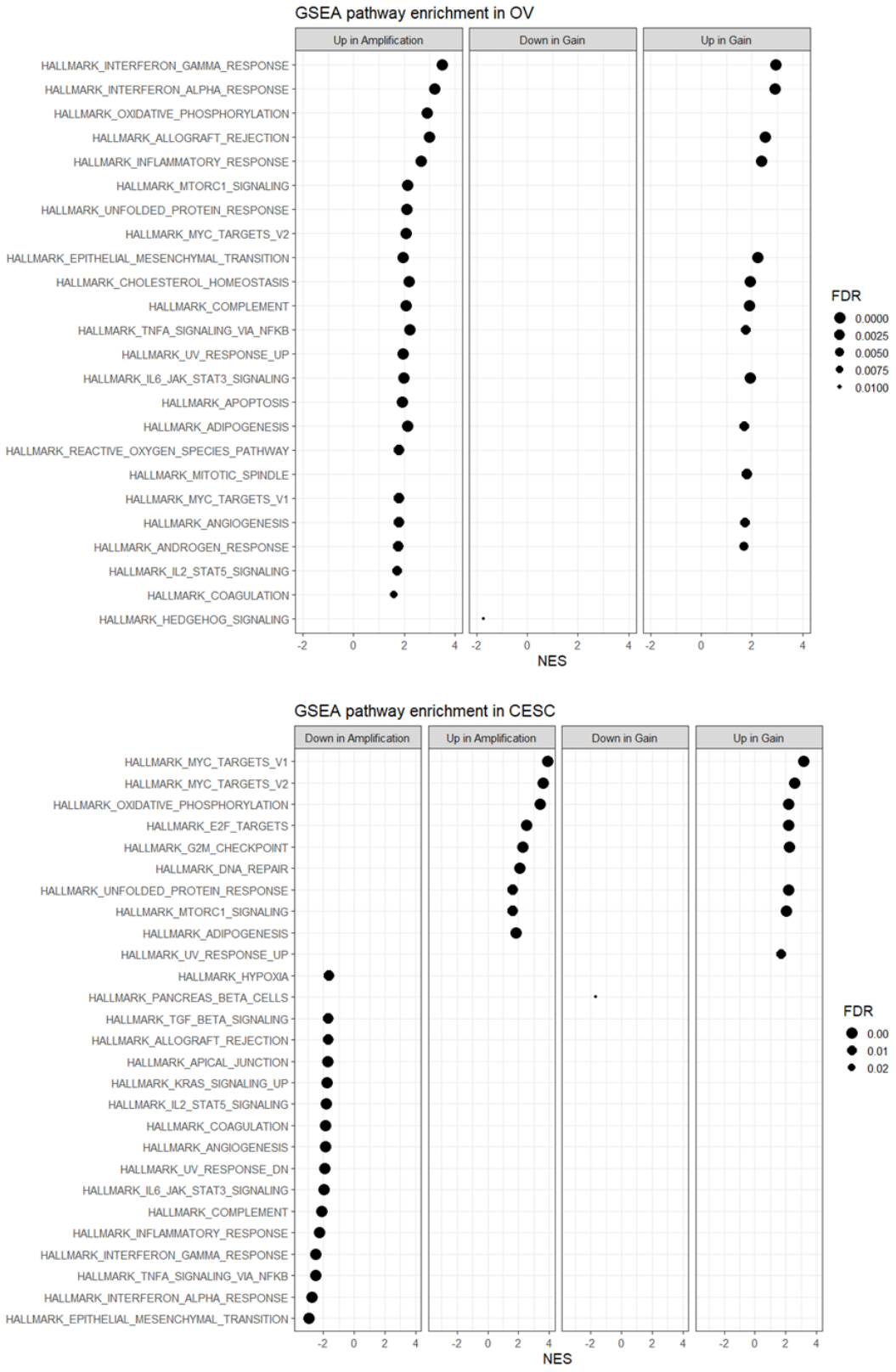

Figure B. 13: Dotplot of GSEA outcome for OV and CESC in PVT1 alteration subgroups. Enriched gene signatures are based on FWER<0.1.

A

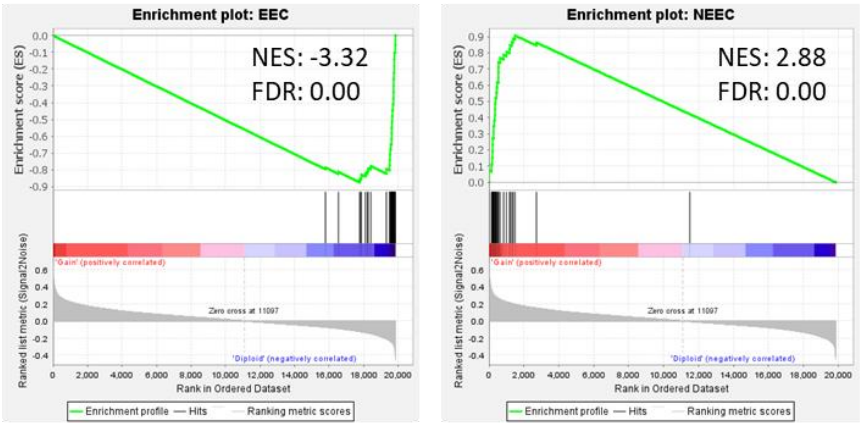

B

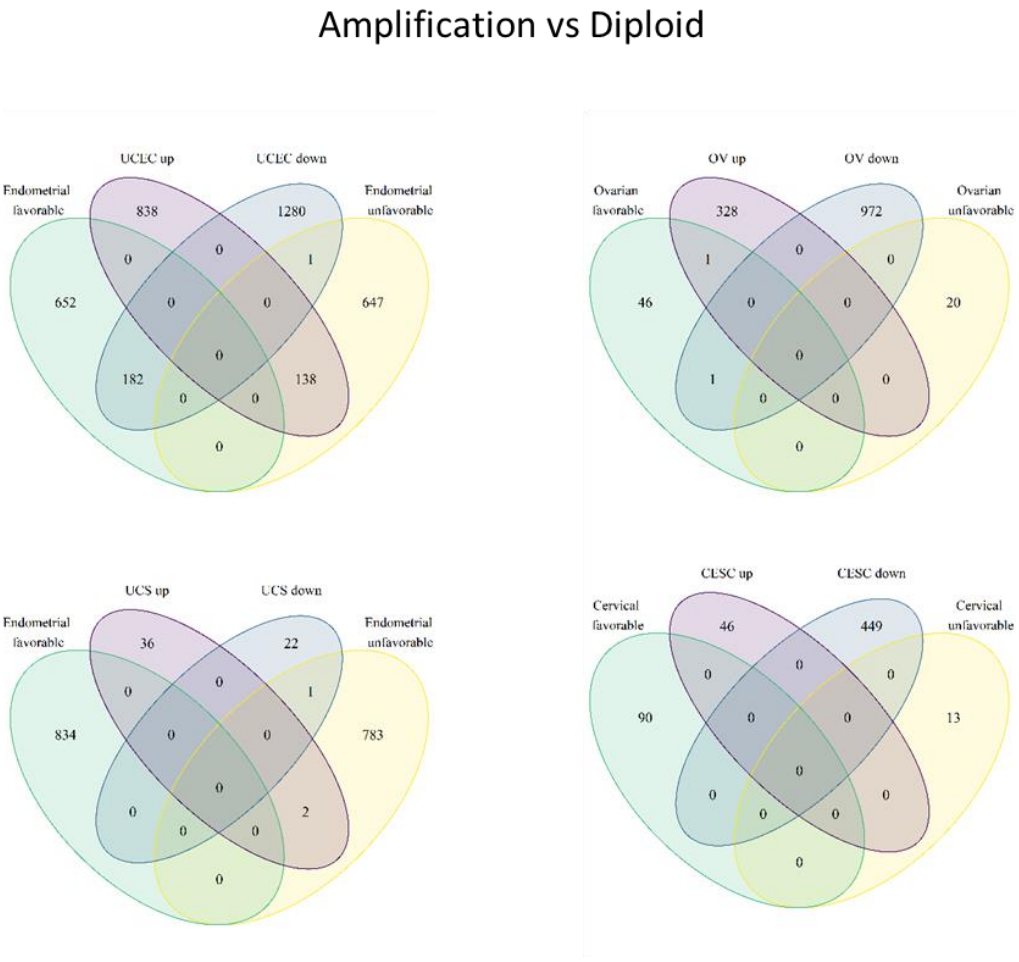

Figure B. 14: PVT1 amplification versus diploid gene signature and prognostic markers. (A) GSEA of endometrioid endometrial cancer (EEC) and non-endometrioid endometrial cancer (NEEC) for gain versus diploid. Enriched gene signatures are based on FWER<0.1. (B) Up- and down-regulated genes compared to favorable and unfavorable prognostic markers for amplification versus to diploid per tumor type.

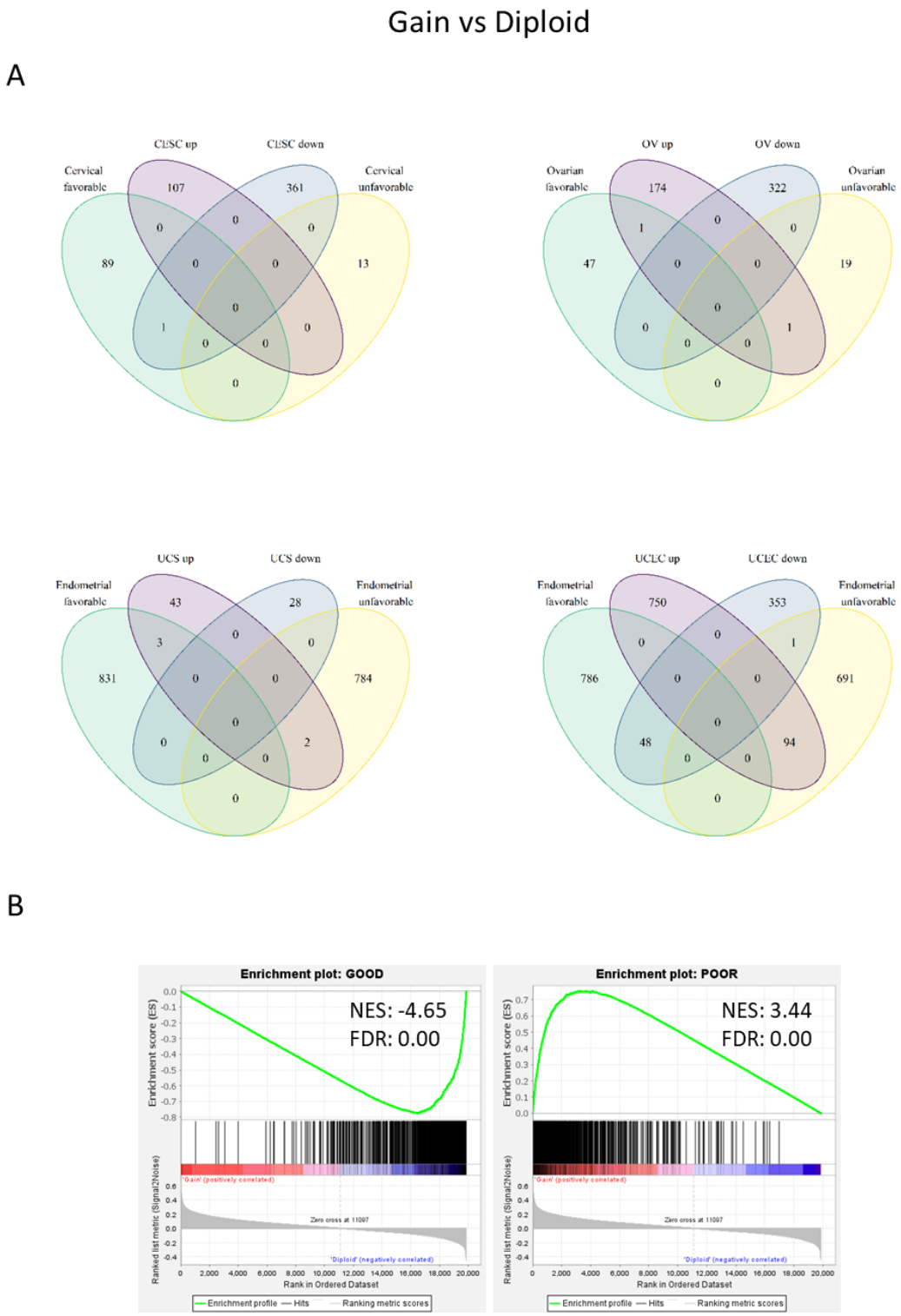

Figure B. 15: PVT1 amplification versus diploid gene expression and prognostic markers. (A) Up- and down-regulated genes compared to favorable and unfavorable prognostic markers for gain versus to diploid per tumor type. (B) GSEA of prognostic markers for gain versus diploid.

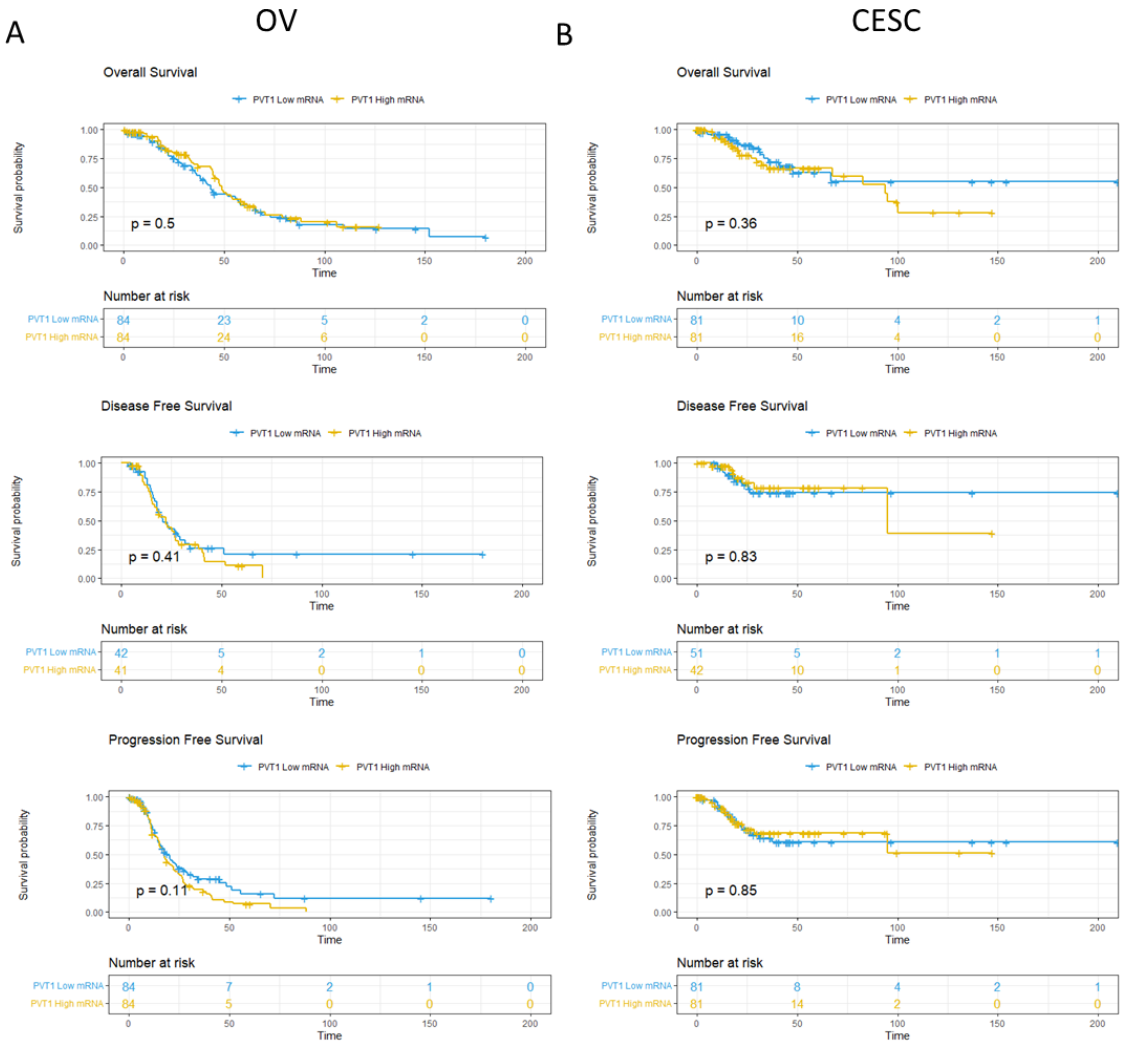

Figure B. 16: Kaplan-Meier survival curves for OV and CESC.
(A) Kaplan-Meir survival curves per PVT1 RNA subgroups in OV. (B) Kaplan-Meir survival curves per PVT1 RNA subgroups in CESC. Global log rank p-value are shown.

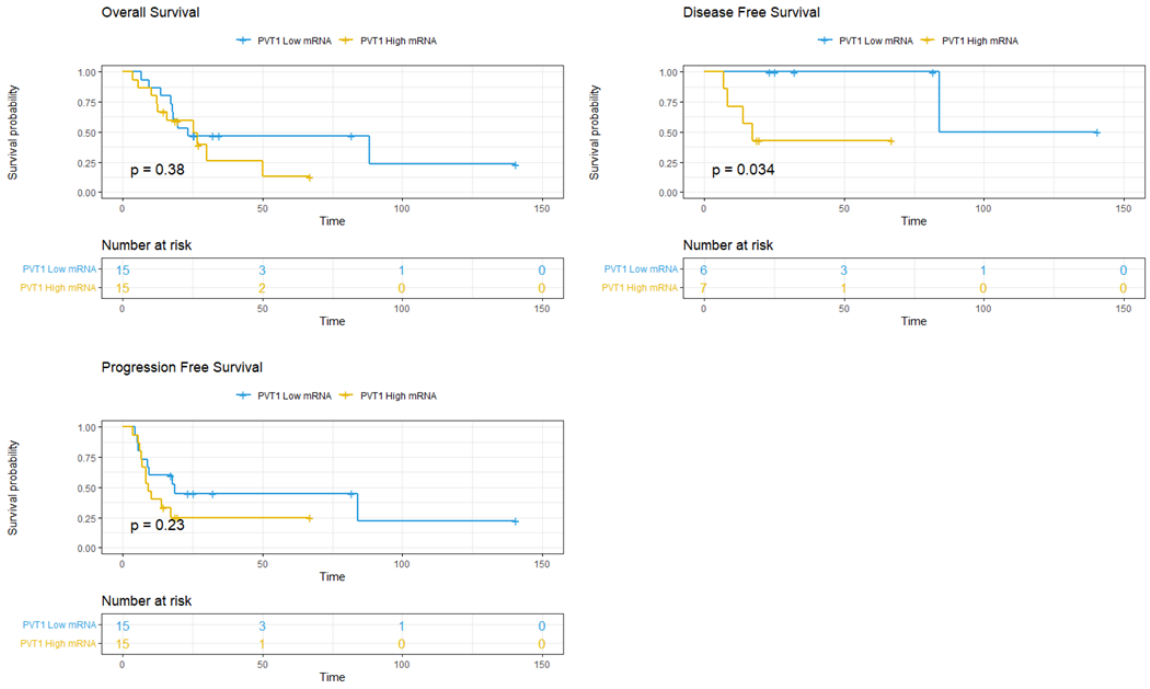

Figure B. 17: Kaplan-Meier survival curves per PVT1 RNA subgroups in UCS. Global log rank p-value are shown.

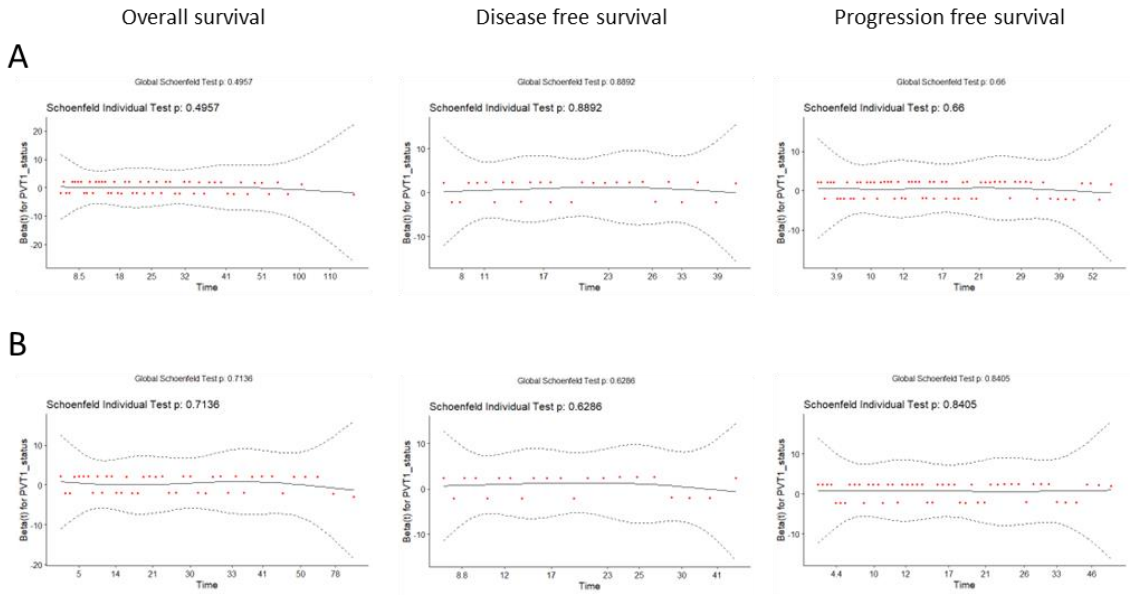

Figure B. 18: Schoenfeld residuals to validate cox proportional hazard model for survival curves.
(A) Schoenfeld residuals for PVT1 RNA subgroups (30% bottom – 30% top) in UCEC.
(B) Schoenfeld residuals for PVT1 RNA subgroups (20% bottom – 20% top) in UCEC.

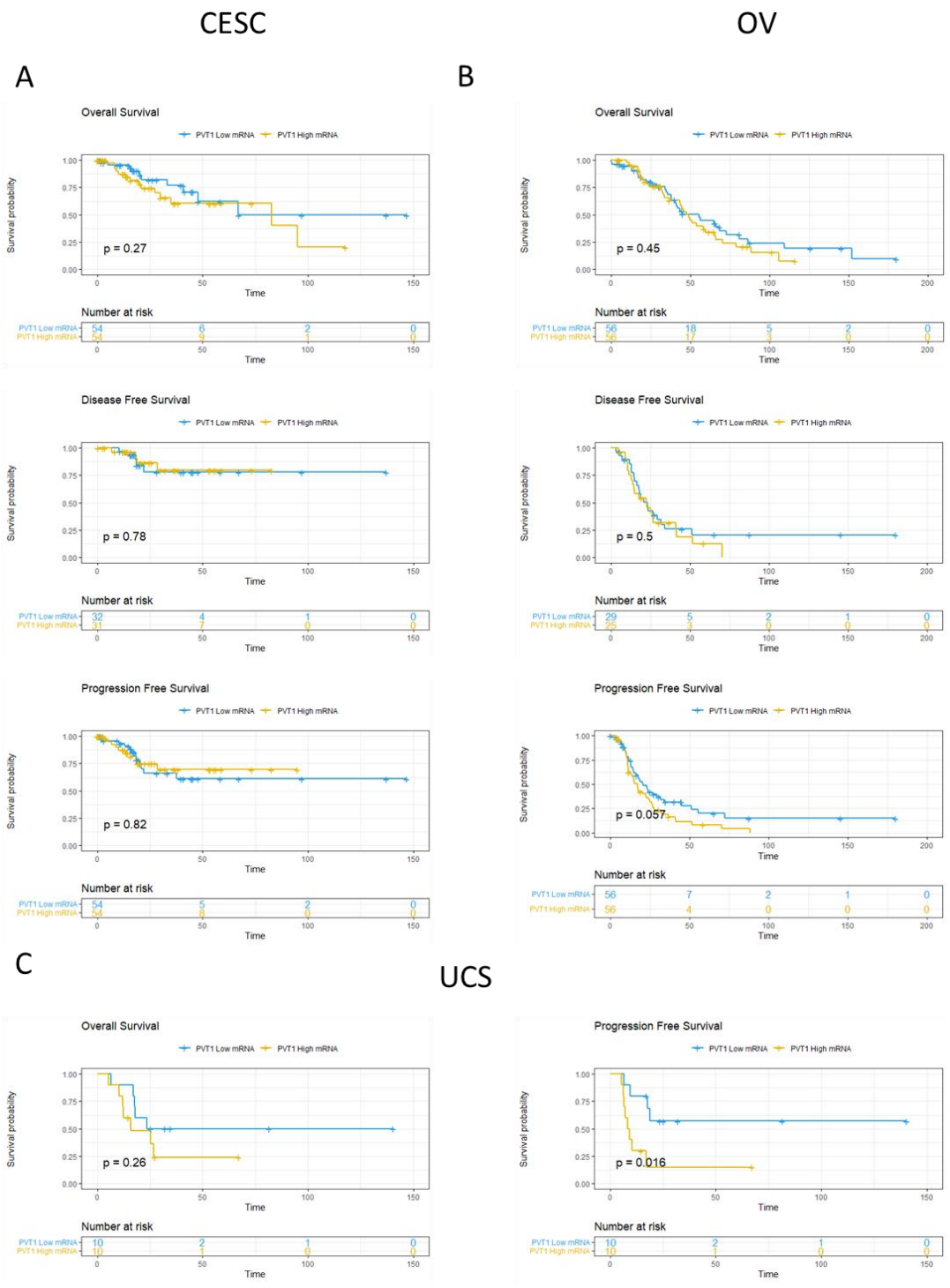

Figure B. 19: Kaplan-Meier survival curves for CESC, OV and UCS.
(A) Kaplan-Meir survival curves per PVT1 RNA subgroups in CESC. (B) Kaplan-Meir survival curves per PVT1 RNA subgroups in OV. (C) Kaplan-Meir survival curves per PVT1 RNA subgroups in UCS. Global log rank p-value are shown.

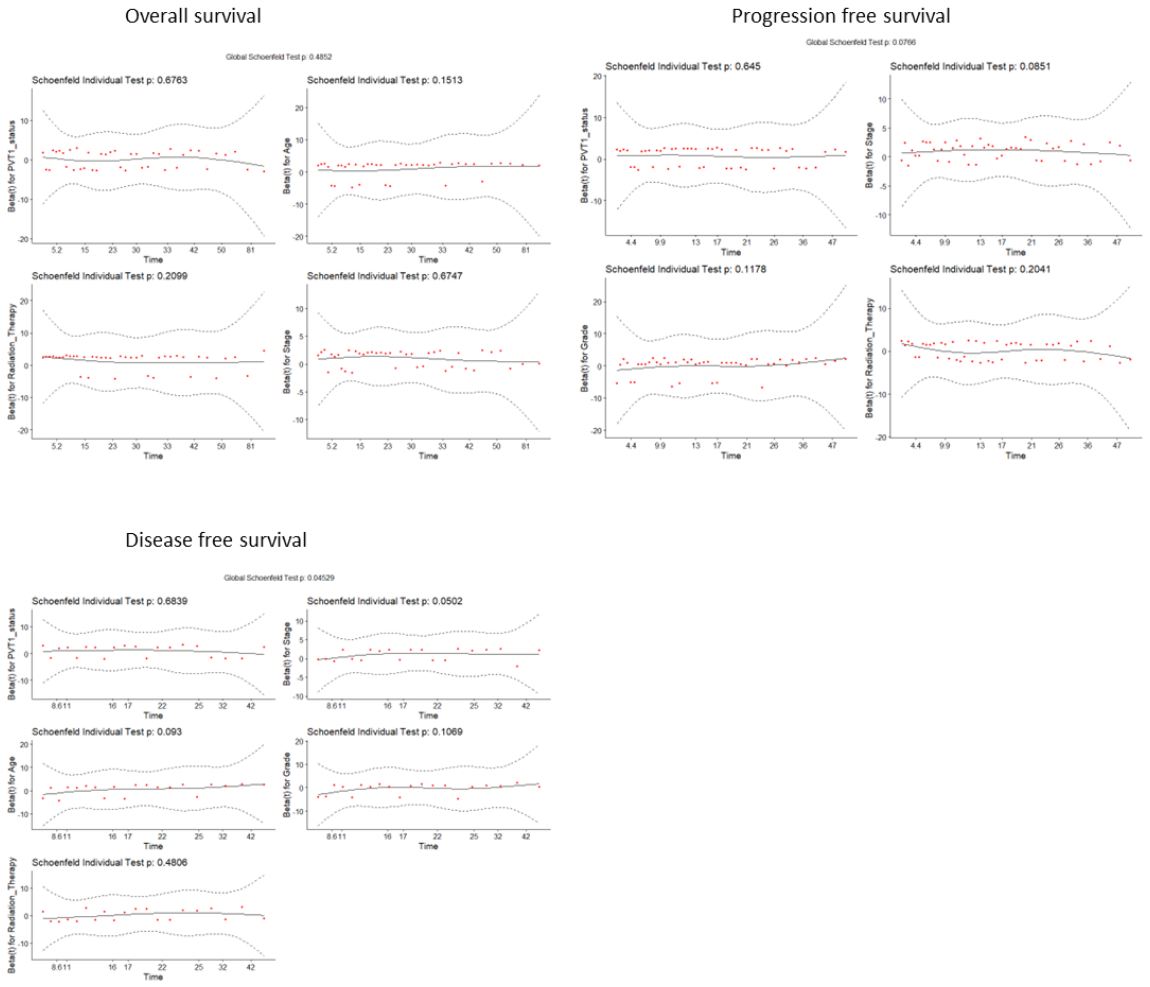

Figure B. 20: Schoenfeld residuals for multivariate analysis with clinical parameters for PVT1 RNA subgroups (20% bottom – 20% top) in UCEC.

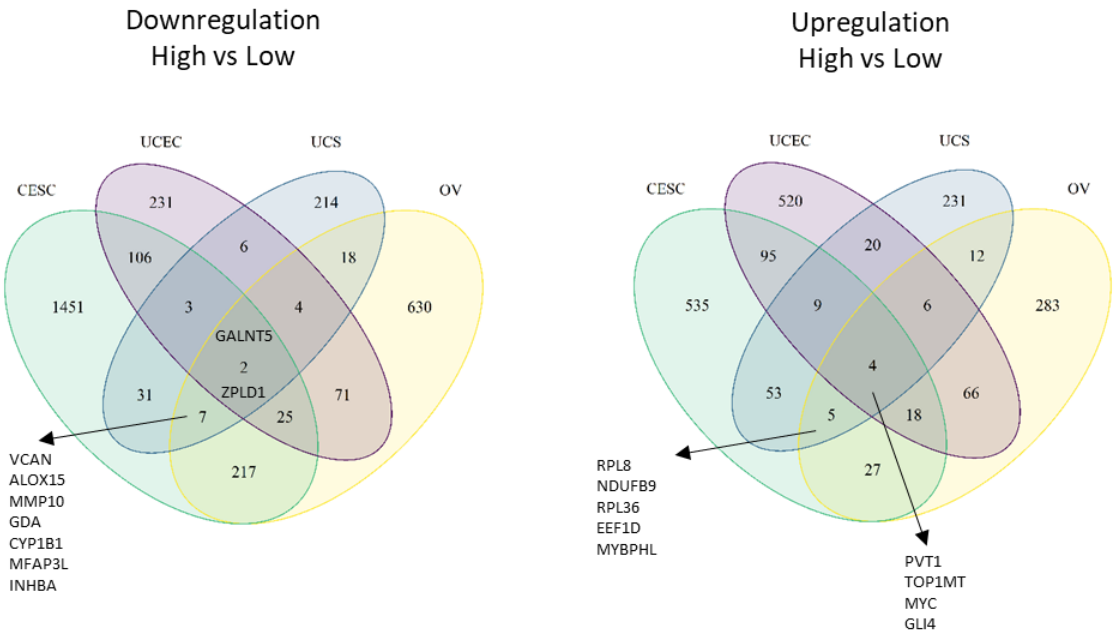

Figure B. 21: Venn diagram of downregulated and upregulated differentially expressed genes between PVT1 high and low RNA subgroups for each tumor type.

Figure B. 22: gProfiler enrichment analysis on up and downregulated differentially expressed genes for each caner study.
(UCEC, CESC, OV and UCS, respectively when available) for PVT1 high and low RNA subgroup.

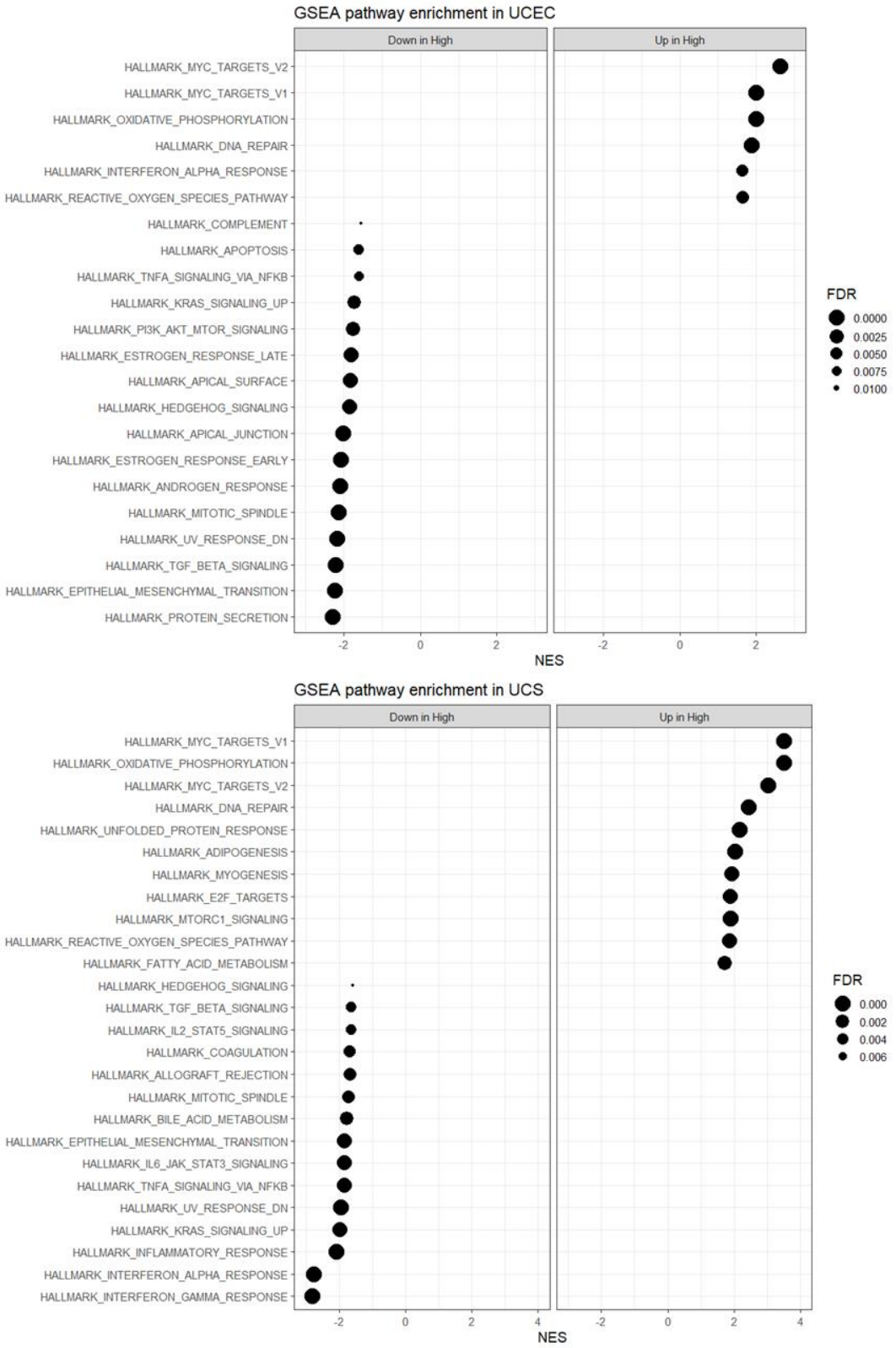

Figure B. 23: Dotplot of GSEA outcome for UCEC and UCS in PVT1 RNA subgroups. Enriched gene signatures are based on FWER<0.1.

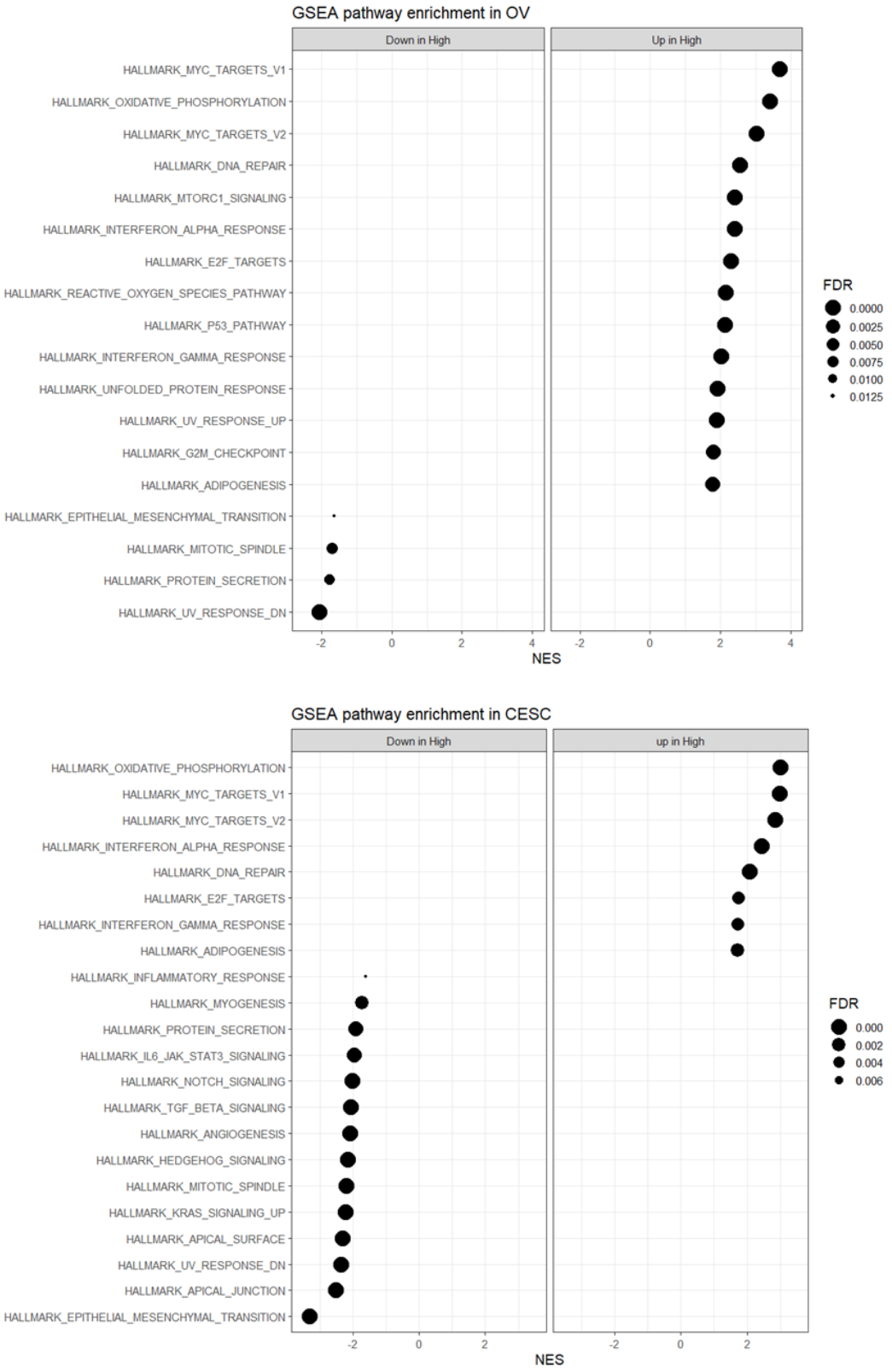

Figure B. 24: Dotplot of GSEA outcome for OV and CESC in PVT1 RNA subgroups. Enriched gene signatures are based on FWER<0.1.

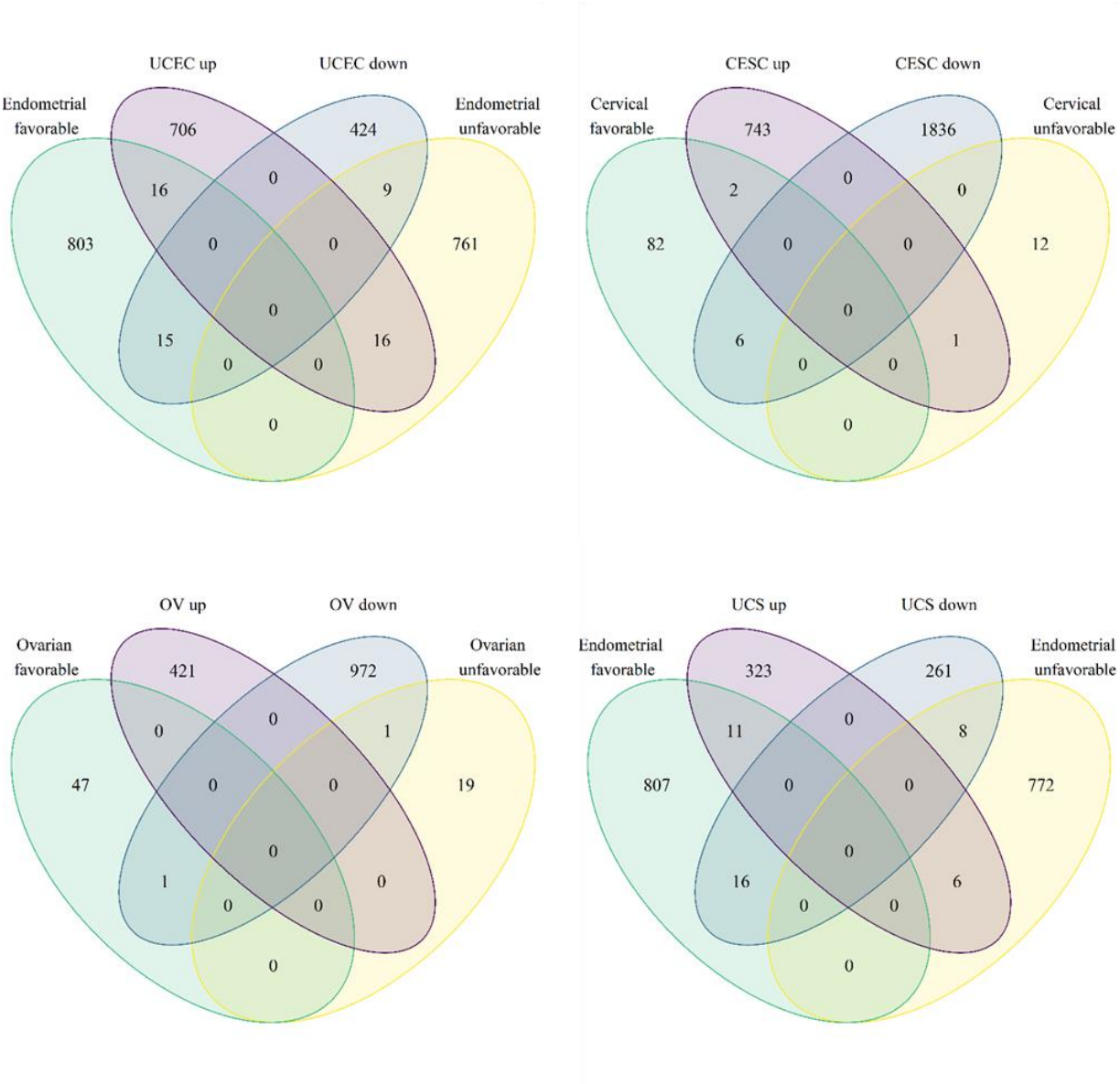

Figure B. 25: Prognostic markers for high and low PVT1.
Up- and down-regulated genes compared to favorable and unfavorable prognostic markers for high versus to low RNA subgroup (20% bottom -20% top sample selection) per tumor type.

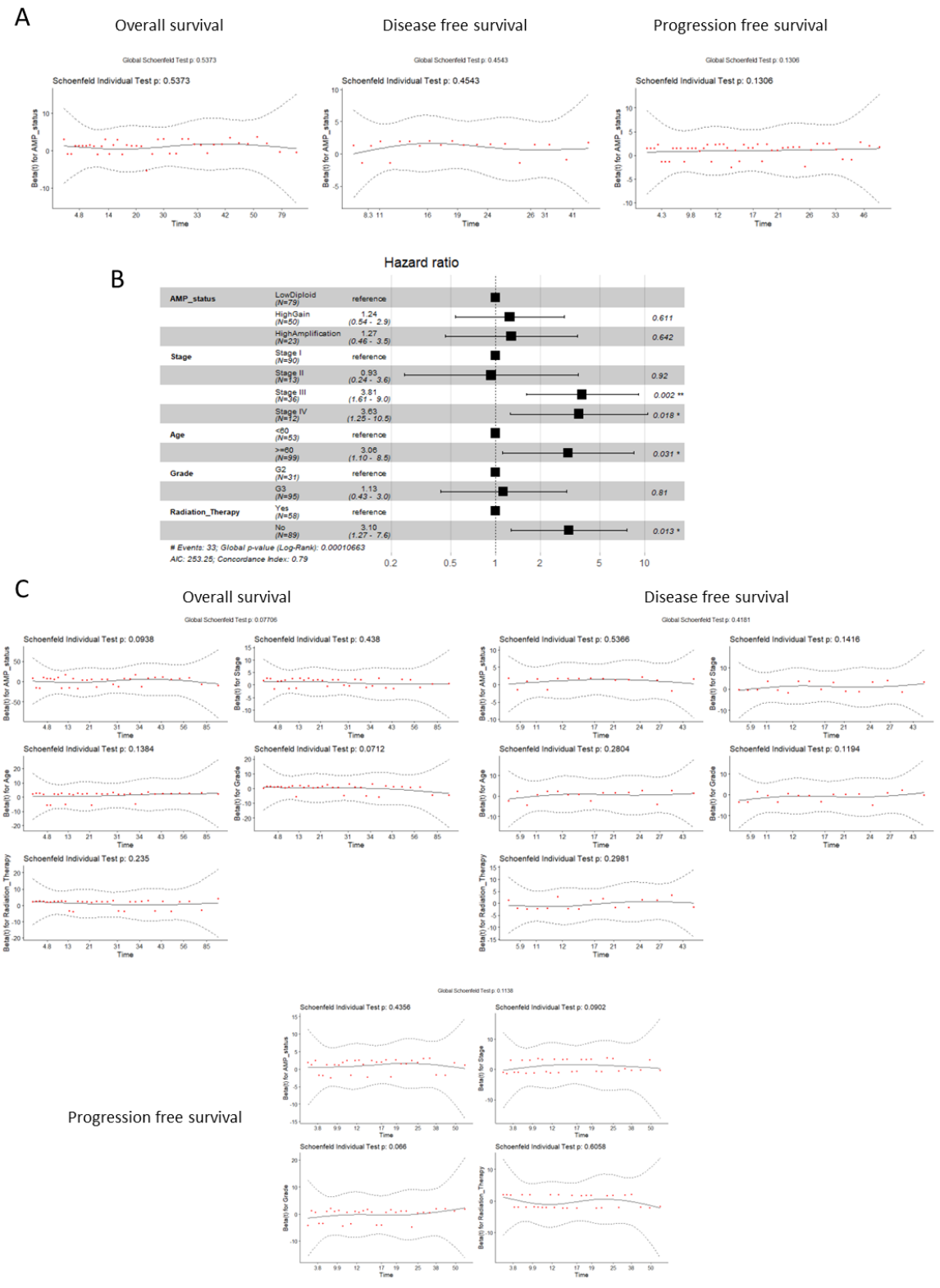

Figure B. 26: Schoenfeld residuals.
(A) Schoenfeld residuals for survival curves for PVT1 RNA expression combined with alterations (low diploid, high diploid, low gain, high gain and high amplification) in UCEC.

(B) Multivariate analysis of PVT1 RNA combined with alterations (low diploid, high diploid and high amplification), stage, age, grade and radiotherapy on overall free survival. (C) Schoenfeld residuals for multivariate analysis with clinical parameters for PVT1 RNA expression combined with alterations (low diploid, high diploid, low gain, high gain and high amplification) in UCEC.

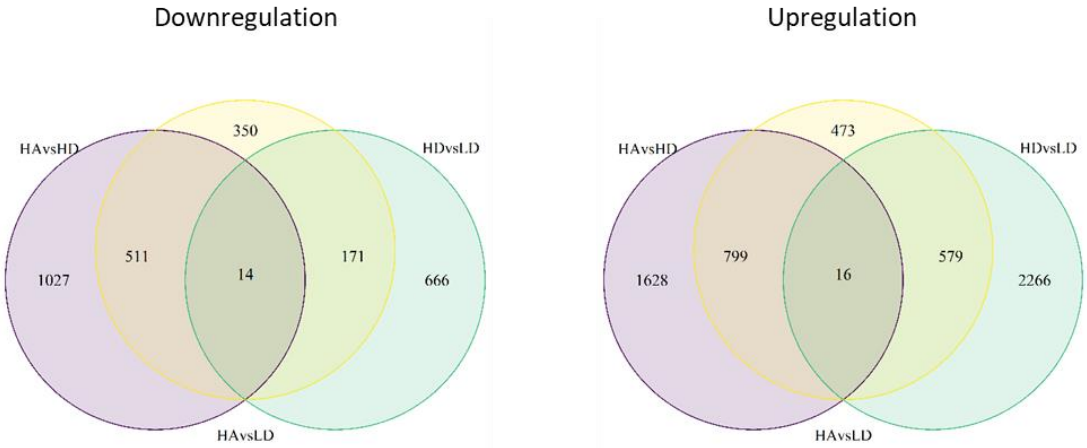

Figure B. 27: Venn diagram of downregulated and upregulated of the different combination.
Venn diagram of downregulated and upregulated differentially expressed genes of the different combination of comparison between the PVT1 RNA combined with alterations subgroup (low diploid (LD), high diploid (HD) and high amplification (HA)).

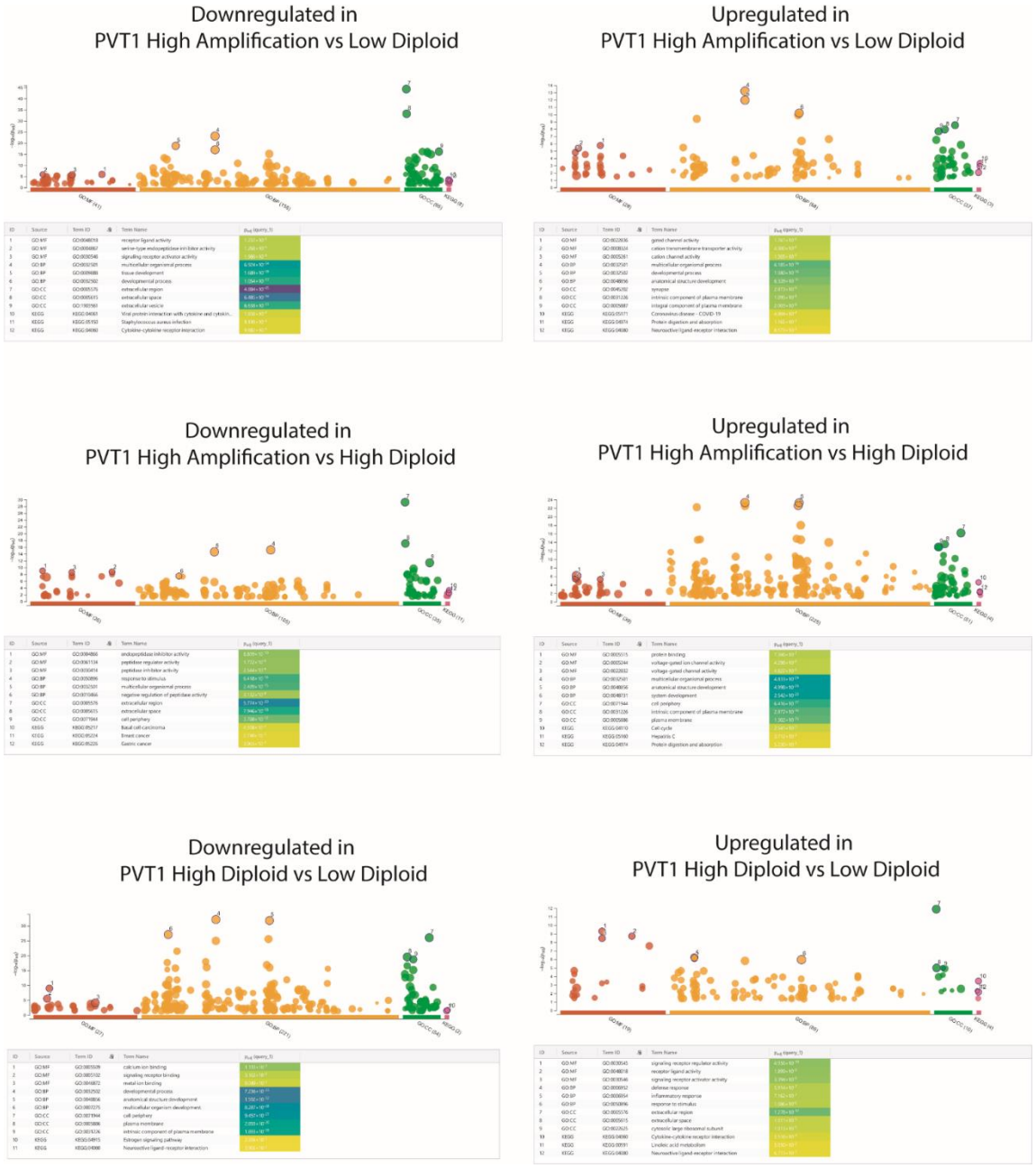

Figure B. 28: gProfiler enrichment analysis on up and downregulated differentially expressed genes of the different combination of comparison between the PVT1 RNA combined with alterations subgroup (low diploid, high diploid and high amplification).

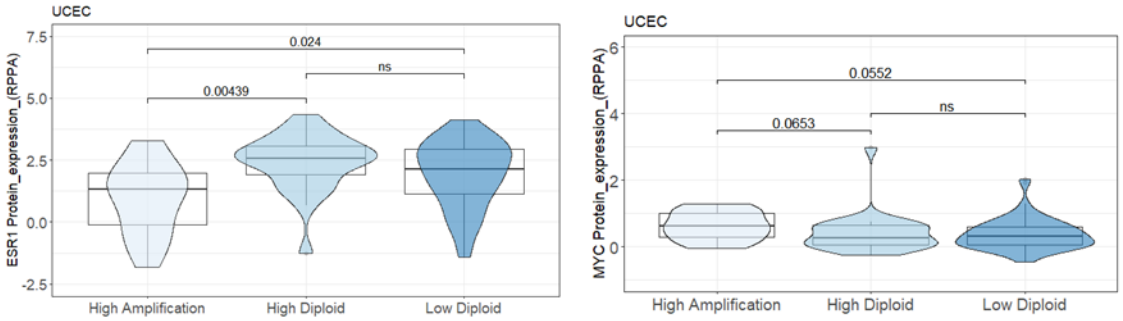

Figure B. 29: ESR1 and MYC protein expression for PVT1 high amplification, high diploid and low diploid. (Kruskal Wallis test).

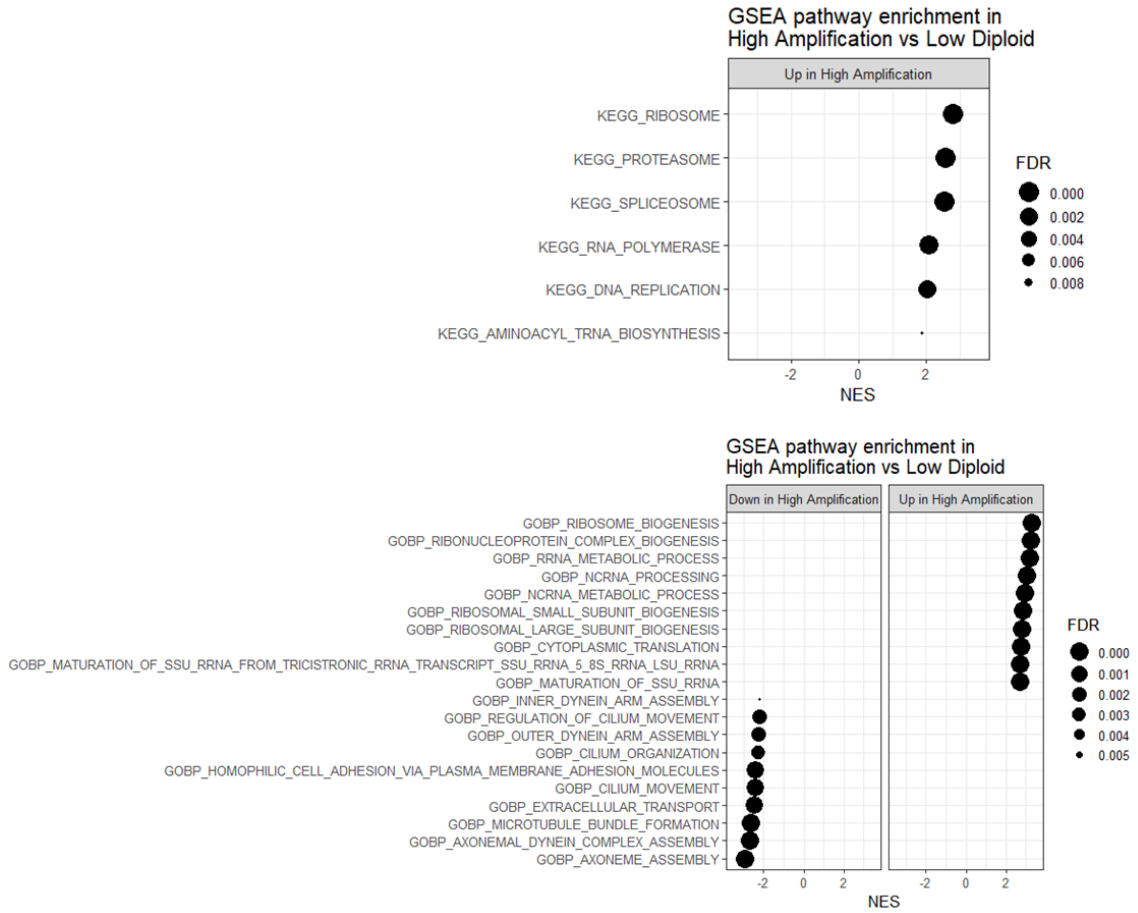

Figure B. 30: Dotplot of GSEA outcome (KEGG and GOBP) for high amplification versus low diploid subgroup in UCEC.
Enriched gene signatures are based on FWER<0.1 (top 10 enrichment pathways are shown if more than 10 enrichment pathways had an FWER<0.1).

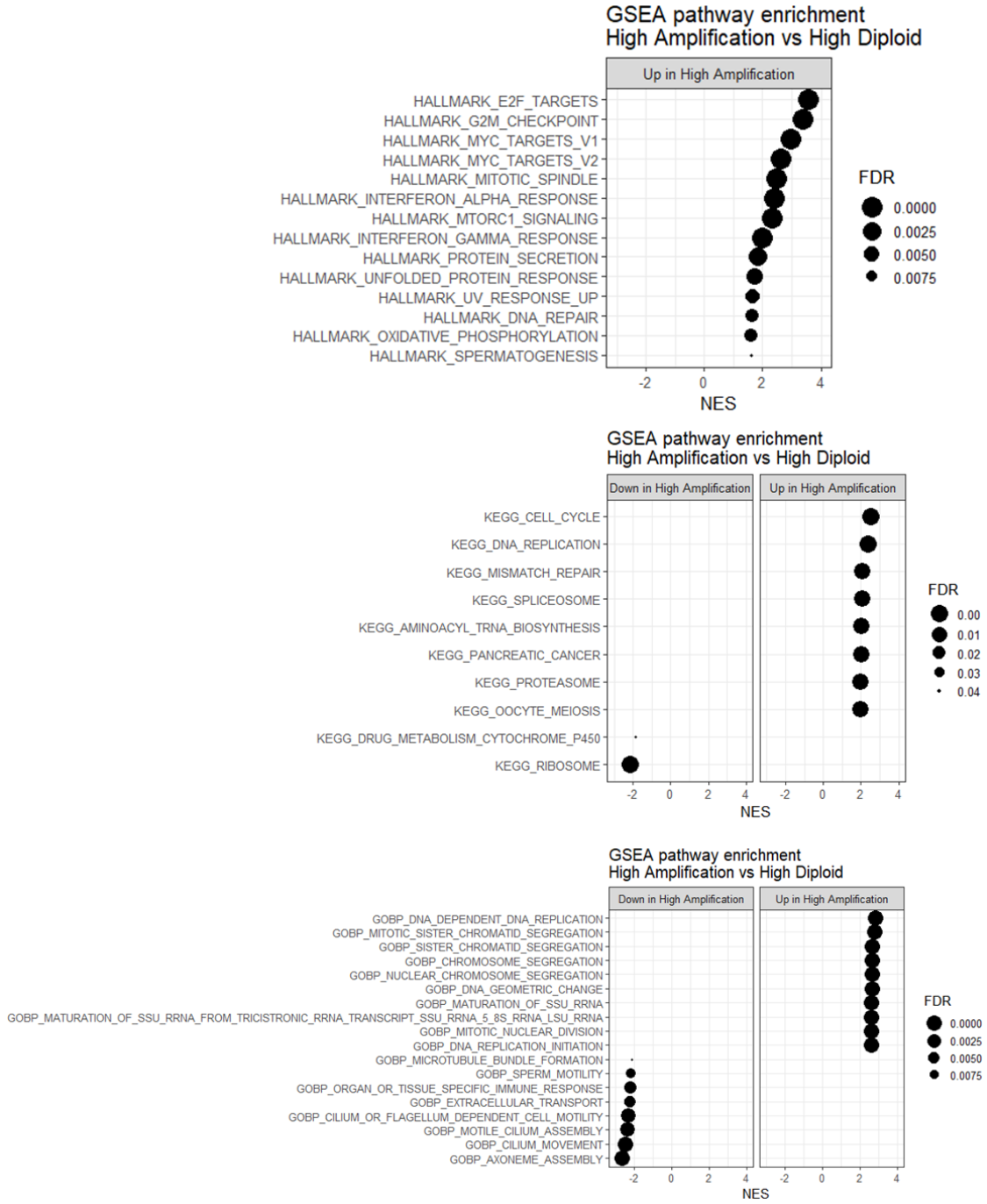

Figure B. 31: Dotplot of GSEA outcome (hallmarks, KEGG and GOBP) for high amplification versus high diploid subgroup in UCEC.
Enriched gene signatures are based on FWER<0.1 (top 10 enrichment pathways are shown if more than 10 enrichment pathways had an FWER<0.1).

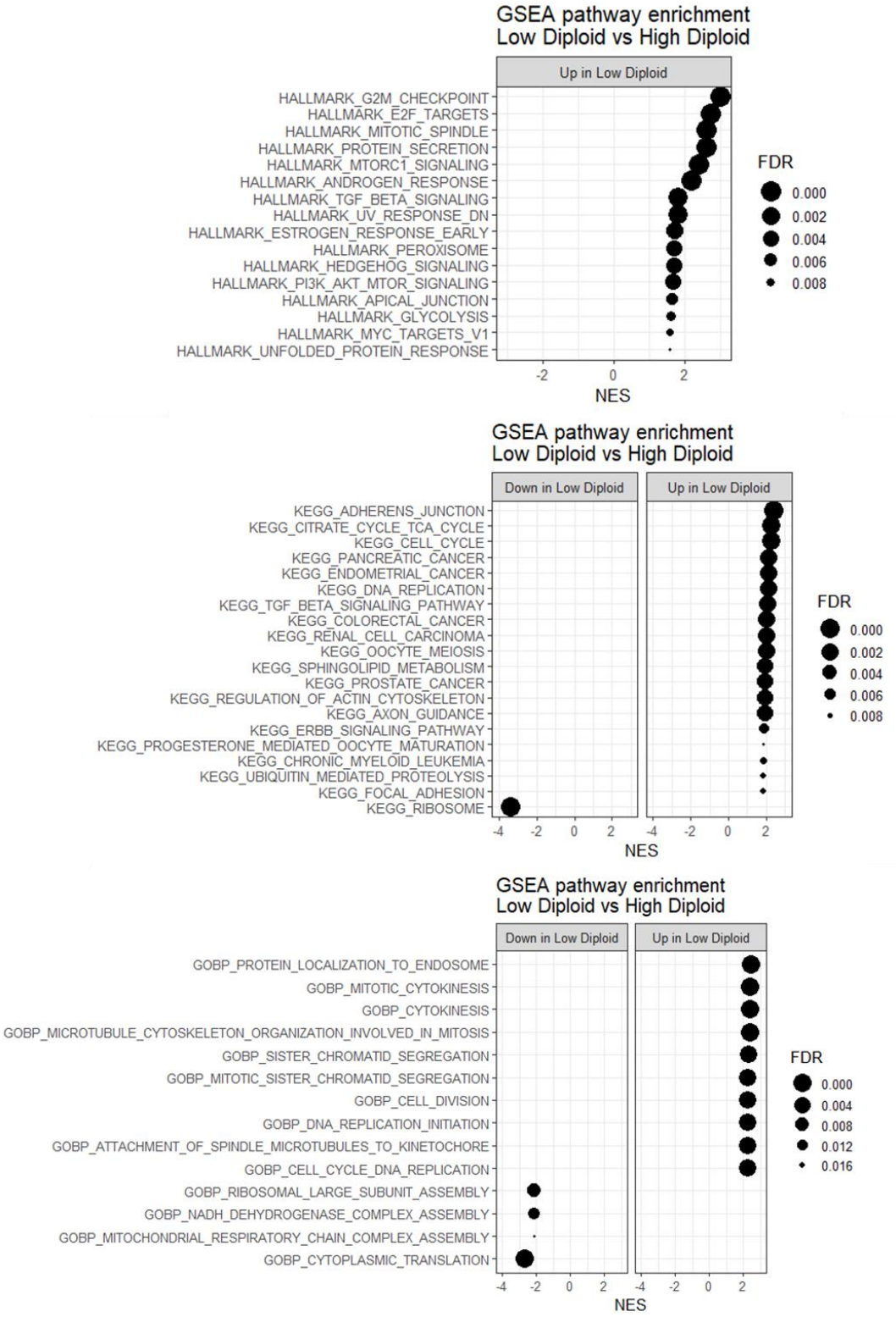

Figure B. 32: Dotplot of GSEA outcome (hallmarks, KEGG and GOBP) for low diploid versus high diploid subgroup in UCEC.
Enriched gene signatures are based on FWER<0.1 (top 10 enrichment pathways are shown if more than 10 enrichment pathways had an FWER<0.1).

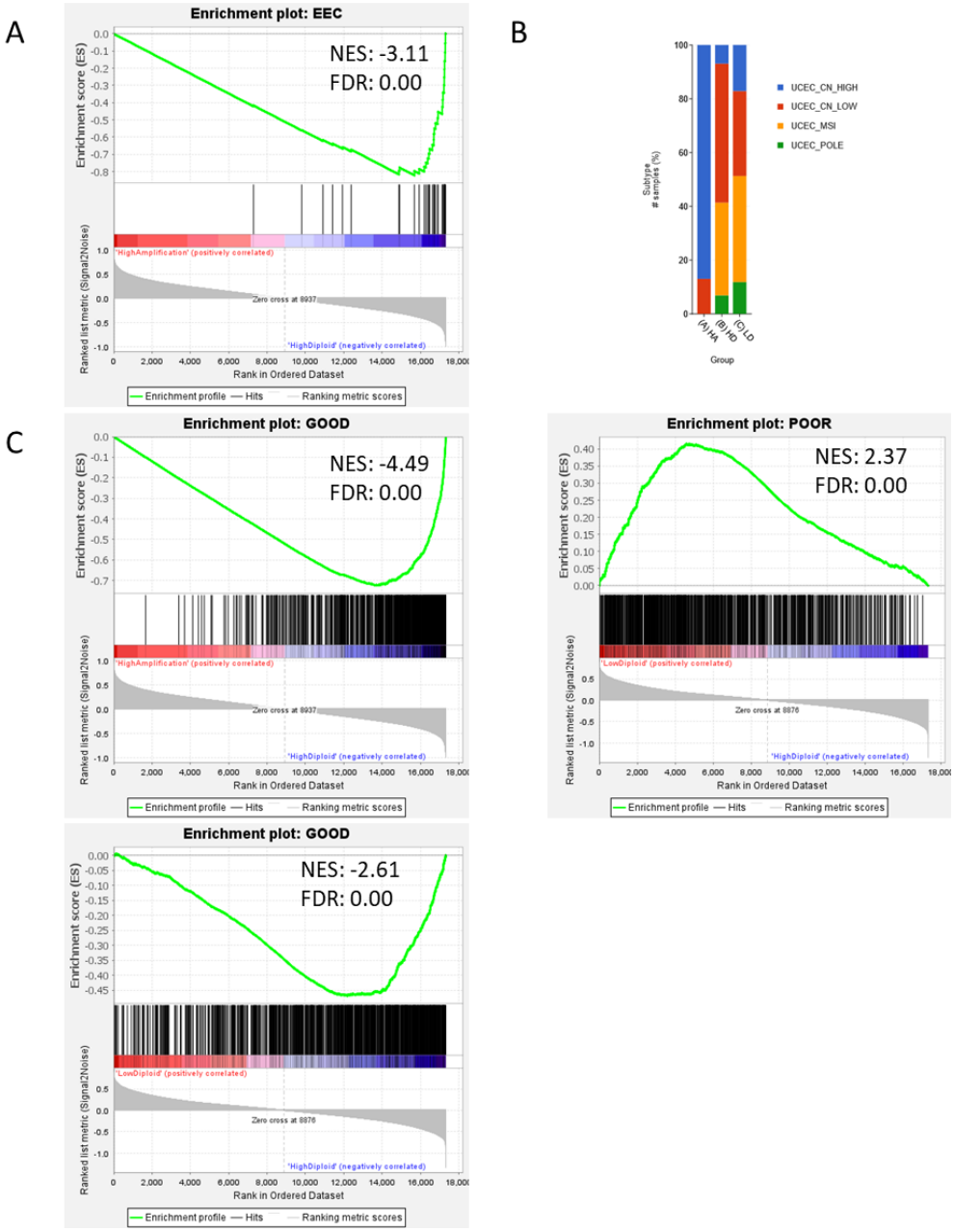

Figure B. 33: GSEA for high amplification versus high diploid.
(A) GSEA of endometrioid endometrial cancer (EEC) and non-endometrioid endometrial cancer (NEEC) for high amplification versus high diploid. (B) Distribution of TCGA UCEC categories (POLE ultramutated, microsatellite instability hypermutated, copy-number low, and copy-number high) in low diploid (LD), high diploid (HD) and high amplification (HA). (C) GSEA of prognostic markers for High amplification versus high diploid and low diploid versus high diploid.

APPENDIX C

CURRICULUM VITAE

KEVIN TABURY

BIOMEDICAL ENGINEER

E-mail: kevin.tabury@gmail.com

https://orcid.org/0000-0002-8004-3718
https://www.linkedin.com/in/kevin-tabury-24321b67/

MY OBJECTIVES

Solution oriented biomedical engineer eager to make a difference in space biology research

PERSONAL

Age // 35 years

Nationality // Belgian & German

SKILLS

- Microscopy
- Molecular biology
- Cellular biology
- Lab-on-chip
- Scientific writing
- R

STRENGTHS

- Reliability
- Creativity
- Communication
- Leadership

LANGUAGES

- French
- English
- German
- Dutch

EXPERIENCE

Jan 2020 - Current
Researcher
SCK CEN

RESPONSIBILITIES:
Investigating biological effects of hadron radiation for space biology and radiation therapy.
Leading the microscopy platform.
Leading the lab-on-chip platform.

Jan 2017 - Current
PhD candidate
UNIVERSITY OF SOUTH CAROLINA

RESPONSIBILITIES:
Investigating the role of long non-coding RNA PVT1 in multiple cancers.

Sep 2009 - Dec 2016
Research Assistant
SCK CEN

RESPONSIBILITIES:
Involved in multidisciplinary projects related to space biology (space effects on the immune system of astronauts), oncology (detection and treatment of prostate, colon and thyroid cancer), cardiovascular disease (non-cancer effects of ionizing radiation) and radiation biomarkers (gene signatures in peripheral blood mono-nuclear cells).

EDUCATION

Jan 2017 - Current
PhD Biomedical Engineering
UNIVERSITY OF SOUTH CAROLINA

SKILLS ACQUIRED:
Molecular biology techniques (DNA, RNA, protein, shRNA, siRNA), cellular biology techniques (Super resolution microscopy, Luminex, ELISA, flow cytometry, western blotting), bioinformatics in R (microarray and RNA sequencing analysis, statistics, modelling), Lab-on-chip (fluidic dynamics, LIFPA).
GPA: 3.81

Sep 2015 - Jun 2016
MSc Industrial Engineering in Biochemical Sciences
Group T/KULeuven

SKILLS ACQUIRED:
Master thesis: 'On-chip development of a multiplex ddPCR assay' - Lab-on-chip devices, microfluidics, micro/nanofabrication and ddPCR - IMEC - Grade of 16.6/20.
MSc - cum laude

Sep 2012 - Jun 2013
Expert in radiation protection class II
IRE/ISISB

SKILLS ACQUIRED:
Broad scientific and technological view on radiological and nuclear techniques

Sep 2006 - Jun 2009
BSc Industrial Chemistry
ISET

SKILLS ACQUIRED:
Bachelor thesis: 'Biomarker study for individual radiosensitivity' - Human blood handling, ionizing radiations, DNA - RNA - protein extraction, microarray analysis and flow cytometry - SCK CEN - Grade of 20/20
BSc - suma cum laude
Award: Industrial chemistry price for highest performance

PUBLICATIONS (4/14)

-Baran R., Marchal S., Campos G.S., Rehnberg E.,Tabury K., et al. (2022)-The Cardiovascular System in Space: Focus on In Vivo and In Vitro Studies. Biomedicines
-Macaeva E., Tabury K., et al. (2021) - High LET carbon and iron ions elicit a prolonged and amplified p53 signaling and inflammatory response comapred to low-LET X-rays in human peripheral blood mononuclear cells. Frontiers in Oncology.
-Moroni, L., Tabury, K., et al. (2021). What can biofabrication do for space and what can space do for biofabrication? Trends in biotechnology.
-Belmans, N., Oenning, A.C., Salmon, B., Baselet, B., Tabury, K., Lucas, S., Lambrichts, I., Moreels, M., Jacobs, R., & Baatout, S. (2021). Radiobiological risks following dentomaxillofacial imaging: should we be concerned? Dento maxillo facial radiology, 20210153 .

PUBLICATIONS IN REVISION / TO SUBMIT

-Tabury, K., Monavarian, M., Listik, E., Shelton, A.K., Choi, A.S., Quintens, R., Arend, R.C., Hempel, N., Miller, C.R., Győrffy, B., & Mythreye, K. (2022). PVT1, a YAP1 dependent stress responsive lncRNA drives ovarian cancer metastasis and chemoresistance. bioRxiv. - in review at Life Science Alliance
-Olde Engberink R., van Oosten P., Tabury K. et al. - The kidney, volume and osmoregulation in space: Current perspective and knowledge gaps - submitted at npj Microgravity
-Radiation in space: current ESA recommandation - To be submitted at npj Microgravity
-Biomarkers of cardiac aging as biosensor to monitor cardiac aging in space. - To be submitted to Frontiers research topic Radiation Risks and Countermeasures for Space Exploration
-Building a stem cell-based human heart - To be submitted toTrends in technologies
-Radiobiology textbook - In revision at Editor - contribution to chapter 3; 6 and 10

TEACHING

Sep 2020 - Current
Master in Space
KULeuven

COURSES:
Advanced Topics in Life Sciences in Space:
-Cardiopulmonary, musculoskeletal and excretory system
-Tissue engineering and regenerative medicine

Jan 2017 - Jun 2019
Teaching assistant
UNIVERSITY OF SOUTH CAROLINA

COURSES:
-Senior Biomedical Engineering Design
-Biomonitoring and Electrophysiology

VOLUNTARY WORK

Jan 2020 - Current
Secretary
BHTC

RESPONSABILITIES:
Secretary of the Belgian Hadron Therapy Consortium

Jan 2017 - Dec 2018
UNIVERSITY OF SOUTH CAROLINA

RESPONSABILITIES:
-Thinking Globally Ambassador-International Student Services
-Member of the instructional development committee of the graduate student association

INTERESTS

Traveling // Cooking // Badminton // Tiny house